International Scientific-Technical and Production Journal

The Paton WELDING JOURNAL

November
2007
11

English translation of the monthly «Avtomaticheskaya Svarka» (Automatic Welding) journal published in Russian since 1948

Founders: *E.O. Paton Electric Welding Institute of the NAS of Ukraine*
International Association «Welding»

Publisher: *International Association «Welding»*

Address:
E.O. Paton Electric Welding Institute,
International Association «Welding»,
11, Bozhenko str., 03680, Kyiv, Ukraine
Tel.: (38044) 287 67 57
Fax: (38044) 528 04 86
E-mail: journal@paton.kiev.ua
http://www.nas.gov.ua/pwj

State Registration Certificate
KV 4790 of 09.01.2001

Subscriptions:
$324, 12 issues per year,
postage and packaging included.
Back issues available.

CONTENTS

MATHEMATICAL MODELLING OF THERMAL-DEFORMATION PROCESSES IN BRAZE-WELDING OF BUTT JOINTS OF THE TITANIUM-ALUMINIUM TYPE

V.I. MAKHNENKO, A.S. MILENIN and **A.P. SEMYONOV**
E.O. Paton Electric Welding Institute, NASU, Kiev, Ukraine

Mathematical model of thermal-deformation processes occurring in braze-welding of butt joints between titanium and aluminium was developed. Analysis of these processes was conducted within the frames of this model, and recommendations were worked out for optimisation of production of passenger aircraft seat tracks comprising dissimilar joints.

Keywords: mathematical modelling, braze-welding, titanium, aluminium, thermal deformation, residual stress-strain state

Welding for making permanent joints in metal parts is finding an increasingly wide use now, in particular, in aircraft engineering, which is a very conservative industry in terms of application of welding technologies [1, 2].

Aluminium, titanium and their alloys are the most common materials for aircraft engineering [3]. From this standpoint, of certain interest are dissimilar welded joints between titanium and aluminium.

Welding of dissimilar joints in many cases is a complex of interrelated physical-chemical, thermokinetic and metallurgical processes, which eventually determine the quality of a welded joint. In turn, this complicates the process of optimisation of a corresponding welding technology [4, 5]. Experimental studies in this area are difficult to conduct and expensive, while the results obtained are not always unambiguous. Therefore, it seems reasonable to use mathematical modelling of the kinetics of the processes taking place in production of dissimilar welded joints by using appropriate numerical methods [6].

The quality and performance of dissimilar welded joints depend both upon the processes of reactive diffusion, which may lead to formation of brittle intermetallic interlayers, and upon the kinetics of the fields of strains, which determine the final shape of a part, and stresses, which may decrease performance of a component, induce formation of hot cracks and stress corrosion processes.

In welding of long parts, change in their shape can be very important. In particular, the problem of preliminary estimation of welding strains became topical in optimisation of the process developed by the Institute of Applied Beam Technologies (BIAS, Bremen, Germany) for production of titanium-aluminium welded seat tracks, i.e. elements of structures of the family of «Airbus» passenger air liners A380 [1].

The structure under consideration is a welded seat track (Figure 1, *a*), which is a flange beam of a variable profile welded with the longitudinal weld. One half of the beam is made from titanium alloy Ti–6Al–4V (chemical composition, wt.%: 5.3–6.8 Al, 3.5–5.3 V, 0.5 N, 0.1 C, 0.0125 H, 0.3 Fe), and the second half is made from aluminium alloy AA6056 (chemical composition, wt.%: 0.7–1.3 Si, 0.5 Fe, 0.5–1.1 Cu, 0.4–0.1 Mn, 0.6–1.2 Mg, 0.25 Cr, 0.1–0.7 Zn).

Experimental studies of the kinetics of temperature field and thermal-deformation state of the beam were carried out during its welding using the same materials and similar but somewhat simplified design, the elements of which are shown in Figure 1, *b*. To avoid formation of brittle reactive phases within the dissimilar contact zone, braze-welding was used to pro-

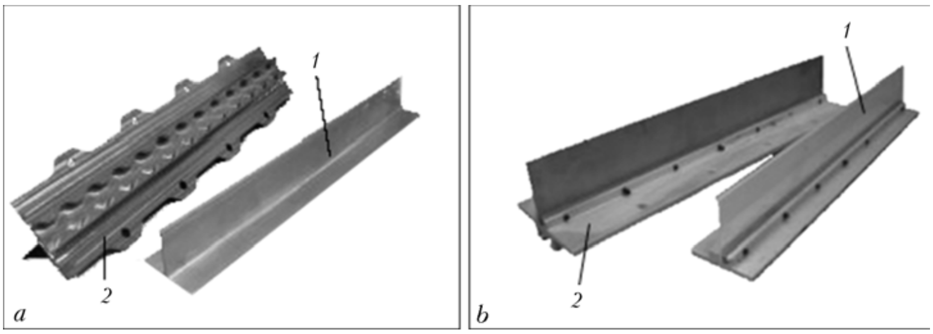

Figure 1. Appearance of parts welded — seat track (*a*) and beam of simplified design for experimental studies (*b*): *1, 2* — aluminium and titanium parts, respectively, of welded beam

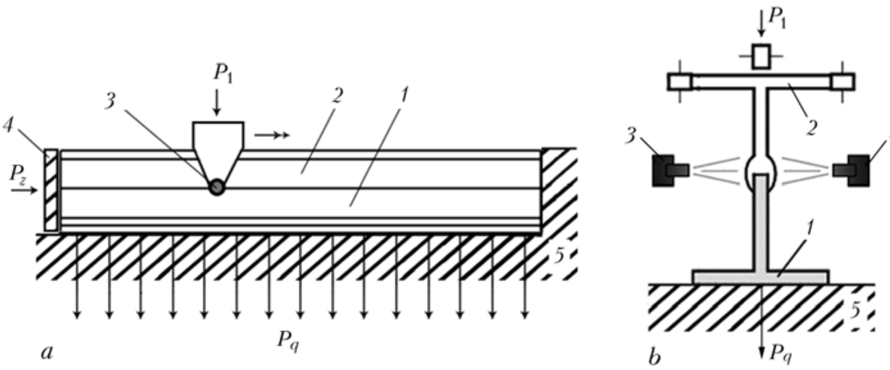

Figure 2. Flow diagram of the process of production of titanium-aluminium joint by laser welding: *a* — side view; *b* — end; *1, 2* — titanium and aluminium parts, respectively, of workpiece; *3* — laser welding heat source; *4* — piston providing axial force; *5* — support table

Table 1. Geometric parameters of dissimilar seat track and welded beam of simplified design

Structure	Beam length, mm	Thickness of part of beam wall, mm		Thickness of aluminium flange of beam, mm	Height of part of beam wall, mm	
		Al	Ti		Al	Ti
Seat track	1000	2.0	1.8	3.2	38.4	42.6
Beam of simplified design	1000	2.0	1.9	5.0	42.0	48.0

duce a permanent joint between the titanium and aluminium parts of the structure. The point of this welding process is that the process parameters are selected so that only the aluminium part of a workpiece is melted, while the titanium part remains solid. In this case, liquid aluminium wets the surface of titanium and forms a braze-welded contact with it [1, 4–6].

Welding of the titanium and aluminium parts of a workpiece was performed with two laser beams on both sides. The beams were simultaneously moved along the weld, as shown in Figure 2 (double arrow indicates to the direction of movement of the laser heat source along a sample welded). The workpiece is in a fixture, which provides its uniform pressing to the support table (distributed pressing force P_q), axial force P_z uniformly affects the end plane of the workpiece by means of a piston, the shape of which copies geometry of the cross section of the beam, and the moving carriage with the laser affects the upper plane, i.e. aluminium flange, with pressing force P_1.

Schematic of the braze-welded joint is shown in Figure 3, and geometric parameters of the dissimilar seat track and beam of the simplified design are given in Table 1.

Operational parameters of the butt welding process were as follows:

Speed of heat source along the seat track joint (beam of simplified design), mm / s 4.33 (3.67)
Power of each source, kW 1.75
Weld spot diameter, mm 5.0
Pressing force at carriage P_1, N 754
Distributed pressing force P_q, N / mm 4.41
Axial force P_z, N 376

The mathematical model was developed and implemented to describe thermal-deformation processes occurring in braze-welding of a dissimilar titanium-aluminium beam of the seat track type.

Efficiency of the laser heat source depends upon such parameters as distribution of power in the weld spot, angle of incidence of the light beam on the surface, state of the surface, etc. Hence, it seemed expedient to experimentally determine the value of the efficiency separately for each particular welding case.

In the case under consideration, the efficiency of the laser affecting each of the parts of the dissimilar surface was found by comparing temperature cycles at different points of the workpiece, experimentally measured during welding using a set of thermocouples, and kinetics of the temperature field determined by numerically solving the equation of thermal conductivity [7].

Properties of the titanium and aluminium alloys used for the calculations are given in Table 2.

The best agreement between the numeric and experimental data on temperature cycles, as well as on the shape of penetration was achieved at a value of

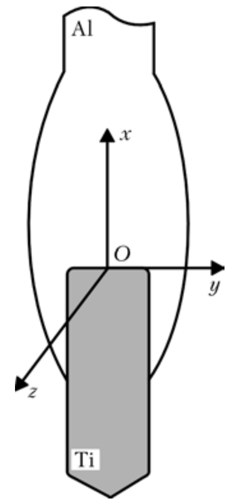

Figure 3. Schematic of braze-welded joint

Table 2. Physical properties of titanium and aluminium alloys used in the mathematical model [8–10]

Physical parameter	Temperature, °C							
	20	100	200	300	400	500	600	700
Ti–6Al–4V								
Thermal conductivity, J / (°C·cm·s)	0.059	0.072	0.086	0.100	0.114	0.128	0.142	0.156
Heat capacity, J / (cm^3·°C)	2.48	2.50	2.57	2.70	2.83	3.01	3.23	3.54
Yield stress, MPa	1060	870	720	630	570	460	350	230
Elasticity modulus, MPa	119	115	110	104	97	91	85	80
Linear expansion coefficient, 10^5·$°C^{-1}$	0.71	0.80	0.89	0.92	0.94	0.96	0.97	0.98
AA6056								
Thermal conductivity, J / (°C·cm·s)	1.1	1.2	1.4	1.5	1.6	1.8	2.0	5.0
Heat capacity, J / (cm^3·°C)	2.50	2.60	2.70	2.80	2.90	2.95	3.00	3.00
Yield stress, MPa	220	213	200	188	140	100	20	20
Elasticity modulus, MPa	98	95	90	80	70	60	50	40
Linear expansion coefficient, 10^4·$°C^{-1}$	0.23	0.23	0.24	0.25	0.26	0.27	0.28	0.28

the efficiency of the welding heat source equal to 0.17 and 0.35 (in affecting the aluminium and titanium surfaces, respectively). The difference in values of the efficiency of the heat effect by the laser on these metals is caused, first of all, by a higher reflection ability of the aluminium surface, compared with the titanium surface.

The efficiency values obtained allow a sufficiently accurate calculation of the kinetics of temperature field in a workpiece during the welding process. Results of this calculation and experimental data are shown in Figure 4.

The method for numerical estimation of stress and strain fields formed during the welding process is based on solving the corresponding problems of non-stationary thermoplasticity by sequentially tracing the evolution of elasto-plastic deformations from the initial state (before the beginning of welding) and up to the final state (after complete cooling and removal of the process fixture [8]). As length of the dissimilar beam welded is much in excess of characteristic sizes of the cross section, the two-dimensional model of the kinetics of the stress-strain state can be used to describe distortion of its axis because of non-uniform heating. The fact that the workpiece was symmetric about plane xOz (see Figure 3) was taken into account in this case.

As shown in Figure 5, *a*, the experimental value of maximal residual flexure of the aluminium flange of the beam of a simplified design at the considered

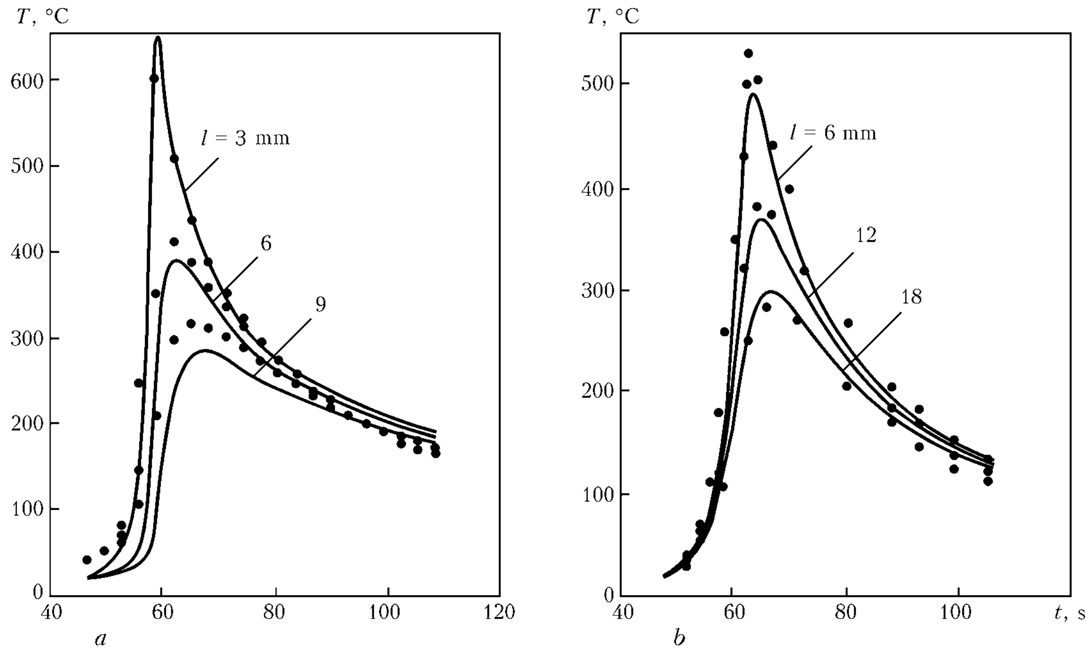

Figure 4. Calculation (curves) and experimental (points) values of temperature cycles obtained at different distance l from the end of titanium edge to the titanium (*a*) and aluminium (*b*) parts of workpiece

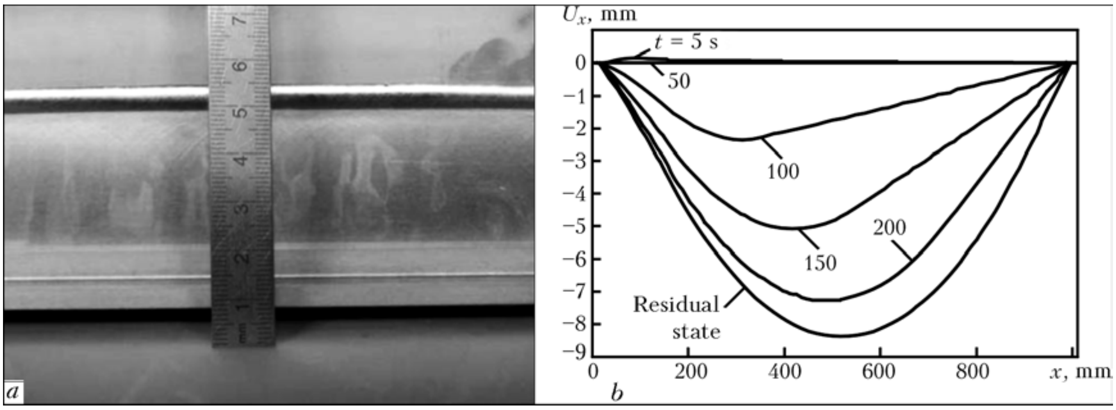

Figure 5. Residual flexure of welded beam of simplified design measured experimentally (*a*), and displacement U_x of its axis along the weld line at different time moments *t* according to calculation (*b*)

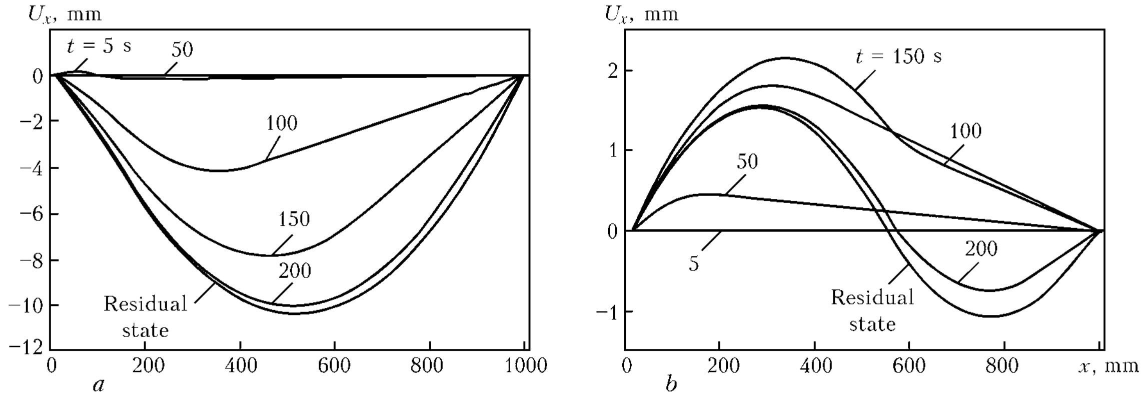

Figure 6. Displacements U_x of axis of braze-welded seat track at different time moments *t* according to numerical calculation: *a* — initial configuration; *b* — optimised position of weld (displacement of 26 mm to titanium part)

process parameters was 8 mm, which correlates with a good degree of accuracy with the calculation data shown in Figure 5, *b*.

In welding of the seat tracks, numerical analysis within the frames of the model showed that maximal residual flexural displacement U_x of the aluminium flange was less than 10.5 mm (Figure 6, *a*).

To exclude subsequent treatment of the workpiece from the technological cycle in order to reduce curvature of axis of the welded beam, the degree of residual deformation can be decreased by optimising the welding process. This can be achieved by varying the force effect on the workpiece in fixture during welding, or by displacing position of the weld line (i.e. varying the ratio of the lengths of the aluminium to titanium parts of the welded beam wall).

As shown by numerical calculations, varying forces in the fixture is of low efficiency, as even the rigid fixation (meaning equality of current flexural displacements of the axis to zero) decreases the maximal residual displacements by 2–3 mm.

The best effect in this case is provided by displacing position of the weld line towards the titanium part of the workpiece (which is desirable in terms of decrease in weight of a structure). Thus, displacement of the weld line by 26 mm in this direction results in a more than 3 times decrease in residual flexure of the seat tracks (Figure 6, *b*).

CONCLUSIONS

1. Values of the efficiency of the heat effect by laser on the aluminium and titanium surfaces, equal to 0.17 and 0.35, respectively, were obtained by comparing experimental and calculation results on the basis of mathematical modelling of the kinetics of temperature field in laser braze-welding of a titanium-aluminium structure (seat tracks of passenger air liners).

2. Investigations of thermal-deformation processes occurring in butt braze-welding of the titanium-aluminium seat track and simplified model structure showed that residual flexural displacements reached values of 10.5 and 8.5 mm, which is in good agreement with the experimental data.

3. Decrease in residual flexures by varying forces applied to a workpiece in fixture, up to a rigid fixation, was found to be of low efficiency.

4. Decrease in the degree of residual deformation can be achieved by displacing position of the weld towards the titanium part of the beam: with the position of the weld line changed by 26 mm, the maximal residual flexure decreases 3 times, compared with the initial geometry of the welded joint.

The authors of this study are grateful to Dr. Thomas Pretorius and his colleagues from BIAS (Germany) for fruitful cooperation, owing to which the results obtained were correctly validated.

1. Kreimer, M., Vollertsen, F. (2005) Processing titanium-aluminum hybrid joints for aircraft applications. In: *Proc. of 3rd Int. WLT Conf. on Lasers in Manufacturing* (Munich, June, 2005), 238–243.
2. Schubert, E., Klassen, M., Zerner, Y. et al. (2001) Lightweight structures produced by laser beam joining for future applications in automobile and aerospace industry. *J. of Materials Proc. Technology*, 115(**1**), 2--8.
3. Williams, J.C., Starke Jr., E.A. (2003) Progress in structural materials for aerospace systems. *Acta Materialia*, **51**, 5775–5799.
4. (1986) *Metallurgy and technology of welding of titanium and its alloys*. Ed. by V.N. Zamkov. Kiev: Naukova Dumka.
5. Rabkin, D.M., Ryabov, V.R., Gurevich, S.M. (1975) *Welding of dissimilar metals*. Kiev: Tekhnika.
6. Ryabov, V.R. (1983) *Welding of aluminium and its alloys with other metals*. Kiev: Naukova Dumka.
7. Makhnenko, V.I., Velikoivanenko, E.A., Pochinok, V.E. et al. (1999) Numerical methods of the predictions of welding stresses and distortions. In: *Welding and Surfacing Rev*., Vol. 13, Part 1. Amsterdam: Harwood A.P.
8. Jordan, A. (2006) *Input data for Abaqus simulation LABRA: theory manual*: Rhode Island: Hibbit, Karlsson & Sorensen Inc.
9. Wischhusen, B.-M., Kreimeyer, M. (2006) *Second progress report of laser joining development for aluminium-titanium seat tracks at BIAS*. Bremen: BIAS.
10. Boyer, R., Welsch, G., Collings, E.W. (1994) *Materials properties handbook. Titanium alloys*. Miami: ASM Int.

WELDING OF ALUMINIUM ALLOYS (directions of research conducted at PWI)

A.Ya. ISHCHENKO
E.O. Paton Electric Welding Institute, NASU, Kiev, Ukraine

The main directions of investigations conducted at the E.O. Paton Electric Welding Institute over half a century in the field of arc welding of aluminium alloys are outlined. Examples of an effective application of technologies of arc welding of aluminium alloys in construction of various structures are given.

Keywords: arc welding, automatic submerged-arc welding, nonconsumable-electrode welding, alternating current, high-amperage arc, asymmetrical current of different polarity, consumable-electrode welding, pulsed-arc welding, narrow-gap welding, aluminium alloys, scandium microalloying

Similar to other developed countries, in Ukraine an increase of the volume of production of aluminium and its alloys is anticipated in the form of wrought semi-finished products, required for manufacture of railway passenger carriages, cars and lorries, buses, aircraft, products of aerospace engineering, chemical, medical and food industries, as well as in construction.

Considerable difficulties arising in fusion welding of aluminium alloys, are associated with a high reactivity of the components in the alloy composition. Interaction with oxygen and susceptibility to hydrogen absorption lead to development of coarse oxide films and porosity in the welds. The strongest alloys are prone to formation of hot cracks and softening in fusion welding. These features are particularly strongly manifested in application of new high-performance aluminium-lithium alloys, which, owing to a low density and increased modulus of rigidity allow a 10–15 % reduction of the structure weight and the respective increase of the tonnage of passenger and transport aircraft and other vehicles.

Research and engineering developments in the field of arc welding of aluminuim and its alloys were started at PWI in 1951 in the laboratory of welding non-ferrous metals and alloys. The laboratory had the task of organizing in a very short time a continuous production of railway tank-cars from AMts alloy 18–20 mm thick for transportation and storage of liquid oxygen and other chemical products, used for rocket launching. Attempts to use inert-gas welding in the plant were unsuccessful, as joining plate metal had to be performed with edge preparation in several passes.

This required a thorough preparation of the surface of the edges being welded and the wire, use of argon and, sometimes, helium. Moreover, welding equipment was imperfect at that time.

The task was solved by development and introduction into mass production of automatic submerged-arc welding over flux of AN-A1 grade. This technology was the leading one in mass production of tanks of 1 to 100 m^3 volume in «Bolshevik» (Kiev), «Krasny Oktyabr» (Fastov) plants, Sumy Mechanical Engineering Plant and a number of other enterprises; of railway tank-car barrels in Mariupol PA «Azovmash». Barrels and tanks were designed for storage and transportation of food and chemical products, namely water, milk, nitric acid, rocket fuel, etc.

In 1960–1970s an active application of higher strength alloys began in manufacture of aerospace systems, ship-, tank- and carriage-construction, chemical industry, construction and other industries. Submerged-arc welding of such objects did not provide the required weld quality or the required joint properties. In welding more than 15 mm metal the risk of slag inclusion or pore formation in the welds became higher, and requirements to maintaining the sanitary-hygienic labour conditions were increased. The above factors led to intensive development of more efficient methods and technologies of inert-gas and electron beam welding. Work in this direction was conducted in parallel, this allowing flexibility in selection of different variants of the technology, depending on the requirements to products, production and service conditions.

Among the processes of inert-gas welding of aluminuim alloys at the start of 1960s the leading position was taken up by nonconsumable-electrode argon-arc welding by a sinusoidal alternating current, which ensured higher quality of the weld metal and mechanical properties of the joints, compared to consumable-electrode argon-arc welding. As regards the arc penetrability, it was limited by insufficient resistance of electrodes from the then most resistant thoriated tungsten. For this reason, tungsten electrodes with a filler of up to 1.5–2.0 % lanthanum oxide (ETL) and with 3.0–3.5 % yttrium oxide (ETY) were developed. Unlike the thoriated ones, they are radiation safe.

Yttriated electrodes allowed increasing the power density of the arc column 1.5 to 2 times without any hazardous overheating of the electrodes, and achieving a significant increase of the effectiveness of melting of the metal being welded. Yttriated electrodes of 10 mm diameter enabled single-pass welding of aluminium alloys up to 20 mm thick by a single-phase high-amperage arc (up to 900–1000 A), and alloys 30–40 mm thick with three-phase arc. The developed respective welding equipment promoted widening of nonconsumable-electrode welding application. Already by mid-1960s technology of automatic high-amperage arc welding of body parts of rocket carriers from AMg6 alloy was mastered in the plants, and the S.P. Korolyov, V.P. Chelomej and M.K. Yangel design bureaus.

Production experience of fabrication of critical structures from AMg6 alloy showed that despite a strict observance of the requirements to metal preparation and technology of nonconsumable electrode welding, inadmissible oxide film inclusions were found in the weld. The idea of intensification of weld pool metal stirring for refining the oxide inclusions and simultaneous metal degassing, was implemented at nonconsumable-electrode pulsed-arc welding. Further investigations allowed establishing the effectiveness of the process and developing specialized equipment. It was possible to reduce 3 times the relative extent of oxide film inclusions in the welds on AMg6 alloy and the probability of formation of its extended inclusions in welding of lithium-containing alloys 1420 and 1460. Abrupt changes of the amplitude during the pulse and pause (modulated current) ensured a 7–10 times reduction of the total volume of voids in the alloy welded joints.

On the other hand, a higher effectiveness of application of asymmetrical square-wave current of different polarity for arc and plasma welding was established. Due to shortening of the time of running of the reverse polarity current to 10–30 % of the total cycle the load on the tungsten electrode is reduced, and in the periods of straight polarity a deeper penetration of the base metal is achieved. As a result, the welding speed was increased, heat input value was lowered, and the weight and overall dimensions of the plasmatron were reduced.

Investigations of physical phenomena running in the arc, allowed achieving a higher concentration of thermal energy in DC helium-arc welding compared to tungsten electrode AC argon-arc welding. This promoted an increase of the arc penetrability, 1.5–2 times lowering of the heat input, and reduction of the HAZ, respectively.

Furtheron it was shown that compared to nonconsumable electrode welding the consumable electrode arc welding process turned out to be less sensitive to the gap width and excessive thickness of the metal being joined, provided a higher welding speed and lower level of residual deformations of the weldments. However, the unstable quality of welds produced in steady arc welding in argon, limited its application in fabrication of critical structures. The new welding processes and equipment for consumable-electrode pulsed-arc welding developed at PWI, were a significant achievement in the field of fusion welding. Technological studies of the welding process using pulsed current generators allowed increasing the arcing stability, significantly reducing metal spattering and evaporation of volatile elements, reducing the quantity and dimensions of oxide inclusions and pores in welds.

Due to that from the middle of 1960s consumable-electrode pulsed-arc welding is becoming ever wider applied in industry, in particular, in fabrication of components of rocket-space complexes in the plants of SPA «Energiya», bodies of light-weight landing armoured vehicles at Volgograd Plant and infantry armoured vehicles at Kurgan Mechanical-Engineering Plant, passenger railway cars and metro cars, truck damping platforms, car refrigerators, ship superstructures, building structures and other items.

High requirements made of welded joints on tanks from AMtsS alloy and commercial aluminium for storage and transportation of aggressive products required development at PWI of a highly-efficient technology of steady-arc welding by a consumable-electrode of a large diameter (3–4 mm) in a mixture of inert gases — helium and argon. Use of these mixtures allowed not only 2 to 8 times reduction of the volume of microvoids in the deposited metal, increasing the mechanical properties and corrosion resistance of welded joints, but also increasing by 40–60 % the welding process efficiency. Such a technology was successfully implemented in fabrication of tanks at Balashikha PA «Kriogenmash», in continuous production of aluminium barrels of railway tank cars in PA «Azovmash».

Use of pulsed-arc welding by a consumable electrode of 1.0–1.6 mm diameter in mixtures of helium and argon gases allowed achieving a higher level of mechanical properties of sheet joints of aluminium-lithium alloys compared to nonconsumable-electrode pulsed-arc welding. The process has become widely accepted in fabrication of rocket frame rings and bodies of infantry combat vehicles at Kurgan Mechanical-Engineering Plant. For consumable electrode welding PWI developed seven types of welding machines, tractors and automatic machines.

Technology of narrow-gap consumable-electrode pulsed- and steady-arc welding in helium and its mixtures with argon has been developed for joining plate structures (up to 150 mm). The method allowed making sound joints in the downhand position and on the vertical plane, as well as reducing several times the number of welding passes, reducing the HAZ and level of residual stresses, saving welding consumables and electric power.

The noted advantages of the new technologies also led to their broad introduction into manufacture of aerospace engineering products from aluminium alloys AMg6, 1201, 1420, including «Energiya-Buran» complex, carrier-rockets and space orbital systems.

Electron beam welding (EBW) is characterized by a unique combination of the following features: high energy density in a small diameter beam, reliable protection of the welding zone and refining impact of the vacuum environment, possibility of achieving very high rates of liquid metal solidification. The most critical and heavy-duty parts and components operating under the conditions of space vacuum, alternating loads and superlow temperatures are produced with EBW application. EBW of diverse parts and components from miniature to large-sized ones of the thickness from several fractions of a millimeter to 200 mm has been mastered in production. In individual cases welding of billets of 400 to 600 mm thickness has been realized. In order to perform EBW units have been developed, with the volume of vacuum chambers from several cubic decimeters to 1500 m^3. In welding of large-sized structures the total extent of welds reaches 100--150 m.

Wider acceptance of this welding process is promoted by development of units allowing operation under the conditions of local or low vacuum. Automatic control of the welding process has been developed, which allows producing high-quality welded joints. This is achieved also by using a system of programming the heat input for different sections of the weld pool volume. Use of beam scanning and programmed heat input in combination with filler wire feed allows lowering the requirements to the accuracy of the butt assembly without detracting from the quality of weld formation at up to 3.0 mm gaps (blank thickness of 50 to 100 mm).

EBW ensures good results in fabrication of stringer panels from sheet material. Welding of stiffeners to a shell of 2–3 mm thickness is performed by two fillet welds, one fillet weld from one side or by a through-thickness weld. In all the cases the welds can be formed without filler application.

Laser welding enables manufacturing such thin-walled structures without using vacuum chambers. In this case it becomes possible to weld any large-sized structures. The welding process is characterized by a higher specific energy density and allows conducting welding at a high speed, but with a low heat input. This promotes lowering of the level of residual strains and stresses in the products, as well as increasing the strength of welded joints by 10–15 % compared to argon-arc welding. The anticipation of a wider application of this welding process is based both on the results of intensive mastering of the technique and technology of welding by this process, and on a successful integrated application of the processes of laser and arc welding. Such hybrid technologies allow combining the advantages of two different welding processes in one, this making it more effective and cost-effective.

Solid-phase joining without base material melting, for instance, by friction stir process, should be regarded as an alternative to the above, most widely used processes of fusion welding. Use of such a joining technology allows elimination of alloy overheating and on other hand provides plastic deformation of weld metal. This is favourable for the level of mechanical properties of the joints and eliminates some of the considered problems of fusion welding of high-strength aluminium alloys.

Development of high-strength aluminium alloys of different alloying systems (Al–Mg, Al–Cu, Al--Zn–Mg–Cu) by All-Russian Institute of Aircraft Materials (VIAM) and, particularly, of the new class of super-light aluminuim-lithium alloys, with which academician I.N. Fridlyander worked with his associates, was the basis for creative contacts between PWI and VIAM for many years. The result of such cooperation was a successful solution of the problems of weldability and introduction of new materials into fabrication of aircfraft, rocket and space systems. The effectiveness of welded structures, for instance, fuel tank and pilot's cabin from aluminium-lithium alloy of 1420 type was confirmed by development and many years of operation of supersonic fighters of MiG-29 series.

In 1990s highly important research was performed together with VIAM and All-Russian Institute of Light Alloys (VILS), his leaders academician A.F. Belov and V.I. Dobatkin, Corresp. Member of RAS, aimed at improvement of the characteristics of advanced light alloys. Special welding consumables (fillers) based on Al–Mg and Al–Cu alloys, containing up to 0.5 % Sc, were also developed. Owing to that a number of high-strength difficult-to-weld alloys began to be joined in a satisfactory manner and weld strength increased by 10–15 %. A more significant effect was obtained at scandium alloying of not only the fillers, but also the base metal of the semi-finished products on the level of 0.1–0.2 %.

Right now the scientists and specialists of the Institute led by B.E. Paton are conducting fundamental investigations in the field of welding light metals and alloys in the following directions:

• study of the phenomena occurring in the welding zone at interaction of light alloy and composite material components with the arc plasma, electron and laser beams, substantiation of the conditions of sound formation of welded joints;

• determination of weldability characteristics of new aluminium alloys of different alloying systems and searching for new methods of overcoming their hot cracking susceptibility and porosity in fusion and solid-phase welding;

• searching for methods of joining dissimilar materials;

• investigation of the regularities of initial solidification and mechanisms of formation of the structure of welds under the non-equlibirum conditions at high cooling rates, intermittent and pulsed power supply, as well as under the influence of microadditives of different structural modifiers;

• investigation of microstructural transformations in the zone of aluminium alloy welding and their influence on physico-mechanical properties of welded joints of aluminuim alloys of different alloying systems;

• determination of the influence of service factors, namely temperature in a broad range from 4 to 60 K, aggressive media, nature of the stressed state, presence of stress concentrators, chemical and physical inhomogeneity of welded joints on the performance and fatigue life of structures from light alloys;

• development of new technologies of making permanent joints of advanced structural materials based on aluminium, including dispersed alumocomposites, intermetallics and dissimilar materials, which are difficult-to-join by regular fusion welding processes;

• substantiation of the criteria of reliable operation of critical welded structures under different conditions, taking into account their structural and chemical inhomogeneity.

A significant achievement of the new third millennium is development of nano-structured materials with exceptionally high properties and nanotechnologies of solid-phase permanent joining of such difficult-to-weld materials as intermetallics based on aluminuim, titanium, nickel, and nano-dispersed composite systems. For this purpose, a new class of effective nano-structured materials has been developed in the form of multilayer films and thin foils, using electron beam vapour-phase technology and other methods of fine dispersion.

ELECTRON BEAM TECHNOLOGY FOR FABRICATION OF RIBBED SHEET WELDED STRUCTURES

Thin-walled panels, i.e. light alloy sheets with stiffeners, are widely used for the fabrication of large-size light-weight casing structures applied in aerospace engineering, ship building and transport. Such panels can be manufactured by hot pressing, but this is feasible only in the case of high-ductility alloys and certain proportions of size of the sheet sections and stiffeners.

The advanced technology was developed for manufacture of welded panels, according to which stiffeners of any cross section are welded to a thin sheet. The technology provides for suppression of residual distortions by using the method of preliminary elastic tension.

Stiffeners can be joined to a panel with two- or one-sided fillet or slot welds. The ratio of thickness of a stiffener to that of a panel can range from 1:1 to 1:10 and higher.

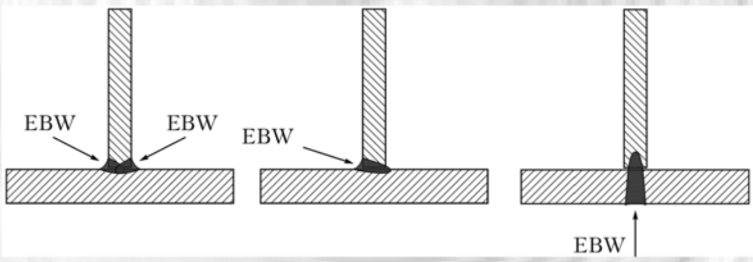

Panels made from high-strength aluminium alloys using electron beam welding have the highest values of structural strength. Residual longitudinal deflection of such panels is not more than 1 mm per running metre of the panel length.

Proposals for co-operation. Development of technical documents, transfer of know-how for the technology, technical consultations and engineering services in commercial application of the technology.

Contacts: Prof. Ishchenko A.Ya.
Tel.: (38044) 287-44-06

PROPERTIES AND STRUCTURE OF HYBRID LASER-PLASMA WELDED JOINTS IN ALUMINIUM ALLOYS

E.G. TERNOVOJ, V.F. SHULYM, V.Yu. KHASKIN, V.D. SHELYAGIN, A.V. LOZOVSKAYA, A.V. SIORA and **A.V. BERNATSKY**
E.O. Paton Electric Welding Institute, NASU, Kiev, Ukraine

The process of production of joints in aluminium alloys by the hybrid laser-plasma method was investigated. Peculiarities of properties and structure of these joints were studied. Welding experiments were conducted both with and without filler wire, which allowed porosity of the welded joints to be eliminated and their properties to be considerably improved.

K e y w o r d s : hybrid laser-plasma welding, aluminium alloys, filler wire, properties of joints, macro- and microstructure, porosity, microhardness, chemical heterogeneity, distribution of hydrogen

Welded structures of aluminium and its alloys have gained wide acceptance in different industries. These alloys are used to fabricate structures operating under conditions of complex alternating loads, increased and low temperatures, and in aggressive environments [1]. Owing to their low weight, sufficiently high specific strength and corrosion resistance, aluminium alloys are extensively applied in ship building, chemical and aerospace engineering, and in motor car construction [2–6].

Structures of aluminium alloys are currently fabricated using fusion welding [7, 8]. Peculiarities of welding of aluminium alloys include high affinity for oxygen, presence of Al_2O_3 oxide films on the welds, and sensitivity to pore formation, this exerting a substantial effect on properties and structure of the welded joints [9–11]. The following methods are used to prevent porosity and provide the required quality of the joints: preliminary preparation of the weld edges and filler materials, and alloying of the weld metal. Preliminary preparation includes mechanical or chemical removal of oxide films from surfaces of the joints and filler material [12]. And the second method provides for the use of filler materials or welding fluxes with additions of alloying elements [13].

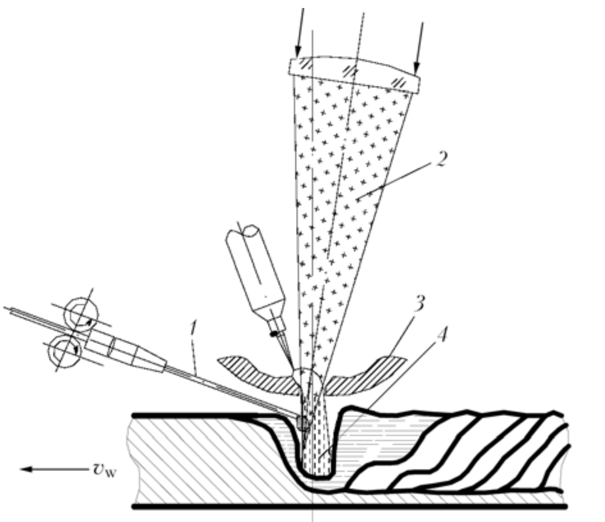

Figure 1. Flow diagram of laser-plasma welding: *1* — filler wire; *2* — laser beam; *3* — plasmatron nozzle; *4* — plasma arc

Hybrid laser-plasma welding is one of the most promising methods for joining aluminium alloys [14–16]. However, peculiarities of the impact by alloying the welds on their physical-mechanical properties with this welding method have not been adequately investigated as yet. So, it is this issue that is the subject of this study dedicated to investigations of welded joints in aluminium alloys. The hybrid laser-plasma welding method (Figure 1) combines advantages of both welding processes (thus mutually eliminating their drawbacks) and allows gaining the hybrid effect [17] from the combined use of laser radiation and electric arc. This is the so-called effect of violation of additivity of the heat impact by the laser beam and arc plasma on the material treated, which is caused by transition from the heat conduction to keyhole penetration welding mode [18–20].

Experiments were carried out using the «Rofin-Sinar» (Germany) diode laser DF 020 HQ with a power of up to 2 kW and wavelength of 0.808–0.940 μm, ingenious-design plasmatron with a power of up to 2 kW and plasma-shaping nozzle diameter of 2.5–3.0 mm, and power unit for welding at a straight-polarity current and in a mode of different-polarity rectangular current pulses [20]. The experiments were conducted on samples of aluminium alloys AMg3 and AMg6, 0.8, 1.5, 2.0 and 3.0 mm thick, which were penetration and butt welded by the laser, plasma and hybrid welding methods. Optimal welding parameters were identified, and properties and structure peculiarities of the joints produced with and without filler wire were determined in the experiments.

The quality of penetration and butt welded joints was evaluated by visual examination and on macrosections. The presence of pores, oxide inclusions, cracks, voids and lacks of penetration in the welds was checked by X-ray flaw detection using the RAP-150 / 300 unit. Chemical composition of the base and weld metals was revealed by spectral analysis using the DFS-36 photoelectric spectrometer, and tensile strength of the welded joints was determined by mechanical tests using the TsDM-4 tensile-testing machine at a temperature of 20 °C. Metallography of geometry and structure of the weld metal was carried out on transverse macro- and microsections using the MBS-9 and «Neophot-32» optical microscopes (with magnification of ×15 to ×150). Structural components were revealed by electrolytic etching in a solution of glacial acetic and chloric acids.

Microhardness $HV0.05$ of the joints was measured on transverse microsections using the LECO microhardness meter M-400 with a step of 0.1 mm. Chemical heterogeneity of the joints was examined using the «Cameca» microanalyser SX-50, and oxygen content of the base metal and metal of the welded joints was determined by the extraction method of local mass-spectral analysis using the EKhO-4M unit with a laser probe 300 μm in diameter. Duration of a radiation pulse was $1 \cdot 10^{-5}$ s, and power of the pulse was 7.5 J.

The investigations were conducted in two stages. The first stage included experiments without the use of filler wire. Penetration and butt weldings of the joints were performed in argon atmosphere using laser radiation or transferred-arc plasma on flat samples measuring 200 × 100 mm, as well as by the hybrid method. Flow rate of the plasma gas was 4 l / min, and that for shielding of the weld pool and optics of the laser head was 10–12 and 0.5 l / min, respectively.

Table 1. Effect of welding (cladding) methods and parameters on macrostructure of welded joints

Experiment No.	Alloy grade	Sample thickness, mm	Welding (cladding) method	Laser power, kW	Welding speed, m / h	Straight / reverse polarity welding current, A	Pulse duration, ms	Macrosection
1	AMg6	1.5	Laser	2.0	108.0	--	--	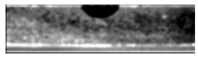
2		1.5	Plasma	--	108.0	100 / 50	50 / 50	
3		1.5	Hybrid	1.5	108.0	77 / 50	50 / 50	
4		1.5	Same	1.2	108.0	63 / 30	50 / 50	
5*		1.5	»	1.5	108.0	85 / 50	50 / 50	
6	AMg3	1.5	Laser	2.0	108.0	--	--	
7		1.5	Plasma	--	108.0	100 / 50	35 / 90	
8		1.5	Hybrid	1.5	108.0	70 / 50	50 / 50	
9*		1.5	Same	1.5	78.0	75 / 50	50 / 50	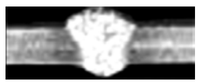
10		3.0	Laser	2.0	14.4	--	--	
11		3.0	Plasma	--	14.4	100 / 50	35 / 35	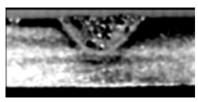
12		3.0	Hybrid	1.5	34.4	100 / 50	35 / 35	

*Here and in Tables 2 and 3 — welding of sample with filler wire.

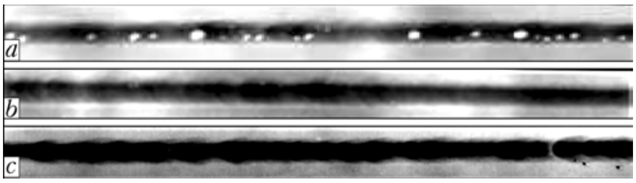

Figure 2. X-ray patterns of joints in aluminium alloys AMg3 (*a*, *c*) and AMg6 (*b*), 2 mm thick, produced by hybrid laser-plasma welding without (*a*, *b*) and with (*c*) filler wire

Power of focused radiation was varied from 0.5 to 2.0 kW. Diameter of the focal spot in this case was 1.2 mm, and deepening of the focus into the sample surface was 0.5--1.0 mm. Parameters of penetration welding and welding by different methods at a speed ranging from 10 to 110 m / h were selected for alloys AMg3 and AMg6 1.5 and 3.0 mm thick.

The second stage of the investigations consisted in performing claddings and welding of the butt joints on alloys AMg3 and AMg6, 0.8, 1.5 and 2.0 mm thick, by feeding filler wire into the weld pool, which was formed using separate heat sources or two heat sources combined at one spot. The experiments were carried out by using the 1.2 mm diameter wire SvAMg6 with a surface polished by the electrochemical method.

As established as a result of the investigations, radiation of the 2 kW diode laser provides penetration of about 0.6 mm deep on the plates of alloys AMg3 (1.5 and 3.0 mm thick) and AMg6 (1.5 mm thick) at a welding speed of 108 and 14.4 m / h, and in butt welding of these alloys 1.5 mm thick at a speed of 108 m / h the penetration depth is 0.7 mm (Table 1). A small penetration depth in laser welding of aluminium and its alloys is attributable to a comparatively large diameter of the focused beam spot, which provides a power density of no more than about $1\cdot10^5$ W / cm^2, while it is reported [20] that to achieve the deep penetration mode the required power density should exceed $1\cdot10^6$ W / cm^2. Plasma of the same power (arc voltage being equal to 20 and 18 V) allows achieving the penetration depth of 1.25 and 1.00 mm, respectively, at the same welding speed. The hybrid combination of these heat sources with a total power of 3.0 and 3.5 kW for alloys of the above thickness provided the full through penetration on a butt joint 1.5 mm thick at a welding speed of 108 m / h, and on a solid plate 3 mm thick at a speed of 34.4 m / h.

X-ray inspection revealed considerable porosity of the joints in alloy AMg3, produced by the hybrid welding method without filler wire (Figure 2, *a*). The similar joints in alloy AMg6, produced by the above three welding methods, also contained pores, but in much smaller amounts (Figure 2, *b*). The joints with high tightness of the welds were produced on the above alloys by hybrid welding using filler wire SvAMg6 (Figure 2, *c*).

Analysis of macrosections of the joints (see Table 1) showed the possibility of achieving the optimal geometry and satisfactory formation of the top and root reinforcement beads by choosing proper welding parameters and filler wire feed speed.

Chemical composition of the base metal and weld metal of the joints in alloys AMg3 and AMg6, 1.5–3.0 mm thick, produced by the hybrid method is given in Table 2. Composition of the weld metal of the joints produced without filler wire hardly differs from the initial composition of the base metal. With the SvAMg6 filler wire added to the weld pool, the content of magnesium used as an alloying element in the weld metal of the AMg3 welded joints increases from 3.3 to 4.8 wt.%.

When comparing values of tensile strength of the AMg3 and AMg6 joints 1.5 and 2.0 mm thick (Table 3), one should note a low strength of the AMg3 joints produced by the hybrid welding method without filler wire. Fracture of such test specimens occurred along the weld axis, the strength factor being about 0.5–0.6 of strength of the base metal. Porosity and oxide inclusions were revealed in the zones of metal fracture. Tensile strength of the AMg6 joints made by hybrid welding with filler wire was $(0.84\text{--}0.87)\sigma_t$ of the base metal, and that of the AMg3 joints was $(0.85\text{–}0.90)\sigma_t$ of the base metal. Fracture of the specimens occurred in HAZ of the base metal. Increased values of tensile strength of the weld metal on the AMg3 joints is attributable to an increased weight content of magnesium in the weld metal, compared with the base metal, which is caused by adding the SvAMg6 filler wire and increasing the weld section. Microstructure of the aluminium alloy welded joints was examined, their microhardness was measured, chemical heterogeneity was studied, and hydrogen content of metal of the joints was determined to prove this hypothesis.

Examinations of microstructure of the AMg3 and AMg6 joints welded without and with filler wire show (Figure 3) that, in addition to the α-solid solution of

Table 2. Chemical composition (wt.%) of base metal and metal of the welds produced on alloys AMg3 and AMg6 by the hybrid method

Alloy grade	Region	Si	Mg	Mn	Cu	Zn	Ni	Ti	Fe
AMg3	Base metal	0.38	3.5	0.5	0.10	0.18	0.03	0.10	0.40
	Weld	0.40	3.2	0.3	0.10	0.12	0.03	0.10	0.40
AMg3*	Same	0.40	4.8	0.3	0.10	0.12	0.03	0.10	0.40
AMg6	Base metal	0.18	6.4	0.6	0.06	0.14	0.03	0.06	0.25
	Weld	0.17	6.0	0.5	0.05	0.08	0.03	0.06	0.27
AMg6*	Same	0.15	6.0	0.5	0.05	0.08	0.03	0.03	0.23

magnesium and manganese, the base and weld metals also contain the binary and more complex β-phases in aluminium, i.e. Mg_2Al_3 or Mg_5Al_3, which are present in the base metal and along the grain boundaries in the form of thin filamentary precipitates, and in the weld metal — in the form of fine eutectic precipitates located between the dendrite branches [21]. Phase precipitates in the weld metal are finely dispersed, and the fusion boundaries have no traces of overheating. Continuous chains of precipitates can be seen along the grain boundaries in HAZ directly at the fusion boundary. The fusion zone in these joints is very narrow, having a fine-grained structure, and is a continuous transition of grains of the base metal into crystalline grains of the weld metal. Dendrites are oriented from the fusion boundary towards the weld metal. A mixture of equiaxed and oriented dendrites can also be seen in the central part of the weld.

It should be noted that the deformation texture of the base metal remains inchanged up to the fusion boundary (Figure 3, *b, d*), and no recrystallisation of grains occurs in HAZ, in contrast to the root part of the weld containing the zone of recrystallised grains. Macro- and microdefects in the form of pores (Figure 4, *a–c*), micropores, oxide films and cracks (Fi-

Table 3. Results of tests to tensile strength σ_t of the base metal and welded joints in alloys AMg3 and AMg6 produced by the hybrid method

Alloy	Base metal	Welded joint
AMg3	222–228 / 215	128–147 / 132
AMg3*		192–207 / 196
AMg6	353–357 / 350	292–309 / 298
AMg6*		290–308 / 295

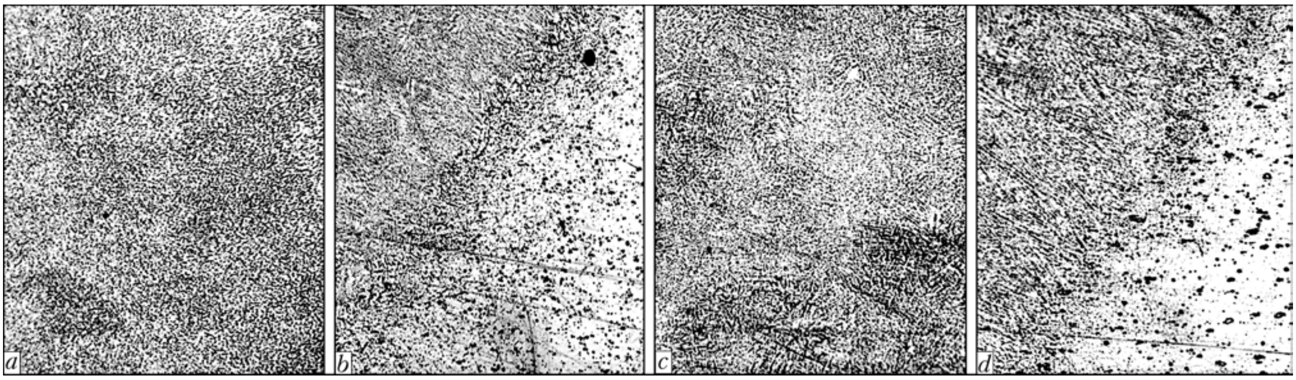

Figure 3. Microstructures (×150) of AMg6 welded joints produced by the hybrid method without (*a, b*) and with (*c, d*) filler wire: *a, c* — weld metal; *b, d* — fusion zone

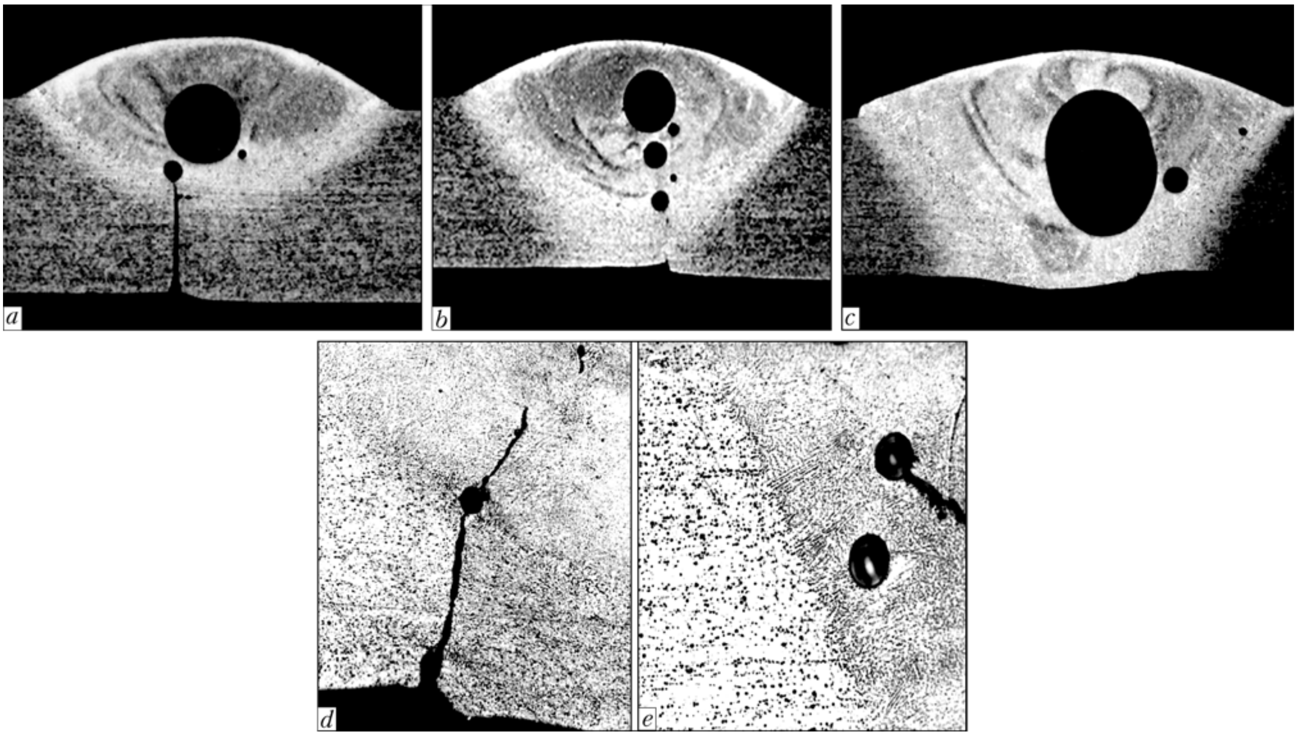

Figure 4. Macro- (×8) and microstructures (×150) with defects in the AMg3 (*a–d*) and AMg6 (*e*) joints produced by laser (*a*), plasma (*b*) and hybrid laser-plasma (*c–e*) welding without filler wire

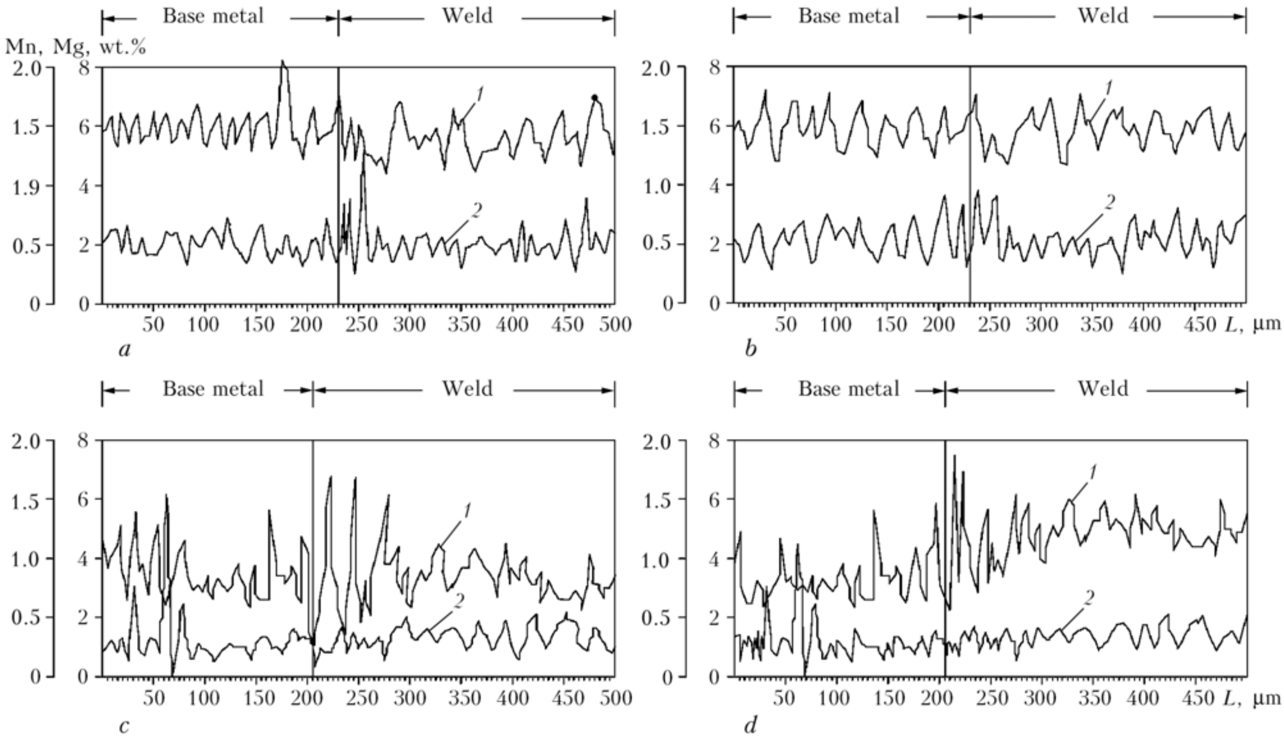

Figure 5. Distribution of magnesium (*1*) and manganese (*2*) in base metal and weld metal of the joints in alloys AMg6 (*a*, *b*) and AMg3 (*c*, *d*) produced by the hybrid welding method without (*a*, *c*) and with (*b*, *d*) filler wire: *L* — length of test region

gure 4, *d*, *e*) are present in the AMg3 and AMg6 alloy joints. The presence of macro- and micropores in the weld metal and fusion zone, especially in alloy AMg3, can be explained by the effect of a highly concentrated heat source on volatile magnesium and, probably, by an increased gas content of the initial AMg3 alloy, compared with AMg6. In addition, formation of porosity can be explained by the presence of oxide inclusions in the molten metal, the inclusions acting as pore initiation centres, which can be well seen in Figure 4, *e*. Microporosity at the interface between the gap of the joint and weld induces formation of microcracks (Figure 4, *d*). This is attributable to the deviation of the heat source from the joint axis taking place during the experiment, which led to the formation of discontinuities and lacks of fusion in the root part of the weld.

In the AMg6 joints produced with and without filler wire, microhardness is uniformly distributed over the entire width of the weld. It is close to that

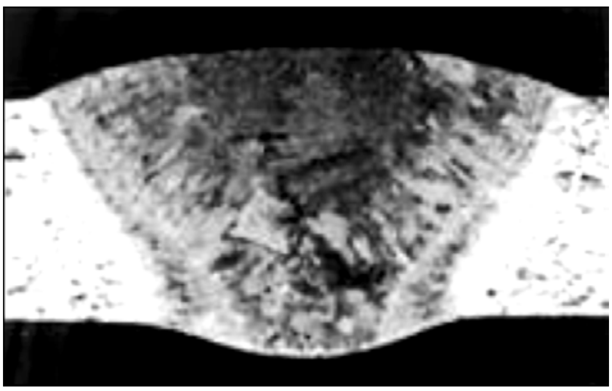

Figure 6. Macrosection (×8) of the AMg3 alloy joint produced by the hybrid welding method using filler wire

of the base metal (about *HV*0.05–75), while at the weld centre it amounts to *HV*0.05–80. This entirely correlates with a sound finely dispersed structure characteristic of a welded joint produced by laser welding at high speeds.

In the AMg3 joints produced without filler wire, increase in microhardness occurs near the central part of the weld (*HV*0.05-65–70). Closer to the fusion zone and in the base metal, it equals *HV*0.05–55. In the AMg3 joint produced with filler wire, microhardness has an increased value over the entire width of the weld and amounts to *HV*0.05–65 at its central part. For both variants, structure of the weld metal at the central part of the weld is characterised by the same degree of dispersion as in the AMg6 alloy joint produced by welding at a high speed. Therefore, fracture of such joints in mechanical tests occurred outside the welds (in HAZ), unlike the joints produced without filler wire.

Investigations of chemical heterogeneity of the welds showed that distribution of a volatile alloying element, i.e. magnesium, in the base and weld metals on the AMg6 and AMg3 alloy joints welded without filler wire was non-uniform (Figure 5). In both cases there was an insignificant decrease (1.0–1.5 wt.%) in the magnesium content of the weld metal, which was proved by the scan patterns shown in Figure 5, *a*, *c*. In the joints produced with filler wire (Figure 5, *b*, *d*), there was a marked (almost by 4.5–5.0 wt.%) increase in the magnesium content of the weld metal on alloy AMg3, and its homogeneous content in the AMg6 alloy joints. An increased magnesium content of the AMg3 alloy joints can be explained by adding filler wire SvAMg6, and is confirmed by results of

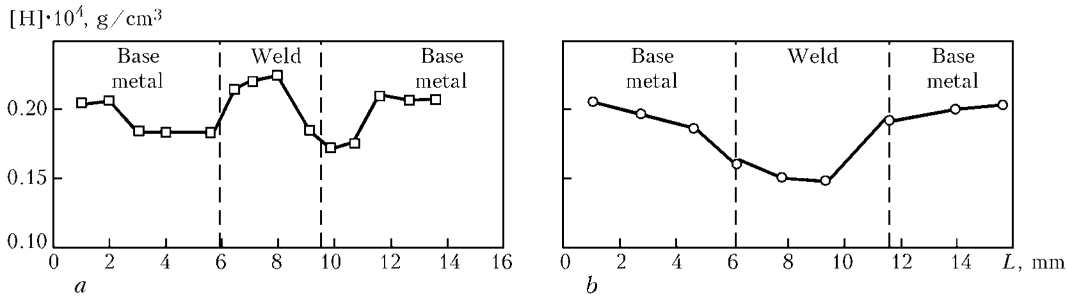

Figure 7. Distribution of hydrogen in the AMg3 alloy joints produced by the hybrid welding method without (*a*) and with (*b*) filler wire

mechanical tensile tests and examinations of microhardness of these joints. Moreover, as shown by X-ray inspection and examination of macrosections, the welds on alloy AMg3 made by the hybrid laser-plasma method using filler wire are free from macro- and micropores (Figure 6). This may be related to decrease in the hydrogen content of these welds caused by adding filler wire with the minimal gas content. This hypothesis was checked by determination of the hydrogen content of the weld metal (Figure 7, *a*, *b*).

Examination of the distribution of hydrogen in different regions of the AMg3 butt joints welded by the hybrid method without filler wire showed that the concentration of hydrogen is highest along the weld axis (higher than in the base metal), which is caused by its diffusion from the fusion zone into the weld metal on the side of the base metal (Figure 7, *a*). Substantial weight content of hydrogen in the base metal leads to formation of increased porosity in the welds, and its sudden differences provoke cracking (see Figure 4, *d*, *e*). The AMg3 alloy joints welded with filler wire exhibit a marked decrease in the hydrogen content of the weld metal (Figure 7, *b*) and, as a result, the absence of pores and cracks, which is proved by the mechanical test results (see Table 3) and X-ray filming (see Figure 2, *c*).

CONCLUSIONS

1. Hybrid laser-plasma welding provides a 2–4 times increase in the penetration depth on aluminium alloys 1.5–3.0 mm thick, compared with laser or plasma welding, as well as a similar increase in the welding speed, compared with plasma arc welding.

2. Coarse pores were detected in welds on the AMg3 alloy joints produced by the hybrid, laser and plasma welding methods without filler wire. The use of filler wire SvAMg6 in hybrid laser-plasma welding of alloy AMg3 allowed porosity of the welds to be eliminated, and tensile strength to be increased by 85–90 % compared with the base metal.

3. Results of examinations of chemical microheterogeneity of the aluminium joints and determination of the content and distribution of hydrogen in them show that porosity of the welds produced by laser-plasma welding is affected by the two main factors, i.e. content of magnesium in the weld metal and presence of hydrogen in the base metal and filler wire.

1. Arbuzov, Yu.P. (1990) *Weldable aluminium alloys.* Moscow: Mashinostroenie.
2. Ryazantsev, V.I., Fedoseev, V.A. (1995) Production of welded cryogenic fuel tanks of aluminium alloys. *Aviats. Promyshlenost*, **7 / 8**, 9–12.
3. Kolganov, I.M., Bashilov, A.S., Bogdanov, B.V. (1994) Production of panels with formed sections of advanced aluminium alloys. *Ibid.*, **9 / 10**, 3–5.
4. Bratukhin, A.G., Redchits, V.V., Lukin, V.I. (1996) Problems of production of welded structures for aerospace engineering. *Svarochn. Proizvodstvo*, **3**, 22--25.
5. Ryazantsev, V.I., Fedoseev, V.A., Mantsev, V.N. (1999) Production of welded car bodies of aluminium alloys. *Ibid.*, **11**, 36–42.
6. Krivov, G.A., Ryabov, V.R., Ishchenko, A.Ya. et al. (1998) *Welding in aircraft construction.* Kiev: MIIVTs.
7. Rabkin, D.M. (1986) *Metallurgy of fusion welding of aluminium and its alloys.* Kiev: Naukova Dumka.
8. Rabkin, D.M., Ignatiev, V.G., Dovbishchenko, I.V. (1982) *Arc welding of aluminium and its alloys.* Moscow: Mashinostroenie.
9. Makarov, I.I., Volynsky, V.N., Prokhorov, N.N. (1976) Influence of pores and oxide inclusions on strength of AMg6 alloy welded joints. *Avtomatich. Svarka*, **4**, 27–30.
10. Lukianov, V.F., Fomin, V.N., Mojseenko, V.P. et al. (1970) Influence of oxide inclusions on strength of welded joints on AMg6 alloy pressure vessels. *Svarochn. Proizvodstvo*, **6**, 24.
11. Zubrienko, G.L., Tenenbaum, F.Z., Petrovanov, V.M. et al. (1977) About some factors influencing the oxide inclusion formation in welds on AMg6 alloy. *Ibid.*, **5**, 24–27.
12. Ryazantsev, V.I., Fedoseev, V.A., Grishin, V.V. et al. (1982) Influence of methods of surface preparation for welding on pore formation in welds of aluminium-magnesium-lithium alloy. *Avtomatich. Svarka*, **6**, 53--54.
13. Ishchenko, A.Ya., Lozovskaya, A.V., Poklyatsky, A.G. et al. (1999) Structure and properties of joints produced in welding of AMg6 alloy using filler wires with scandium. *Ibid.*, **4**, 19--25.
14. Ueyama, T., Tong, H., Yazawa, I. et al. (2003) Aluminium alloy sheet welding by the laser AC pulsed MIG hybrid process. *J. JILM*, 41(**12**), 567--574.
15. Shtaufer, G. (2000) Laser hybrid welding. In: *New Materials and New Prospects:* Proc. of Int. Conf. on Welding and Joining (Israel, 18–20 June, 2000), 53--61.
16. Tusek, J. (1996) Synergic operation of welding arc and laser beam — for practical application or for scientific research only? *Varilna Tehnika*, 45(**2**), 39–46.
17. Diebold, T.P., Albright, C.E. (1984) «Laser-GTA» welding of aluminum alloy 5052. *Welding J.*, 63(**6**), 18–24.
18. Dilthey, U., Lueder, F., (1999) Expanded capabilities in welding of aluminium alloys with laser-WIG hybrid process. *Aluminium*, 75(**1 / 2**), 64–75.
19. Ueyama, T., Tong, H., Yazawa, I. et al. (2003) Hybrid welding (laser + AC pulsed MIG) of thin aluminium sheets. *Keikinzoku Yosetsu*, 41(**12**), 9–16.
20. Paton, B.E., Gvozdetsky, V.S., Krivtsun, I.V. et al. (2002) Hybrid laser-microplasma welding of thin sections of metals. *The Paton Welding J.*, **3**, 2–6.
21. Rabkin, D.M., Lozovskaya, A.V., Sklabinskaya, I.E. (1992) *Metals science of aluminium alloys.* Kiev: Naukova Dumka.

INVESTIGATION OF THE FRACTURE MODE OF WELDED JOINTS OF HIGH-STRENGTH ALLOY V96tss UNDER THE CONDITIONS OF OFF-CENTER TENSION

T.M. LABUR, A.Ya. ISHCHENKO, T.G. TARANOVA, V.A. KOSTIN and **G.M. GRIGORENKO**
E.O. Paton Electric Welding Institute, NASU, Kiev, Ukraine

Regularities of initiation and propagation of cracks in V96tss alloy under the conditions of off-center tension have been studied. Fractographic analysis was used to establish the causes and mechanisms of initiation of fracture sites in individual sections of welded joint HAZ after different conditions of welding heating.

Keywords: aluminium alloy, welding heating, nonconsumable electrode, electron beam, heat-affected zone, off-center tension, fracture microstructure, fractographic analysis, crack initiation, crack propagation, fracture

Zirconium and scandium addition to aluminium alloys ensures formation of a finely-dispersed structure without dendrites, strengthened by disperse precipitations of intermetallics based on the above elements [1–3]. Refinement of grain size at addition of these elements leads to delayed decomposition of the solid solution in aluminium alloys and subsequent coagulation of decomposition products during welding. The welded joints are characterized by a higher strength, which allows them to be used in development of critical welded structures of flying vehicles with high values of strength and reliability in operation [4, 5].

Under the operation conditions, the morphology and composition of intermetallic compounds often determine the processes of initiation and propagation of cracks at fracture [3–10]. A large body of data on the features of initiation and growth of microcracks in aluminium alloys is indicative of the urgency and importance of this problem. In the above works the authors note that a tough fracture mode related to formation of pits (micropores) and their subsequent coalescence during realization of plastic deformation, prevails in aluminium alloys. The pit dimensions are determined by grain size and distance between the inclusions. A non-uniform distribution of fine and large pits is observed in the fractures of complex-alloyed aluminium alloys.

In publications there is no information on the features of running of the processes of crack initiation and propagation in the welded joints of high-strength aluminium alloy V96tss. We made an attempt using qualitative approaches of electron microscopy to establish the influence of the structural and physical inhomogeneity, found in welded joints, on crack initiation and nature of their distribution. Such a method of investigation not only complements the available data obtained on the basis of fracture mechanics, but also is the basis for a valid expertise of the features of development of cracks at welded structure damage, as well as studying different stages of their fracture.

The nature of structural transformations occurring in the metal of the high-strength aluminium alloy V96tss at the thermal cycle of welding, was studied using a scanning electron microscope (SEM) JSM-840, fitted with microanalysis system Link 860 / 500. Interaction of the electron beam of the scanning microscope with the structural components, containing such elements as magnesium, copper, zirconium, scandium, creates different contrast of the image of the studied phases, which enables making a qualitative and quantitative evaluation of the influence of the shape and dimensions of the particles on crack initiation and propagation in the structure of alloy V96tss, depending on the thermophysical conditions of heating running in the HAZ at different methods of fusion welding, namely nonconsumable electrode (TIG) and electron beam (EB) welding. The following heating conditions were used here: overheating at T = 550 °C, 3 s; quenching at T = 460 °C, 1 h; annealing at T = = 360 °C, 20 min; tempering at T = 360 °C, 3 min; ageing at T = 140 °C, 7 h. Air and water were used for simulation of different cooling conditions. Influence of thermophysical conditions on fracture resistance characteristics in the studied sections of the HAZ of welded joints of alloy V96tss is shown in Figure 1.

Analysis of fracture relief of the broken samples showed that the thermal conditions of welding influence the structural-phase changes in the metal, phase content and nature of their distribution in the metal volume which, in its turn, influences the features of running of the processes of crack initiation and propagation. In all the fractures of samples of alloy V96tss a zone of plastic deformation is found at the notch tip (Figure 2), which is the macroscopic characteristic of fracture and is a section of fracture, where the main crack initiates in the sample at testing. Indeed, the dimensions of the zone of plastic deformation (Table) determine the influence of the alloy structure on its performance and mechanical properties, as the structural sensitivity of the material is due to the features

Influence of heat treatment on geometrical dimensions (mm) of plastic deformation zone

Heating conditions	a_1	a_2	a_3	L	α
Overheating	1.91	0.94	0.34	4.90	17°33′
Quenching	1.50 / 2.15	0.73 / 1.29	0.24 / 0.99	3.84 / 4.49	20°14′ / 31°12′
Annealing	1.79 / 2.12	1.30 / 1.34	0.62 / 0.50	2.78 / 2.14	33°09′ / 59°38′
Tempering	2.10	1.32	0.51	2.37	46°10′
Ageing	2.32	1.50	0.53	1.70	62°08′
Initial condition	2.01	1.14	0.40	1.40	60°04′

Note. The numerator gives the results of testing at EBW; the denominator — at TIG welding.

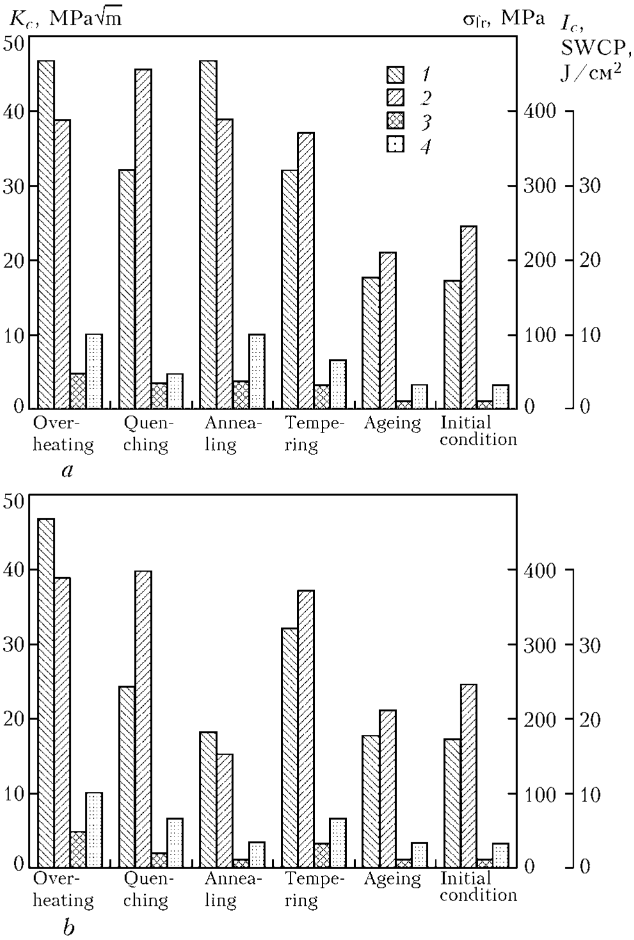

Figure 1. Dependence of the values of fracture resistance of V96tss alloy in different sections of the HAZ on heating conditions at EBW (*a*) and TIG welding (*b*): *1* — stress intensity critical factor K_c; *2* — rated breaking stress σ_{fr}; *3* — energy of crack initiation J_c; *4* — specific work of crack propagation (SWCP)

of the structural components and proportions of the geometrical dimensions of this zone. The latter in the studied samples point to a different level of the starting stressed state of the metal at initiation of cracks, the presence of which must be due to the content and dimensions of particles precipitating at phase particle heating. Their volume fraction determines the length and quantity of embryo microcracks, as well as the nature of local stress in the vicinity of their location. This influences the level of inner stresses and dimensions of the plastic deformation zone. As the radius in the crack tip is the same in all the samples (R = = 0.1 mm), there is every ground to believe that the size of the plastic deformation zone and, therefore, also the toughness of metal of the studied samples are determined by inner stresses which depend on the volume fraction of inclusions, as well as the conditions of heating and cooling in welding. Note that a plastic zone of a considerable length (4.90, 4.49, 3.84 and 2.80 mm) was obtained as a result of sample fracture under the conditions of a plane-stress state, when the metal especially actively absorbs the plastic deformation energy.

Unlike the above case, in the samples in the initial condition or after ageing, the extent of the plastic zone decreases by 30–35 %. This is indicative of development of conditions for elastic deformation in them at propagation of the main crack, when energy relaxation is insufficient for realization of plastic deformation.

Thus, at increase of the volume fraction of particles the structural and phase transformations occurring in the welded joint HAZ, may induce both the plane-strain and plane-stress state in the metal during their fracture. This allows assuming the dominating influence of particles on the conditions of crack initiation at fracture of welded joints of V96tss alloy, on which the values of fracture toughness characteristics depend at all the stages of crack propagation (Figure 2, *b*–*d*).

Let us consider the features of the relief in the studied samples simulating the conditions of V96tss alloy in HAZ. In a sample the condition of the metal of which corresponds to the zone of weld fusion with the base metal, where overheating is always in place, fracture runs in parallel to the applied load axis. In the fracture relief individual fragments of the structure are observed with hot solidification cracks formed at heating (Figure 3, *a*). At investigation of the relief of a section containing intermetallic compound $Al_3(Zr, Sc)$, it is established that its particles fail in the brittle mode (Figure 3, *b*). Particles of a coarser (3–6 μm) size delaminate from the matrix, and those of a fine (0.6–1.5 μm) size preserve a coherent bond with the matrix (Figure 3, *c*). Brittle nature of fracture of these particles can be due to running of the process of segregation of the alloying and impurity elements on grain boundaries under the conditions of overheating (550 °C, 3 s). Propagation of the thus formed microcracks further on occurs by the tough mechanism due to a high ductility of the matrix. Formation of fracture sites in the form of pits ahead of the crack can be related to relaxation of stress caused by accumulation of high density dislocations, which is preceded by formation of microvoids.

The path of the main crack propagation in the studied samples after heating up to the quenching temperature (460 °C, 1 h) with subsequent cooling in water differs from that found in the base metal. The site of microcrack initiation in this case are clusters

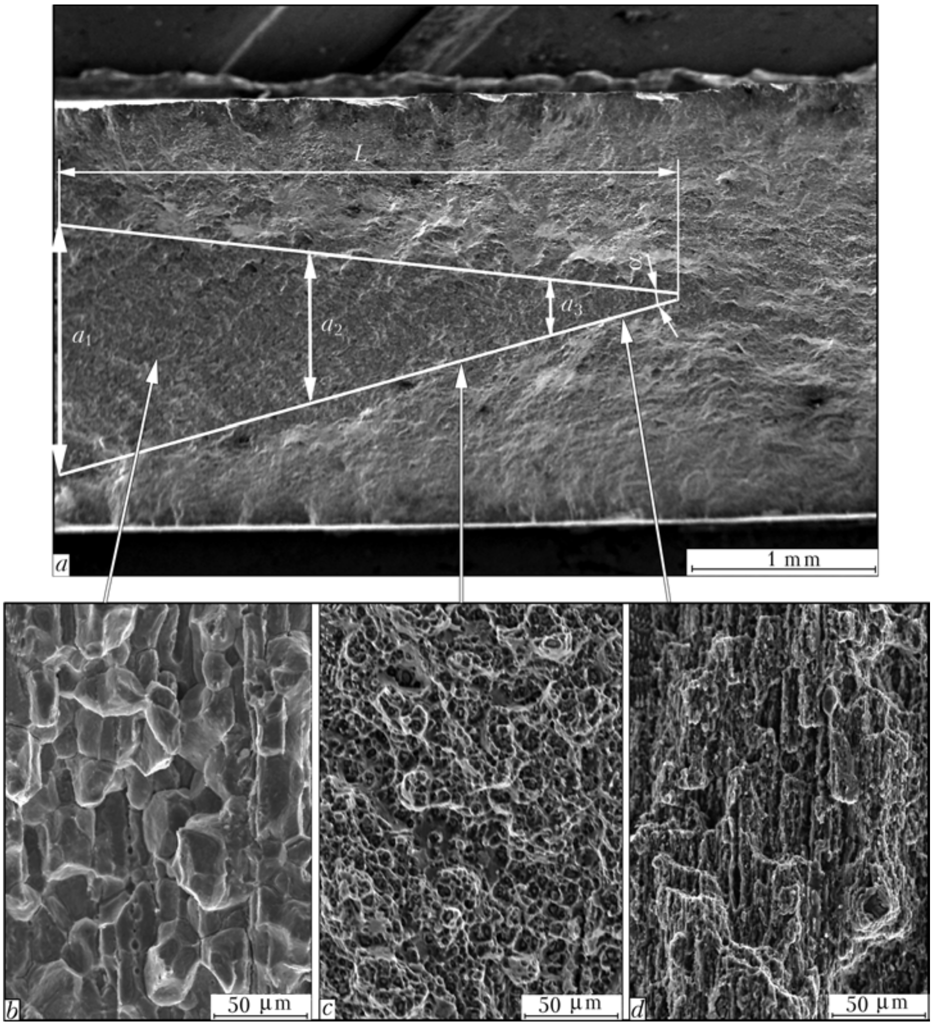

Figure 2. Geometrical dimensions of the plastic deformation zone (*a*) and microstructure of the characteristic sections of its fracture surface — intercrystalline (*b*), transcrystalline tough (*c*) and transcrystalline brittle (*d*)

of precipitating inclusions (Figure 4). Presence of characteristic ridges on the fracture surface, found at electron microscopy investigation, points to a discrete nature of the process of crack development (Figure 4, *a*). As they propagate the width of the ridges increases, which is, possibly, due to the increase of stress intensity in this section of the structure. Short hot cracks are also observed in the fracture in the plastic deformation zone. In addition, structure sections were detected, where crack initiation starts from the eutectic (Figure 4, *b*). In the center of fracture in the studied sample the site of the main crack initiation are coarse intermetallic compounds containing $Al_3(Zr, Sc)$ modifiers. Cracking or delaminating into components as the main crack propagates, they form clusters of particles with different content of scandium (15 wt.% in the center, 26 wt.% at the edge) and zirconium (respectively 18 and 6 wt.%). The mode of their fracture gives rise to the assumption that the site of the local breaking stress is their central part with subsequent development of delamination into peripheral regions. The duration of each of the stages of crack formation is determined by particle size. The cause for the action of such a fracture mechanism supposedly is a different

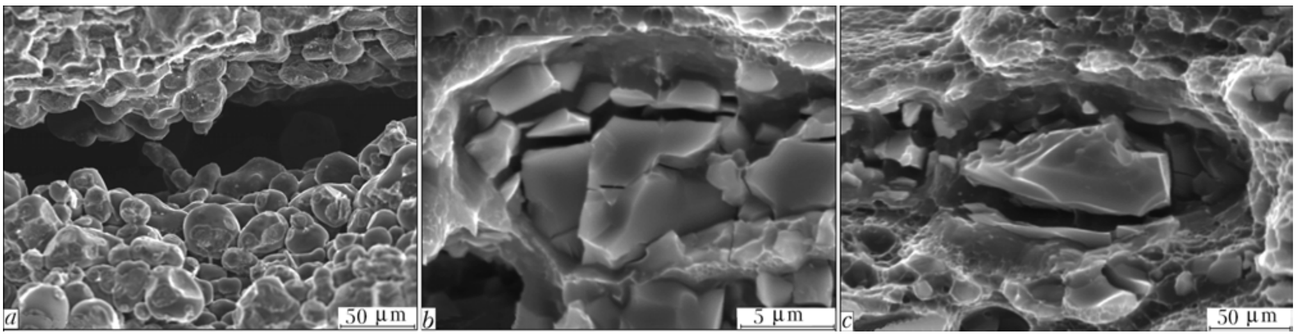

Figure 3. Fractograms of fracture surface of V96tss alloy in overheated condition: *a* — hot solidification crack; *b* — cleavage of intermetallic compounds; *c* — delamination of intermetallic compounds from the matrix

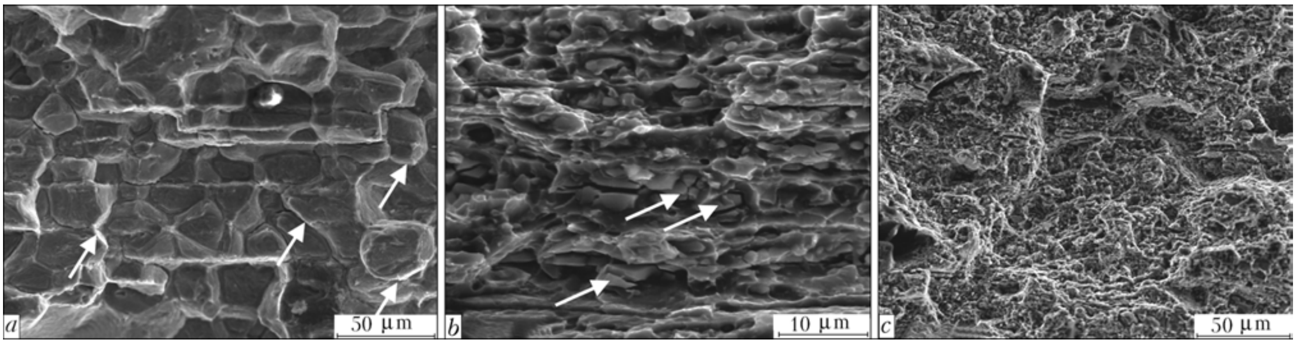

Figure 4. Fractograms of fracture surface of V96tss alloy in as-quenched condition: *a* — particle clustering section; *b* — section along the grain boundaries; *c* — section of facet location

proportion of zirconium and scandium in the metal of each subsequent layer.

Under the conditions of heating V96tss alloy up to the annealing temperature a shortening of the length of the plastic deformation zone is noted (see the Table). Angle α formed at its tip in this case is equal to 59°38′. In such a sample a low (1.1 J / cm^2) value of the energy of crack initiation is found, which is indicative of a considerable brittleness of the alloy structural components under the given conditions of thermal impact. The associated phase transformations lead to coarsening of the structural components located along the grain boundaries, which is the cause for a mixed nature of alloy sample fracture (Figure 5, *a*). Alongside the tough mechanism of formation of fine and shallow pits, sections are observed which are formed by the cleavage mechanism, running across the coarse intermetallic compounds (Figure 5, *b*). The crack propagates predominantly along the grain boundaries, where a low-melting eutectic forms during welding heating (Figure 5, *d*). Thus, embrittlement of welded joints of V96tss alloy produced by TIG welding is due to the process of coarsening of the structural components and formation of a significant volume fraction of the eutectics. The fracture sites are hot cracks. Their different shape (long and round) and extent are indicative of a non-uniform stressed state of the metal under the thermophysical conditions of nonconsumable-electrode welding. Content of particles of intermetallic compound $Al_3(Zr, Sc)$ is low, therefore they do not participate in the crack initiation process.

At sample cooling in water after heating to T = = 360 °C and soaking for 20 min, which corresponds to the thermal cycle of EBW, the fracture surface acquires numerous features of tough fracture. This leads to an increase of the values of fracture toughness (see Figure 1). In this case, small facets with ridges form during realization of plastic deformation. The site of crack initiation in this case, are structure sections, containing fragments of microvoids in the form of hot cracks. Their small number and short length (0.2–0.5 mm) lead to realization of a tough fracture mechanism (Figure 5, *c*) at higher values of the crack initiation energy parameter compared to a sample cooled in air.

In the metal in as-tempered condition a short zone of plastic deformation forms (2.37 mm, see the Table). Small dimensions of the facets formed at fracture are observed (Figure 6, *a*), which provides sufficiently high values of all the fracture toughness characteristics (see Figure 1). A multitude of fragments of intermetallic compounds located along the grains and elongated in the base metal rolling direction are found on the fracture surface, which leads to formation of facets of the same shape. As the influence of the heating conditions is negligible, no essential change of the alloy texture is observed compared to the base metal. The fracture sites are phases containing zirconium and scandium. Quantitative analysis of elements of the broken adjacent fragments of such phases leads to the assumption that the cause for their fracture is delamination, arising from weak atomic bonds between the layers as result of their different content of scandium and zirconium (Figure 6, *b*).

In a sample of V96tss alloy, when the metal is in the state of artificial ageing, a shortening of the plastic deformation zone at the notch from 2.37 to 1.70 mm (see the Table) and a change of the relief are observed (Figure 7). The facets mostly have a shallow depth, small dimensions, and they are greatly elongated in the direction of rolling. Presence of indications of both tough and brittle fracture in the studied sample fracture (Figure 7, *a*) points to a mixed mode of crack propagation. Its initiation occurs by brittle cleavage mechanism. The process of crack propagation is realized during plastic deformation of the matrix along the sliding lines. A feature of fracture of coarse particles containing zirconium and scandium is cracking (Figure 7, *b*). The content of these elements in the layers formed at the inclusion top and bottom, differs by about 5 times.

Fracture of alloy V96tss in the initial condition is of a mixed nature, when two or more fracture mechanisms act simultaneously [10]. It means that at testing under the conditions of off-center tension different factors start interacting in the studied sample. Therefore, the mode of fracture of V96tss alloy somewhat differs from that found in ductile aluminium alloys. Such behaviour of the metal can be realized under the conditions, when the stress level at plastic deformation is insufficient for fracture by the mechanism of pore coalescence. Presence of particles broken by cleavage

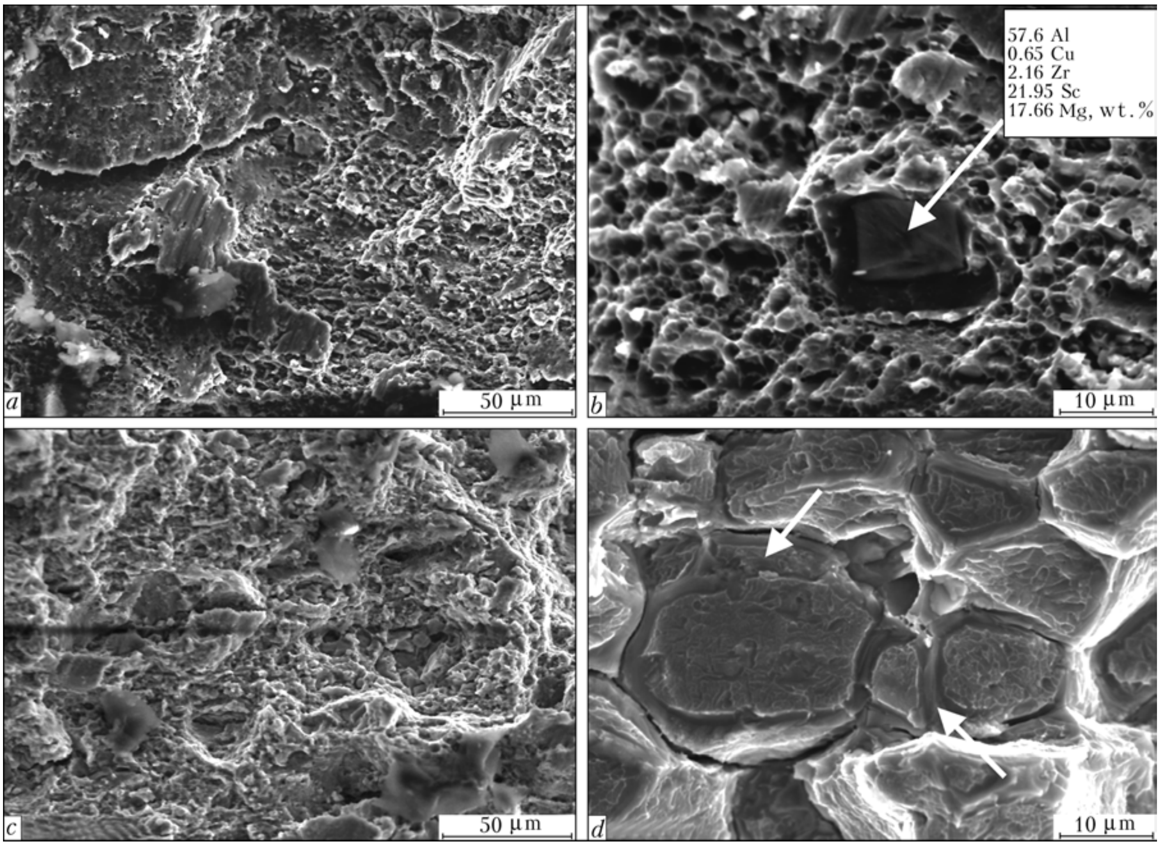

Figure 5. Fractograms of fracture surface of V96tss alloy in as-annealed condition: *a* — section with a mixed fracture mode; *b* — cleavage of intermetallic compound (shown by an arrow); *c* — tough fracture section; *d* — eutectics (shown by arrows)

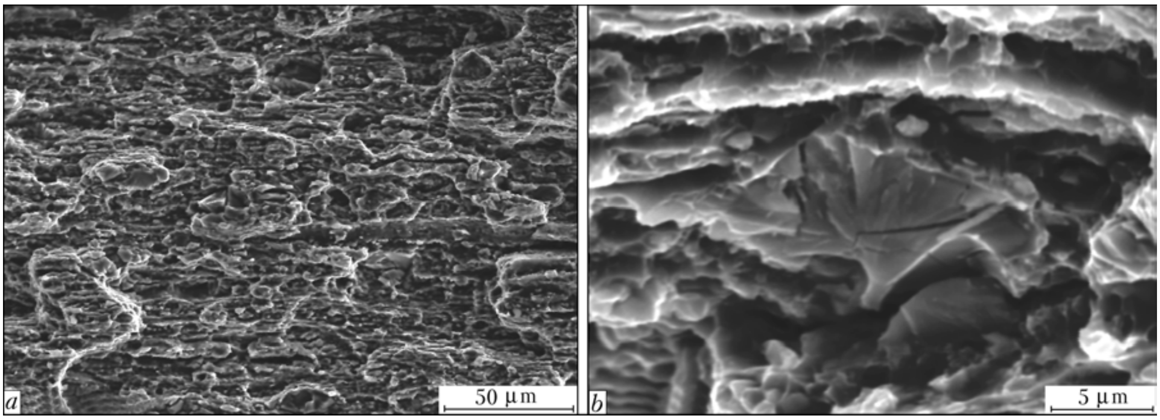

Figure 6. Fractograms of fracture surface of alloy V96tss in as-tempered conditions: *a* — section with mixed fracture mode; *b* — delamination section

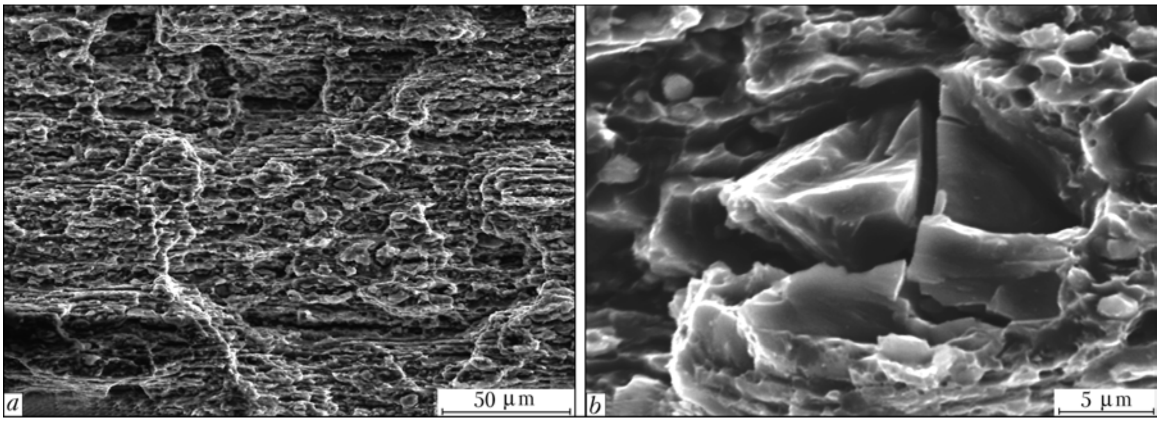

Figure 7. Fractograms of fracture surface of V96tss alloy in the condition of artificial ageing: *a* — section with a mixed fracture mode with delamination along the direction of rolling; *b* — section with cracking of a coarse intermetallic compound

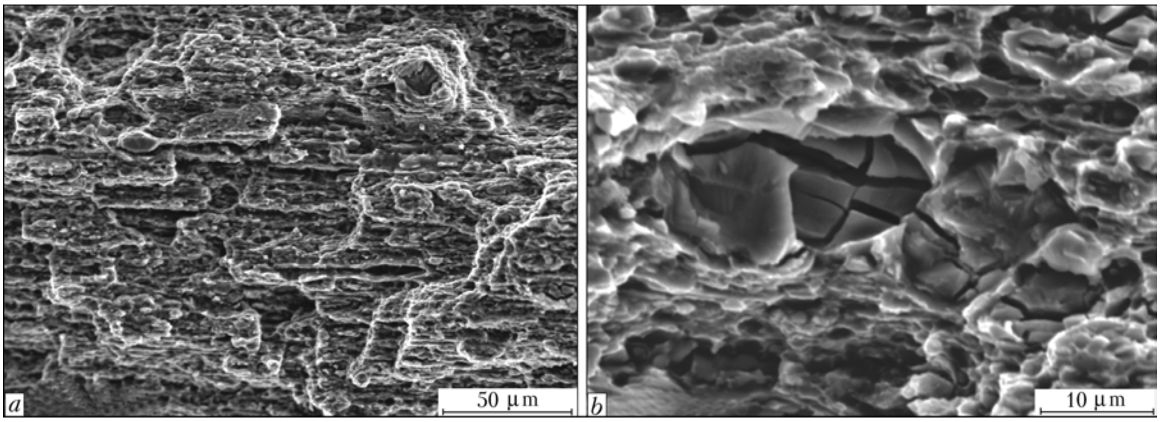

Figure 8. Fractograms of fracture surface of V96tss alloy in the initial condition: *a, b* — the same as in Figure 7

in the fracture, as well as sections formed by the tearing mechanism, is indicative of non-uniformity of mechanical properties of the structural components of V96tss alloy (Figure 8). A significant number of fine cracks on the inclusions confirms the fact that they initiated at the stage of the main crack propagation. Their growth occurred as the main crack front drew closer. Eutectic formations are observed on the boundaries between the grains near the primary inclusions of zirconium and scandium. Zirconium content in them is 2 times smaller than that of scandium.

CONCLUSIONS

1. Based on investigation of fractures of V96tss alloy, the method of fractographic analysis was used to determine the general regularities of initiation and propagation of cracks at off-center tension of samples after different conditions of welding heating.

2. Thermophysical conditions of heating accompanying the fusion welding process (TIG and EBW) have an essential influence on the capability of V96tss alloy to undergo plastic deformation near the brittle inclusion location, thus preventing crack initiation. Appearance of crack initiation sites is closely related to a change of the condition of intergranular space as a result of coarsening of intermetallic compounds, formation of low-melting eutectics, as well as increase of the dimensions and volume fraction of phases and inclusions. Metal overheating leads to development of inhomogeneity by the content of alloying elements and impurities, in connection with their segregation along the grain boundaries, formation of brittle intergranular interlayers of oversaturated phases, particularly on the fusion boundary, where the interlayers form a dense frame around the grains. The associated increase of the level of stress concentration facilitates crack initiation as a result of phase cracking or violation of the contact with the matrix, this lowering the strength and ductility values of V96tss alloy: σ_{fr} = = 211 MPa; K_c = 17.7 MPa$\sqrt{m}$; J_c = 1.1 J / cm^2; SWCP = 3.2 J / cm^2.

3. Development of the main crack in V96tss alloy proceeds predominantly as a result of tearing away of metal directed normal to load application. It is accompanied by cracking of phases containing alloying elements, and delamination of inclusions, having zirconium and scandium in their composition.

1. Elagin, V.I., Zakharov, V.V., Rostova, T.D. et al. (1993) Regularities of alloying of aluminium alloys with scandium. *Vestnik Know-How*, **2**, 62–66.
2. Zakharov, V.V., Rostova, T.D. (1996) Shear bands in aluminium alloys containing scandium and lithium. *Metallovedenie i Term. Obrab. Metallov*, **4**, 18--21.
3. Fridlyander, I.N. (2002) Aluminium alloys in flying vehicles during the periods of 1970–2000 and 2001–2015. *Tekhnologiya Lyog. Splavov*, **4**, 12--17.
4. Ishchenko, A.Ya., Labur, T.M. (1999) *Weldable aluminium alloys with scandium*. Kiev: MIIVTs.
5. Davydov, V.G. (1997) State-of-the-art of metals science and technological investigations of aluminium-lithium alloys. *Tekhnologiya Lyog. Splavov*, **5**, 15–25.
6. Kishkina, S.I. (1981) *Fracture resistance of aluminium alloys*. Moscow: Metallurgiya.
7. Gordeeva, T.A., Zhegina, I.P. (1978) *Analysis of fractures in evaluation of material reliability*. Moscow: Mashinostroenie.
8. (1989) *Strength calculations and testing in machine-building, classification of kinds of damage surfaces (fractures) of metals*. Moscow: Standart.
9. Romanov, O.N. (1981) Structural fracture mechanics — new prospective trend in the problem of metal fracture. *Fiziko-Khim. Mekhanika Materialov*, **4**, 28–32.
10. (1982) *Fractography and atlas of fractographs*: Refer. Book. Moscow: Metallurgiya.

FRICTION STIR WELDING AND SURFACING OF COPPER AND ITS ALLOYS

M.L. ZHADKEVICH[1], N.G. TRETYAK[1], P.M. KAVUNENKO[1], V.I. ZELENIN[1], V.A. MOKHORT[1] and **E.V. ZELENIN[2]**
[1]E.O. Paton Electric Welding Institute, NASU, Kiev, Ukraine
[2]NTUU «Kiev Polytechnic Institute», Kiev, Ukraine

Peculiarities of structure of welded and surfaced joints of the L60 brass and the M1 copper produced by friction stir welding were investigated. High quality of welds, absence of defects and inhomogeneities in the welding zone was noted. Technology for friction stir surfacing of copper by production of overlapped slot welds was developed.

Keywords: friction stir welding and surfacing, brass, copper, phase composition, copper mould

The friction stir welding (FSW) process, developed in 1991 in The Welding Institute (TWI) [1], allows performing butt, corner and overlap joints of sheet billets. The main parameter of the FSW process mode are welding speed (speed of the tool movement), rotational speed of the tool, pressure and movement forces of the tool, angle of the tool inclination, and its dimensions [2]. In addition, friction conditions, which depend upon used material of the tool and the material being welded, and stress of the billet material flow at the deformation temperature are taken into account.

Most widely this method is used for welding of aluminium and its alloys in ship building, railway transport, automotive industry, construction [2–4], and for connection of alloys, for example, copper containers for storage of nuclear waste [5, 6] or copper backings (a version of heat sinks) in the spraying equipment.

The authors developed on the FSW basis the technology for friction stir surfacing (FSS) of copper and its alloys. Scheme of this process is presented in Figure 1. The component being surfaced and filler materials in the form of a plate are fixed by means of clamps. A revolving working tool is brought in touch with the filler plate and gradually immerses into it so far as it will go into shoulder of the tool. Due to friction of the tool on surface of the filler plate and the billet being surfaced heat, necessary for transition into plastic state of the filler material and of a portion of the component metal, is released. Due to movement of the tool production of the slot weld is ensured. Sequential making of such overlapping welds allows depositing filler material on a component.

Welding and surfacing experiments were carried out with application of plates from the M1 copper (GOST 859–78) of 5 and 20 mm thickness and the L60 brass (GOST 15527–70) of 6 mm thickness. Welding and surfacing were performed on a specially equipped milling machine with 10 kW power of the drive (Figure 2).

FSW and FSS processes were performed at a speed of the spindle rotation 900–1250 rpm and speed of the tool movement 50 / 70 mm / min. Working tool, made from the tungsten-based refractory material, had relatively simple constructive shape (diameter of the shoulder was 25 mm). Angle of inclination of the tool to surface of the billet being welded or surfaced was 2–3°. In case of surfacing of the billet of 20 mm thickness a plate of 5 mm thickness was used as a filler material.

Macro- and microstructures of the specimen cross section metal were first investigated using the MBS-10 microscope. The specimens were ground, polished, and then within 60 s they were subjected to etching in a special solution, consisting of 10 g of orthophosphoric acid, 0.3–0.4 g of chromium anhydrite, and two drops of hydrogen peroxide. Microstructure and chemical composition of the metal were investigated using the PEMMA-101A scanning electronic microscope-microanalyser. Hardness *HRB* was determined according

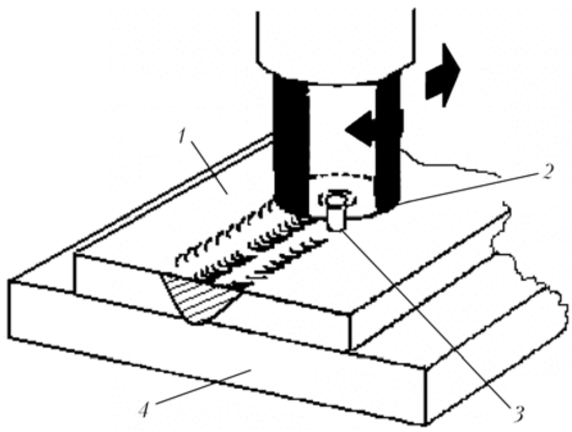

Figure 1. Scheme of FSS process: *1* — filler material; *2* — shoulder; *3* — pin of special profile; *4* — copper billet

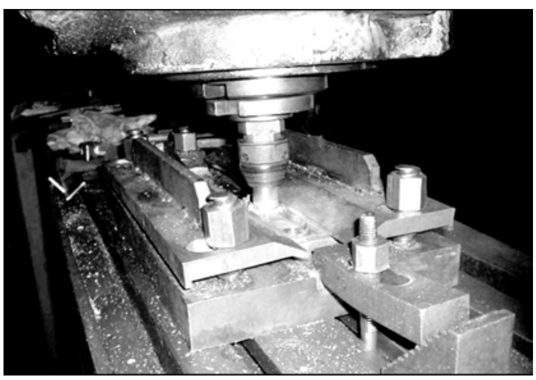

Figure 2. Laboratory installation for FSW and FSS

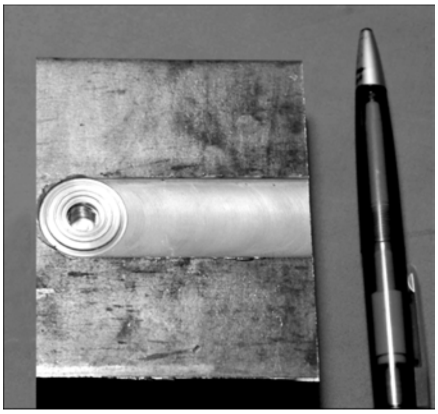

Figure 3. Exposed surface of L6 brass joint produced by FSW

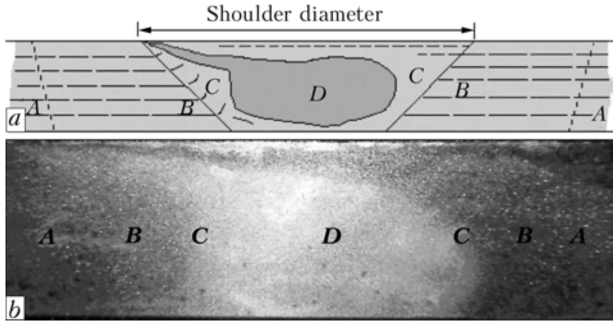

Figure 4. Scheme of arrangement of structural zones in FSW (*a*) [8] and macrostructure of brass joint (*b* — ×5): *A* — base metal; *B* — HAZ; *C* — thermo-mechanically affected zone; *D* — dynamic recrystallization (nugget) (×5)

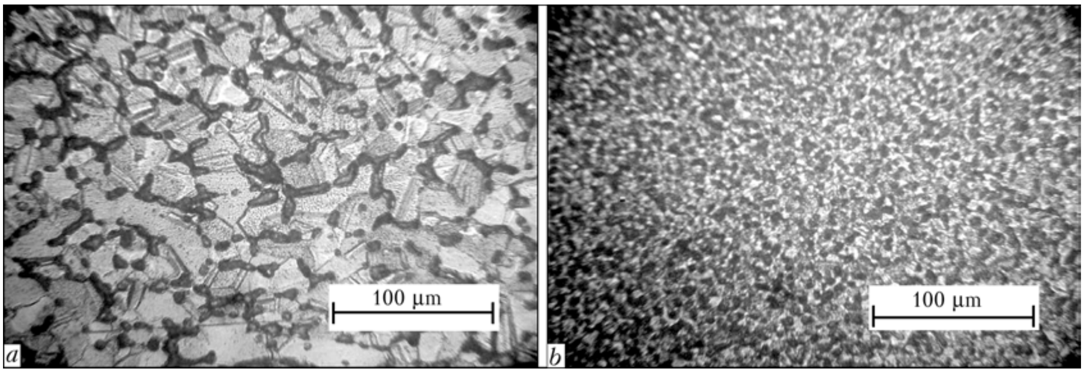

Figure 5. Microstructure of base metal (L6 brass) (*a*) and metal in weld nugget zone (*b*)

to the standard methodology, and phase composition — using diffractometric method.

Appearance of the produced joint is shown in Figure 3. One can see in the Figure that exposed surface of the weld is smooth with traces of the shoulder. Analysis of the joint sections showed absence of defects in the form of pores, cracks, and discontinuity flaws.

In Figure 4 distribution of different structural zones in the weld section is shown [7].

Metallographic analysis showed that main changes of the structure occurred in zones *C* and *D*, where mainly occurs stirring of the metal in welding. Size of the grain in center of the weld (in the nugget zone) significantly differs from grain size of the base metal. In Figure 5, *a* microstructure of the base metal, consisting of two $\alpha + \beta_{II}$ phases with mean size of the grain 50–60 μm, is shown, and in Figure 5, *b* — microstructure of the recrystallization zone metal of a welded brass specimen, grains in which were refined down to 5–7 μm is presented, whereby in the nugget zone changes of chemical composition do not occur, which is confirmed by the X-ray microspectral analysis.

Change of hardness depending upon distance from the weld center within its cross section is shown in Figure 6. Hardness of the stir zone metal is by *HRB* 10–12 higher than that of the base metal.

Results of chemical and X-ray microspectral analysis of the base and weld metals, presented in Figure 7, prove presence of the same structural zones, consisting of $\alpha + \beta_{II}$ phases, and absence of changes in chemical composition of the weld metal in comparison with the base metal.

The latter confirms good prospects of using FSW method for joining copper alloys, containing easily evaporating elements. So, it is noted in [8] that in fusion welding of brass evaporation of zinc occurs, which not just significantly changes chemical composition of the weld metal and mechanical properties thereof, but can also cause formation of big number of pores, which negatively effect strength characteristics of the weld. This limits application of welded joints at high temperature gradients and mechanical loads.

In the course of FSS of copper and its alloys possibility of production of the high-quality surface layer without presence of defects and inhomogeneities in the stir zone (Figure 8) was established, where due to dynamic recrystallization the metal had grain of a smaller size in comparison with the base metal that caused in its turn improvement of service characteristics of the deposited material.

Metallographic analysis of specimens, cut out from surfaced metal billets, showed that size of the grains in the stir zone significantly differs from size of the base metal grain. It is established that during stirring significant (5–10 times) refining of the grain occurs, the structural zones being the same (Figure 9).

In case of performance of FSS on copper specimens significant change of the deposited metal hardness did

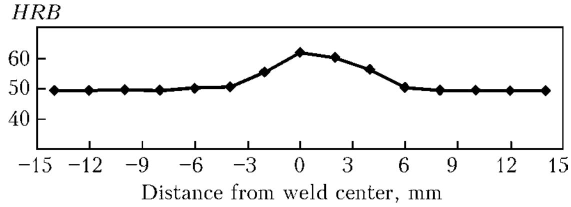

Figure 6. Distribution of hardness in L60 brass joint of 6 mm thickness produced by FSW

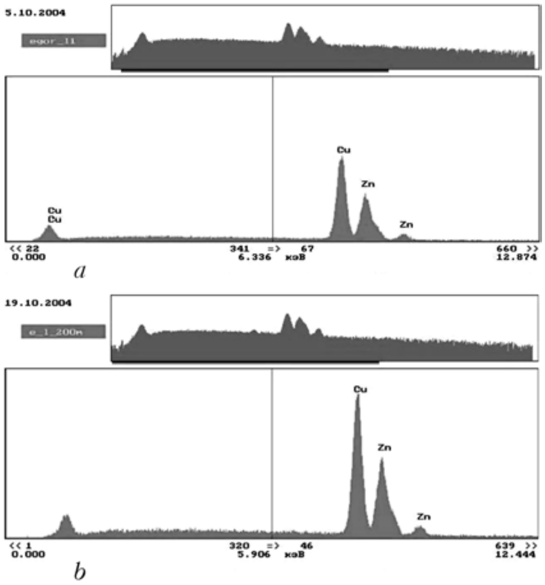

Figure 7. Energy spectrum of elements in base L60 brass (*a*) and nugget zone (*b*)

Figure 8. Metal macrostructure of deposited layer of M1 copper (×5)

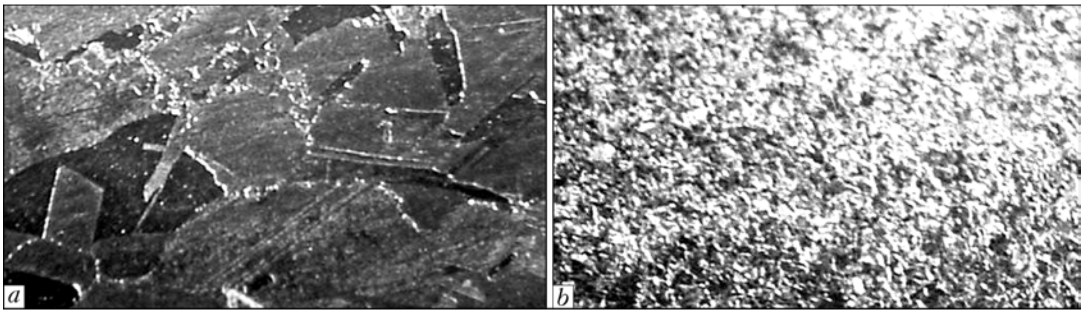

Figure 9. Microstructure of base metal (*a*) and deposited layer of M1 copper (*b*) (×5)

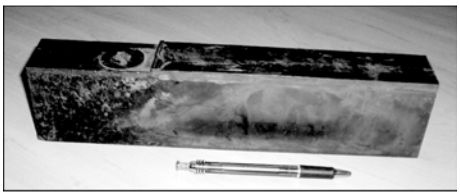

Figure 10. Appearance of surfaced fragment of copper mould plate of machine for continuous casting of steel

not occur. Hardness of the stir zone metal was by 10 % higher than that of the base metal. Deformations, caused by welding stresses, were absent. Chemical analysis results of the deposited layer and base metals confirmed identity of their chemical composition and absence of oxide inclusions in the surfacing zone.

On the basis of carried out experiments, designed for restoration of initial dimensions, specimens from the copper mould plate of machines for continuous casting of steel were surfaced (Figure 10). For implementation of mentioned surfacing technology on commercial scale a design of the head for FSW and FSS was developed, which can be used in composition of serial portal metal-removal machine tools, whereby thickness of the billets being welded or the deposited layer may achieve 20–30 mm.

CONCLUSIONS

1. In FSW of the L60 brass quality welds without presence of defects and change of chemical composition in the stir zone were produced, whereby the weld metal hardness increased by 15–20 % in comparison with the base metal.

2. Principally new technology for FSS of copper was developed by producing overlapped slot welds.

3. Fragments of the copper mould plate of the machine for continuous casting of steel were surfaced, and design of the head for implementation of the commercial FSS technology was developed.

1. Thomas, W.M., Nicholas, E.D., Needham, J.C. et al. *Improvements relating to friction welding*. EU 0615480B1. Publ. 1995.
2. Midling, O.T., Hval, M., Johansen, H.G. et al. (1998) Process optimization of friction stir welding in fabrication of aluminium ship panel. In: *Proc. of 3rd Int. Forum on Aluminium Ships* (Haugesund, May 27–28, 1998), 2–10.
3. Kawasaki, T., Makino, T., Todori, S. et al. (2000) Application of friction stir welding to the manufacturing of the next generation «A-train» type rolling stock. In: *Proc. of 2nd Int. Symp. on FSW* (Gothemburg, Sweden, June, 2000), 26–28.
4. Johnsen, M.R. (1999) Friction stir welding takes off at Boeing. *Welding J.*, Febr., 35–39.
5. Cederqvist, L. (2005) A weld that lasts for 100,000 years. *Svetsaren*, 60(**2**), 31–33.
6. Okamoto, K., Hirano, S., Doi, M. et al. (2002) Fabrication of backing plate of copper alloy by friction stir welding. J. JWS, **70**, 192–193.
7. Threadgill, P. (1997) Friction stir welds in aluminium alloys — preliminary microstructural assessment. *TWI Bulletin*, March / April, 30–33.
8. Abramovich, V.P., Dementsevich, V.P., Efimov, L.A. (1988) *Fusion welding of copper and alloys on its base*. Leningrad: Mashinostroenie.

FRICTION STIR WELDING OF ALUMINIUM ALLOYS (Review)

A.Ya. ISHCHENKO, S.V. PODIELNIKOV and **A.G. POKLYATSKY**
E.O. Paton Electric Welding Institute, NASU, Kiev, Ukraine

The state-of-the-art of friction stir welding, working tool designs, joint types when this welding process is used, features of formation of joints of different aluminium alloys and their properties are considered. The main applications of friction stir welding are described.

Keywords: friction stir welding, aluminium alloys, welding tool, welded joint structure, weld properties, applications, welded structures

Method of friction stir welding (FSW) was developed by The Welding Institute (TWI) in 1991 [1]. Intensive study of this process in order to improve the technology and develop new equipment led to its effective application in manufacture of high technology products in such industries as carriage-, ship-, aircraft construction and many others. FSW belonging to the processes of solid-state joining of materials is devoid of the drawbacks inherent to the processes of welding with metal melting. Investigators of this process believe that if 10 % of the total volume of welded joints in the USA is replaced by FSW, hot house gas emissions will be reduced by 500 mln pounds per year. The estimated cost effectiveness for US industry from FSW introduction into industrial production is equal to 4.9 bln USD per year [2].

The essence of the process consists in the following (Figure 1). A tool in the form of a rod consisting of two main parts: shoulder or lip (thickening) and tip (protruding part) is used for welding. Dimensions of these structural elements are selected depending on the thickness and material of the parts being welded. The tip length is set to be approximately equal to that of the part to be welded. Shoulder diameter can vary from 1.2 to 25 mm. The tool rotating at a high speed in the butt area is brought into contact with the blank surface so that the tip is introduced into the blanks to the depth approximately equal to their thickness, and the shoulder touches their surface. After that the tool moves along the joint line at the speed of welding. Friction results in the metal heating right up to plastic condition, its stirring by the rotating tool and driving it into the vacant space behind the tool moving along the butt. The volume, in which the weld forms, is limited by the tool shoulder from above. After the end of welding, the rotating tool is removed from the butt beyond the blank. In view of the asymmetry of weld structure in the cross-section of welded joints made by FSW, a distinction is made between the on-coming side, where the direction of the tool rotation coincides with that of welding and opposite side — that of retraction.

FSW is mainly applied for joining materials with a comparatively low melting temperature, primarily aluminium [3] and magnesium [4] alloys. Successful welding by this process of copper [5], nickel and titanium alloys [2], as well as steels [6] has been performed. FSW is used to weld aluminium alloys up to 75 mm thick in one pass [7]. FSW allows producing overlap joints of aluminium sheets of the thickness from 0.2 mm [8]. Welding speed of 6082 alloy 5 mm thick can be up to 6 m / min [9].

The main parameters of FSW process are welding speed, tool rotation frequency, force of tool clamping and displacement, angle of tool inclination, and its dimensions.

The clamping and displacement forces depend on the type of material being welded, its thickness and welding speed. Welding of samples of 7010-T7651 alloy 6.35 mm thick at welding speed variation in the range from 59 to 159 mm / min and tool rotation speed from 180 to 660 rpm showed that at increase of the rotation speed the heat input into the metal increases, and the welded joint forms a microstructure with more uniform grains [10]. The strength and ductility properties are also improved up to a certain limit. At increase of welding speed it is necessary to increase the tool rotation speed to achieve optimum conditions. However, for a complete absence of defects, as well as ensuring all the required properties, reliability and adaptability-to-fabrication it is necessary to strictly select the modes, the most suitable for particular products.

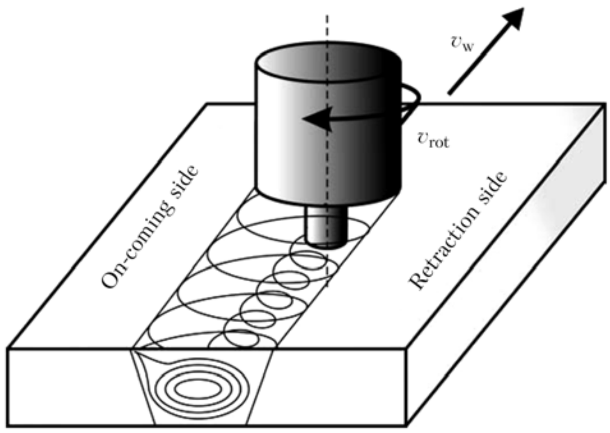

Figure 1. Schematic of FSW process

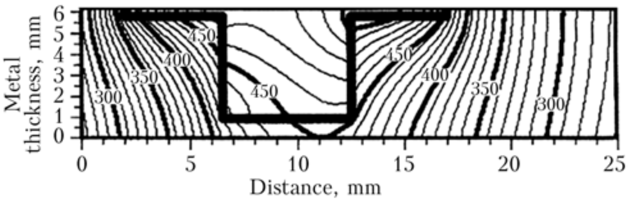

Figure 2. Temperature distribution in the sample longitudinal direction

Most of the researchers mention the following FSW advantages, compared to other methods of producing permanent joints [11, 12]:

- preservation of base metal properties to a considerable extent in the welding zone compared to fusion welding processes;
- absence of harmful evolutions and ultraviolet radiation during welding;
- ability to produce sound welds on alloys, which are prone to formation of hot cracks and porosity in fusion welding;
- no need to use filler material or shielding gas, remove surface oxides on the edges before welding, as well as slag and spatter after welding;
- absence of alloying element losses in the weld metal.

Levels of Cr, Cu, Mn, Cr^{+6} precipitations at FSW of steels, as reported by Rockwell Scientific, USA, are much lower (< 0.03, < 0.03, < 0.02 and < 0.01 mg / mm^3, respectively) than in argon-arc welding (0.25, 0.11, 1.88 and 0.02 mg / mm^3, respectively) [2]. Comparison of production costs when using FSW and consumable-electrode welding (MIG) showed that the initial capital investment at FSW is higher but with increase of production volumes FSW application becomes more cost-effective than arc welding [11].

Judging from TWI experimental data, the maximum temperature at FSW is equal to about 70 % of the melting temperature, and is not more than 550 °C for aluminium. Heat input at FSW is lower than in argon-arc welding by approximately 2 times, and for 6N01-T5 alloy 4 mm thick it is equal to 190 and 390 J / mm, respectively (welding speed of 500 mm / min) [13]. In [14] temperature distribution in the plate being welded was plotted using mathematical simulation of thermal processes at FSW (Figure 2). A lower temperature of the metal in the joint zone at FSW compared to MIG welding accounts for a lower level of angular deformations in the welded joint. At FSW the angular deformation is equal to 1 / 5–1 / 7 of its values at MIG welding [12] (Figure 3).

It is assumed that at FSW the residual stresses in the metal are low owing to a low level of metal heating

Figure 3. Comparison of angular deformation at FSW (lower sample) and MIG welding (aluminium alloy of 6000 series, 2 mm thickness)

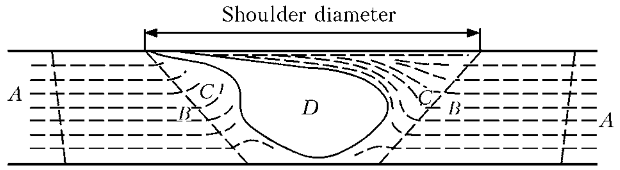

Figure 4. Schematic of the zones of butt joint made by FSW (for designations see the text)

temperatures. A rigid restraint applies high limitations to plate deformation, which prevents metal shrinkage at cooling of the dynamic recrystallisation zone and HAZ in the longitudinal and transverse directions, leading to transverse and longitudinal residual stresses. At FSW of 2024-T3 and 6013-T6 alloys it is found that the longitudinal residual stresses are higher than the transverse residual stresses (welding speed was equal to 300–1000 mm / min, tool rotation speed was 1000–2500 rpm). High tensile stresses are observed predominantly in the HAZ metal. At lowering of welding speed and tool rotation speed the residual stresses are decreased. Maximum values of longitudinal tensile stresses reach 30–60 % of the welded joint yield limit and 20–50 % of the base metal yield limit [15].

Macrostructure of welded joints at FSW has features, not characteristic of welds produced by fusion welding processes. Formation of a nugget in the joint center with oval concentric rings differing in their structure is typical for FSW [16]. Adjacent to the nugget is a complex profile which is characteristic for the weld upper part. Presence of oval rings is due to the features of metal stirring by the tool tip. In the welded joint at FSW four zones are singled out, which are schematically presented in Figure 4. Directly adjacent to zone *A* (base metal) is zone *B*, where the blank metal remains undeformed and changes its structure only under the impact of heating (HAZ). Zone *C*, where the metal is subjected to considerable plastic deformations and heating, is called the zone of thermomechanical influence. Zone *D* is the joint nugget, where dynamic recrystallization proceeds. Metal hardness decreases in the direction from the base metal to weld center, and the minimum value is reached in the HAZ metal (Figure 5). Hardness lowering in the HAZ metal occurs as a result of over-ageing, decrease of dislocation density or due to both of these mechanisms.

The high level of mechanical properties of welded joints is reported by many researchers. At FSW in welded joint of 6082-T6 alloy σ_t = 245 MPa, whereas in the base metal σ_t = 317 MPa. For 6082-T4 aged after welding σ_t = 308–310 MPa. Fatigue testing reveals a higher level of mechanical properties of the joints at FSW, compared to similar ones in argon-arc welding [18].

Authors of [19] studied the mechanical properties of joints produced by FSW of 5083 alloy at cryogenic temperatures, which was of interest at preparation of fabrication of tanks for liquefied hydrogen. Samples of 30 mm thickness were welded at the speed of 40 mm / min. Studies at 77 K in liquid nitrogen, at 20 K in liquid hydrogen and 4 K in liquid helium

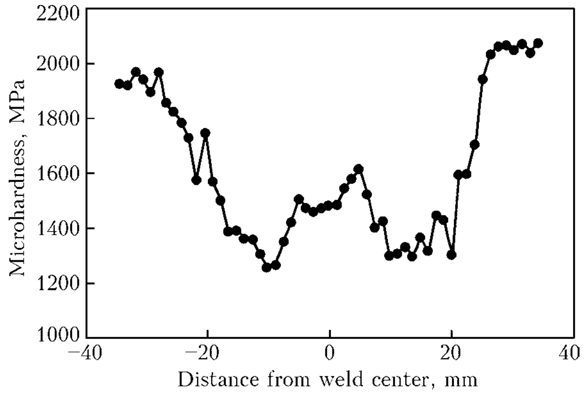

Figure 5. Hardness distribution in the zone of welded joint of 7075-T735 alloy [17]

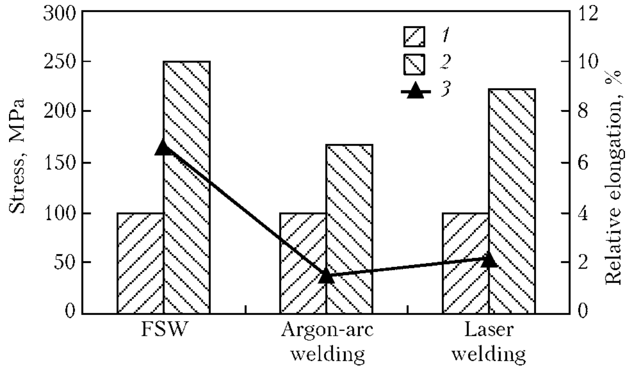

Figure 6. Mechanical properties of welded joint made by different welding processes: *1* — yield limit; *2* — ultimate strength; *3* — relative elongation

showed that the level of joint properties at FSW is higher than in argon-arc welding.

The authors of [20] studied the problems of FSW of casting aluminium alloys. In industrial production casting alloys often have to be welded to billets produced by extrusion. ADC1 and A6061-T6 alloys 4 mm thick were used. Results obtained at FSW were compared with similar ones in argon-arc and laser welding. As is seen from Figure 6, FSW ensures better properties of joints. Ultimate strength is equal to 80 % of A6061-T6 strength. In bend testing fracture at FSW runs through the base metal. Positive results of FSW of dissimilar alloys, as well as aluminium alloys to steels, are reported in work [21]. At FSW of steel SS400 and alloy A5083 2 mm thick the ultimate strength corresponded to 240 MPa, which is equal to 86 % of aluminium alloy strength.

As a disadvantage of FSW process, the authors of [2, 12] note formation of a hole at the end of the weld, equal to tip diameter, which requires taking the weld beyond the working section of the blank, or filling the hole after welding using other methods, such as friction welding-in of special plugs.

Improvement of the technology and equipment allows overcoming the existing drawbacks, as well as widening the fields of application of the process. Although FSW is applied mainly for butt and overlap welds, fillet, tee, and spot welds can be also made.

Spot FSW can be realized by two methods. The first is immersion spot welding patented by Mazda, Japan, in 2003. Here the rotating tool is immersed into a part, bringing the metal in the joint zone into a plastic state with subsequent stirring under the shoulder. After that the tool is lifted leaving a characteristic depression in the part. The second method is spot FSW with weld filling patented by GKSS in 2002 [2]. For this method a tool is used, in which the tip and shoulder have separate drive systems. The rotating tool is lowered into a part, the tip presses out and stirs the metal under it, and after that it is removed. The metal under the shoulder fills the depression, and thus a weld without a hole is produced (Figure 7).

Welding tool is usually made from tool steels H13 (AISI), SKD 61, SKD 11, SKH 57 (JIS) and stainless martensite steel SUS 440C (JIS). In this case it is possible to use composite tools, in which the tip is made from cobalt alloy MP159, and the shoulder — from H13 [22]. For FSW of steels up to 0.5 thick MegaStir developed a tool from polycrystalline cubic boron nitride. Its fracture resistance is higher and allows giving the tip a shape required for a favourable flowing of the metal in welding zone (Figure 8). The tool is placed at a small angle of 2–3° relative to the part surface [16, 23], this providing the highest quality values.

The tool simultaneously having the same role as the substrate of blanks being joined is shown in Figure 9 [24]. NASA is developing a self-regulating tool, in which the tip length is determined by forces acting on it. At deviation of the load on the tip from the specified value, automatic correction of its length occurs, this allowing welding of blanks of a variable cross-section and avoiding formation of a hole when making circumferential welds.

For welding aluminium alloys of a considerable thickness tool families Whorl^{TM} (Figure 10) and Triflute^{TM} [25] were developed, which allow performance of single-pass welding of aluminium alloys 50 mm thick. New variants of FSW are Re-Stir^{TM}, Skew-Stir^{TM}, and Com-Stir^{TM} technologies [26]. Re-Stir^{TM} technology with variable rotation of the tool clockwise and counterclockwise allows eliminating weld asymmetry characteristic of the traditional FSW. In Skew-Stir^{TM} technology the tool is slightly inclined relative to the machine spindle so that the point of intersection of the axes of the spindle and tool, which was called the focal point, can be located above, under or in the blank being welded, depending on the material properties and mode parameters. Such a feature allows

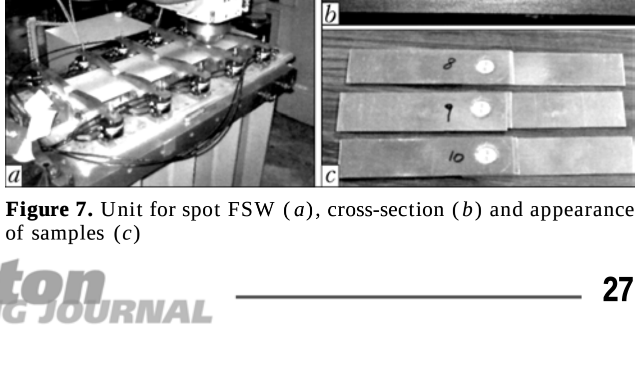

Figure 7. Unit for spot FSW (*a*), cross-section (*b*) and appearance of samples (*c*)

Figure 8. Appearance of the tool from polycrystalline cubic boron nitride [2]

producing a wider weld at tool rotation during welding. A-Skew^{TM} and Flare-Triflute^{TM} tools ensure formation of stronger overlap joints. A feature of Com-Stir^{TM} technology consists in combining the rotational and orbital motions of the tool during welding.

This results in wider welds, which is used mainly when joining dissimilar materials. A system has been developed with two parallel tools Twin-Stir^{TM} [27].

Development of advanced FSW technologies is going on. At the University of Missouri (Columbia, USA) development of FSW with concurrent heating at current passage through the tool tip is performed. The Center of Processing and Joining Advanced Materials, USA is developing FSW with induction preheating of material, which will allow increasing the welding speed, lowering the forces acting on the tool, and reducing its wear [2]. In work [28] the possibility of laser application for metal preheating at FSW of magnesium alloys was studied.

Owing to a small number of factors, influencing the FSW process, and sufficiently simple equipment design, this process is ideally suited for automation and robotisation [29]. Tricept 805 unit allows welding of aluminium of up to 10 mm thickness.

FSW is already widely used in manufacture of various high-tech products. General Dynamics Land Systems and Edison Welding Institute performed joint work, the purpose of which consists in ensuring the required ballistic characteristics of joints of armor plates from aluminium alloy 2195-T87 for sea armour

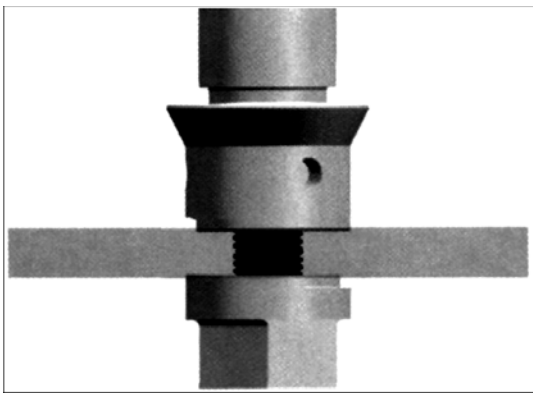

Figure 9. Bobbin Tool design

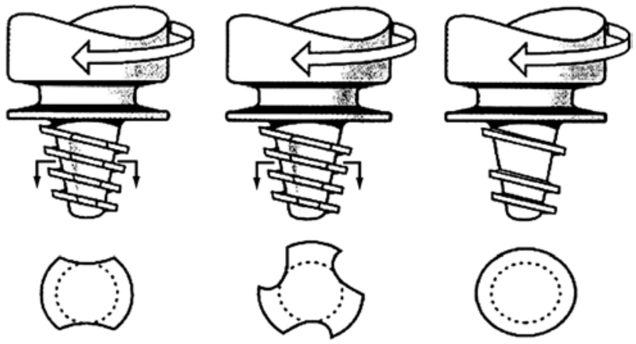

Figure10. Schematics of design variants of Whorl^{TM} tool

vehicles. Welding of plates of 31.8 mm thickness by FSW instead of argon-arc welding allowed achieving more acceptable strength properties of the joints and more ductile welds (2 to 3 times). As a result the welded joints (including fillet joints) have successfully passed ballistic testing [22].

To prevent deterioration of properties of superconducting niobium-titanium wire, it should be joined to a rigid element from pure aluminium at the temperature below 400 °C. This was earlier done by soldering, but soldered joints had a low strength. FSW ensured the required properties of the welded joint in liquid helium [12].

Starting from 2003, Ford Motor Co., USA, manufactured several thousand Ford GT cars, in which FSW is used for welding the central section. It accommodates a fuel tank isolated from the inner section [2]. FSW improves the accuracy of dimensions and by 30 % increases the strength of the joints compared to similar components in gas-shielded arc welding. In [30] the process of manufacturing the body of Mazda RX-8 car by spot friction welding is described (Figure 11). In 2003 more than 100,000 cars were manufactured, the doors of which were made using spot FSW [7]. Successful application of this process allows the company to plan making such joints on a new generation of cars of MX-5 model.

FSW process is actively studied in the aerospace industry (Figure 12) [24]. In 2001 this process was introduced into production of the external tank of a carrier-rocket for reusable space vehicles. The technology envisages welding eight longitudinal welds on

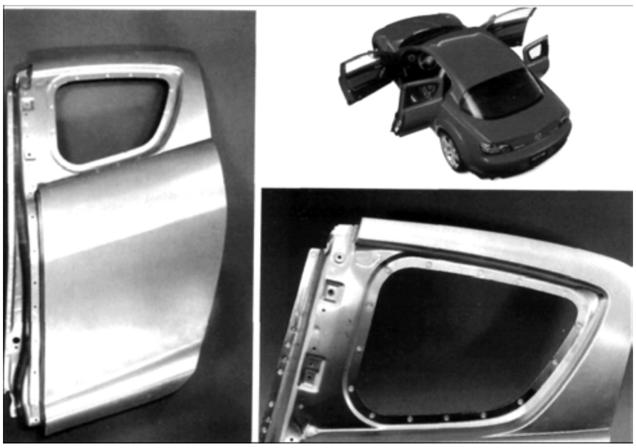

Figure 11. Joints made in Mazda RX-8 car using spot FSW [2]

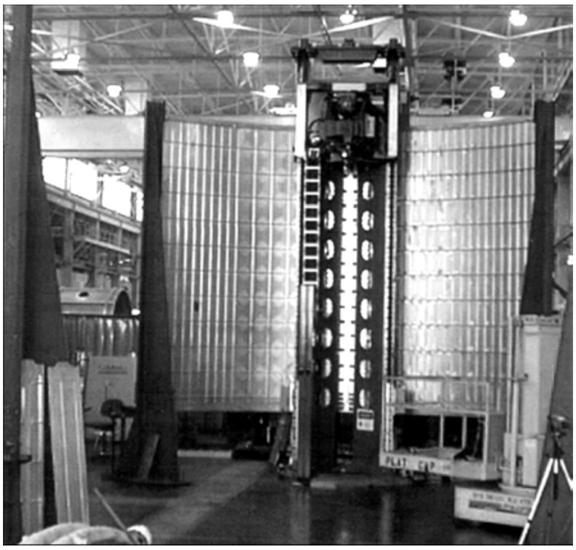

Figure 12. Equipment for FSW in the vertical position

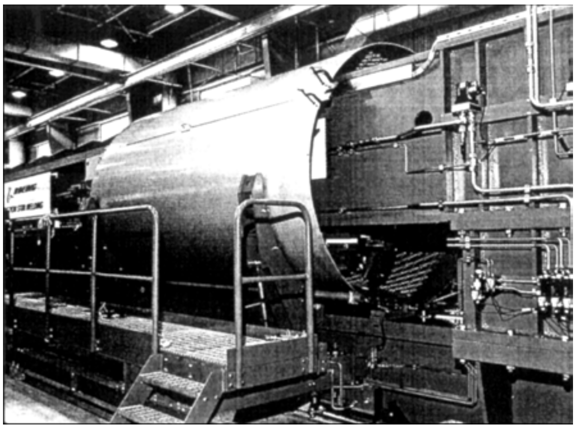

Figure 13. Unit for FSW of a fuel tank of Delta rocket in Boeing plant

a tank of 2195 alloy for liquid hydrogen and four longitudinal welds on a tank for liquid oxygen, which is equal approximately to 1 / 2 mile of welds on each tank. Equipment for repair FSW in the vacuum of space is being developed. The concept of FSW application is based on that the high speed of tool rotation (3000 rpm) allows reducing the forces required for welding performance.

Boeing Company started using FSW in manufacture of Delta II and III rockets (Figure 13) [31]. Welding is performed on a fuel tank 8.4 m long, a liquid oxygen tank 12 m long and on other structures. FSW ensures an increase of the quality (one defect per 76.2 m of weld) compared to argon-arc welding (one defect per 8.4 m of weld), shortening of the time required for the welded structure fabrication. Production of Delta II rockets rose from 8 to 17 pcs per year.

Study [32] reports on the work on FSW of finned panels for an aircraft wing from alloys 2024, 7475, and 7050 4 mm thick. The high quality of the joints is ensured when using FSW on Airbus A350 and two new versions of A340 (A340-500, and A340-600) [2]. Eclipse Aviation is finishing certification of a business-class jet plane Eclipse 500 with components made by FSW (Figure 14).

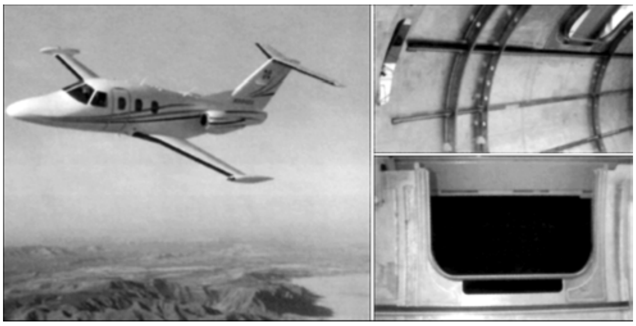

Figure 14. Eclipse 500 aircraft with components made by FSW

Thus, the presented review is indicative of the fact that FSW is successfully developing and finding application in different industries. Most of the publications are devoted to welding of aluminium alloys of medium and comparatively large thickness. It should be noted that difficulties usually arise when joining blanks 0.5–3.0 mm, as well as more than 40 mm thick.

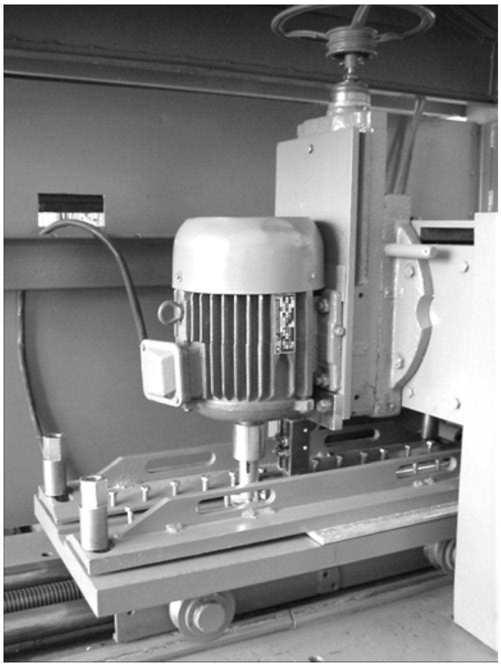

Figure 15. Appearance of an experimental unit for FSW of sheet (1.8–2.5 mm) aluminium alloys

Mechanical properties of aluminium alloy joints made by FSW

Aluminium alloy	σ_t, MPa	α, deg
AMg6	343	180
1420	362	96
1201	294	180
1460	325	180

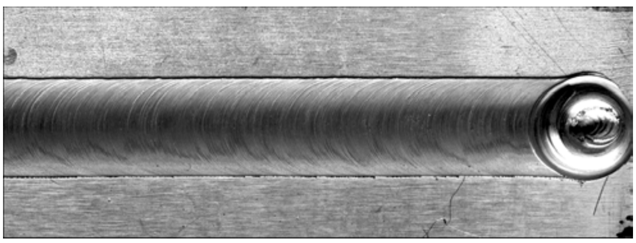

Figure 16. Appearance of a weld produced by FSW (aluminium alloy AMg6 2 mm thick)

In this connection, as well as in view of the arising complications, when ensuring the accuracy of assembly of thin-walled blanks for welding, PWI conducted studies of FSW process on a special experimental unit (Figure 15). The work was performed on aluminium alloys AMg6, 1201, 1460 of 1.8–2.5 mm thickness. Figure 16 gives the appearance of AMg6 alloy welded joint produced by FSW process. Effectiveness of welding tools with different profiles of the working part was verified simultaneously. It is established that with this welding process the joints feature a high level of mechanical properties –– strength factor of welded joints is equal to 0.7–0.9 % of that of the base metal (Table).

1. Thomas, W.M., Nicholas, E.D., Needham, J.C. et al. *Friction stir butt welding*. Pat. 5460317 US. Publ. 1995.
2. Arbegast, W.J. (2006) Friction stir welding. After a decade of development. *Welding J.*, 85(**3**), 28–35.
3. Ito, T, Motohashi, Y., Goloborodko, A. et al. (2005) Microstructures and room temperature mechanical properties in friction-stir-welded joints of 7075 aluminum alloys. *J. JWS*, 74(**3**), 9--13.
4. Aritoshi, M. (2005) Friction stir welding of magnesium alloys sheets. *Ibid.*, 74(**3**), 18–23.
5. Nakata, K. (2005) Friction stir welding of copper and copper alloys. *Ibid.*, 74(**3**), 14–17.
6. Klingensmith, S., Dupont, J.N., Marder, A.R. (2005) Microstructural characterization of a double-sided friction stir weld on a superaustenitic stainless steel. *Welding J.*, **5**, 77–85.
7. Martin, J. (2006) Pushing the boundaries — friction stir goes deeper than before. *TWI Connect.*, Jan. / Febr., 1.
8. Teh, N.J. (2006) Small joints make a big difference. *Ibid.*, 143(**3**), 25--29.
9. Ericsson, L.G., Larsson, P. (2003) Rotary friction welding — researches and new applications. *Tekhnologiya Mashinostroeniya*, **6**, 81–84.
10. Hassan, A.A., Prangnell, P.B., Norman, A.F. et al. (2003) Effect of welding parameters on nugget zone microstructure and properties in high strength aluminium alloy friction stir welds. *Sci. Technol. Weld. Joining*, 8(**4**), 257–268.
11. Defalco, J. (2006) Friction stir welding vs. fusion welding. *Welding J.*, 85(**3**), 42--44.
12. Okamura, H., Aota, K., Ezumi, M. (2000) Friction stir welding of aluminum alloy and application to structure. *J. JILM*, 50(**4**), 166–172.
13. Aota, K., Okamura, H., Masakuni, E. et al. (2001) Heat inputs and mechanical properties of friction stir welding. In: *Proc. of 3rd Int. Friction Stir Welding Symp.* (Kobe, Japan, 27–28 Sept., 2001).
14. Lambrakos, S.G., Fonda, R.W., Milewski, J.O. et al. (2003) Analysis of friction stir welds using thermocouple measurements. *Sci. Technol. Weld. Joining*, 8(**5**), 385–390.
15. Dalle Donne, C., Lima, E., Wegener, J. et al. (2001) Investigation on residual stresses in friction stir welds. In: *Proc. of 3rd Int. Friction Stir Welding Symp.* (Kobe, Japan, 27–28 Sept., 2001).
16. Volpone, M., Mueller, S.M. (2005) Friction stir welding (FSW): le ragione di un successo. *Rivista Italiana della Saldatura*, **1**, 23–30.
17. Chao, Y.P., Wang, Y., Miller K.W. (2001) Effect of friction stir welding on dynamic properties of AA2024-T3 and AA7075-T7351. *Welding J.*, **8**, 196–200.
18. Ericsson, M., Sandstorm, R. (2003) Influence of welding speed on the fatigue of friction stir welds, and comparison with MIG and TIG. *Int. J. of Fatigue*, **25**, 1379–1387.
19. Hayashi, M., Oyama, K., Eguchi, H. et al. (2001) Mechanical properties of friction stir welded 5083 aluminum alloy at cryogenic temperatures. In: *Proc. of 3rd Int. Friction Stir Welding Symp.* (Kobe, Japan, 27–28 Sept., 2001).
20. Nagano, Y., Jogan, S., Hashimoto, T. (2001) Mechanical properties of aluminum die casting joined by FSW. *Ibid.*
21. Kimapong, K., Watanabe, T. (2004) Friction stir welding of aluminum alloy to steel. *Welding J.*, **10**, 277--282.
22. Colligan, K.J., Konkol, P.J., Fisher, J.J. et al. (2003) Friction stir welding demonstrated for combat vehicle construction. *Ibid.*, **3**, 34–40.
23. Shibayanagi, T., Maeda, M. (2004) Characteristics of microstructure and hardness in friction stir welded 7075 aluminum alloy joints. *Transact. of JWRI*, 33(**1**), 17–23.
24. Ding, J., Carter, R., Lawless, K. et al. (2006) Friction stir welding flies high at NASA. *Ibid.*, **3**, 54–59.
25. Dolby, R.E., Johnson, K.J., Thomas, W.M. (2004) The joining of aluminium extrusions. *La Metallurgia Italiana*, **3**, 25--30.
26. Pekkari, B. (2004) The future of welding and joining. *Svetsaren*, **1**, 53–59.
27. Thomas, W., Staines, D. (2006) Better joints using two contra-rotating FSW tools. *TWI Connect.*, May / June, 7.
28. Kohn, G., Greenberg, Y., Makover, I. et al. (2002) Laser-assisted friction stir welding. *Welding J.*, **2**, 46--48.
29. Cook, G.E., Smartt, H.B., Mitchell, J.E. et al. (2003) Controlling robotic friction stir welding. *Ibid.*, **6**, 28–34.
30. Kato, K., Sakano, R. (2004) Development of spot friction welding and application for automobile body. *J. Light Metal Welding & Construction*, 42(**11**), 8–13.
31. Imuta, M., Kamimuki, K. (2004) Development and application of friction stir welding for aerospace industry. In: *Proc. of the IIW Int. Conf. on Technical Trends and Future Prospectives of Welding Technology for Transportation, Land, Sea, Air and Space* (Osaka, Japan, 15–16 July, 2004), 53–64.
32. Kumagai, M. (2003) Application of FSW for aircraft. *Welding Technology*, 51(**5**), 74–78.

EXTENSION OF SERVICE LIFE OF METAL STRUCTURES FROM LOW-ALLOY STEELS BY HIGH-FREQUENCY MECHANICAL PEENING AFTER REPAIR WELDING

V.V. KNYSH and **V.S. KOVALCHUK**
E.O. Paton Electric Welding Institute, NASU, Kiev, Ukraine

To extend the life time of metal structures in repair welding using the standard technology, it is recommended to treat the fusion zone between the repair weld and base metal by high-frequency mechanical peening (HFMP). HFMP strengthening of the welded joints on steel 09G2S in as-welded condition and after repair welding provides a 3--5 times increase of their cyclic life in single-frequency zero-to-tension axial stress cycle.

Keywords: repair welding, welded joints, steel, high-frequency mechanical peening, service life extension

Different structural-technological methods are used for extension of joint cyclic life [1–3] in the process of fabrication of metal structures, working under the conditions of alternative loading. However, fatigue cracks appear in welded joints of structural elements after a certain period of operation, sometimes before the period of design service life is over. Replacement of damaged structures by new ones requires considerable investments and time that is why in some cases their operation is temporary continued until repair work is done even after fatigue cracks have appeared in them. In order to extend the fatigue time, well-known methods are used for retardation of fatigue cracks, as well as additional strengthening technologies. They are based as a rule on relief of tensile or favorable compression residual stresses, in case they are artificially induced, close to the tips of propagating cracks by local heating, explosion or impact treatments, by hole drilling in cracks tips and placing high-strength bolts into the holes with their tightening [3–6]. It is possible to achieve more effective recovery of load-carrying capacity of joints with fatigue cracks by complete removal of damaged metal with a crack and following maintenance with applying of arc welding. However, in this case also it is necessary to lower stress concentration in the zones of weld transition to the base metal, relieve or redistribute tensile and create favorable compressive residual stresses in repair welds or adjacent HAZ by different methods for essential extension of joint service life using traditional welding technologies and consumables. It is possible to achieve full or partial residual stress relieving by appropriate heat treatment of the entire element or its separate zones [7]. Inducing compressive residual stresses in welded joints is possible in the process of their manufacturing or repair by welding when using material with austenite-martensite structure as welding wire. Wire with the content of 10 Cr, 10 Ni and 80 Fe (wt.%) [8] in the base can be used for these purposes. When such weld metal or external (facing) layer is cooling down, transformation of austenite crystalline structure into martensite runs at the last stage of cooling, resulting in increase of the metal volume and appearance of residual compressive stresses [9]. When welding with traditional consumables, residual compressive stresses in the welded joint zone can be induced artificially after manufacturing or repair by welding through general or local surface plastic deformation as a result of static overloading, explosion or impact treatments [10, 11]. Combined strengthening methods, promoting the greatest extension of metal structures life, can be used.

One of the most effective, efficient and economically advantageous methods of extension of cyclic fatigue life of joints as a result of surface plastic deformation of weld metal or weld-to-base metal transition zone is high-frequency mechanical peening (HFMP) with the use of ultrasonic converters [12–15]. Fatigue tests of large-sized cross-shaped specimens (Figure 1), manufactured from low-alloy 09G2S steel were carried out for evaluation of such treatment effectiveness aimed at extension of cyclic life of joints after their repair by welding. Such specimens have high value of stresses concentration coefficient and tensile stress level in as-welded condition commensurate with their values in real welded metal structures. Welds of longitudinal stiffeners of specimens were made by manual-arc welding with stick electrodes UONI-13/55 with complete penetration. After specimen welding, weld-to-base metal transition zones were treated by HFMP on the length of 70 mm from the edge of the stiffener on the side of OO' axis. Such specimen geometry allowed determination of fatigue resistance of welded joint in the initial state, strengthened by HFMP technology in as-welded condition, as well as after their repair by welding without strengthening and with strengthening by HFMP on the same specimens and under the same loading conditions.

Fatigue tests of the specimens were done in a soft mode of zero-to-tension stress cycle in servohydraulic machine URS 200/20 with 5 Hz loading frequency. Developing fatigue crack of 20 mm length on specimen surface was taken as a criterion for ending the tests. During testing fatigue cracks initiated as a rule along

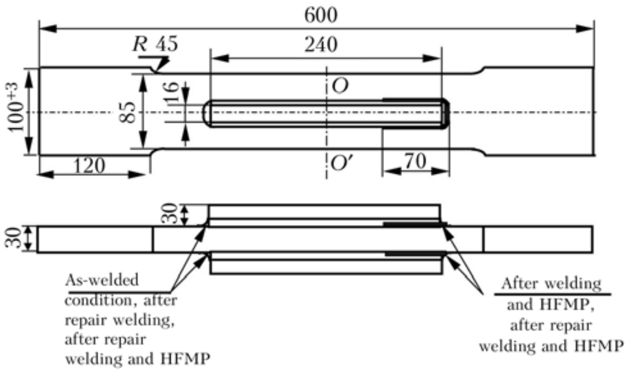

Figure 1. Specimen sizes of manufactured and repaired welded joints for evaluation of efficiency of HFMP application

the fusion line of end-fillet lap weld with the base metal. The first cracks initiated in the non-reinforced welded joints. Tests were interrupted when the crack reached the critical length; metal with fatigue crack was cut out by finger mill and the formed recess was welded by UONI-13 / 55 electrodes. Specimen tests were continued after the repair in the initially set loading conditions, till fatigue cracks of critical sizes formed in the repaired or initially strengthened by HFMP joints. Newly formed cracks were repaired by welding again. Part of the specimens were tested under the initially set loading conditions till fatigue cracks formed in the initial state after repair; and a part of them — after extra strengthening of repair welds by HFMP technology.

The results of fatigue tests obtained during the work are given in Figures 2 and 3. Evaluation of applied repair effectiveness for extension of welded joints cyclic life is given in Figure 4 by coefficient of fatigue life improvement K_{FLI} as the following ratio:

$$K_{FLI} = N_s / N_{in},$$

where N_s is the joint cyclic life at a certain stress level after HFMP strengthening in as-welded condition after repair by welding, after repair by welding with the use of HFMP for strengthened and unstrengthened joints in as-welded condition; N_{in} is the cyclic life of the joint at the same level of stresses in as-welded state.

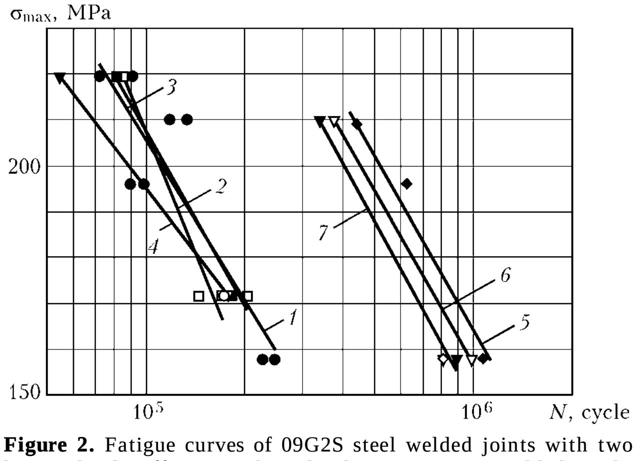

Figure 2. Fatigue curves of 09G2S steel welded joints with two longitudinal stiffeners without hardening: *1* — as-welded condition; *2–4* — correspondingly the first, second and third repairs by welding; *5–7* — correspondingly the first, second and third repairs by welding with subsequent HFMP treatment

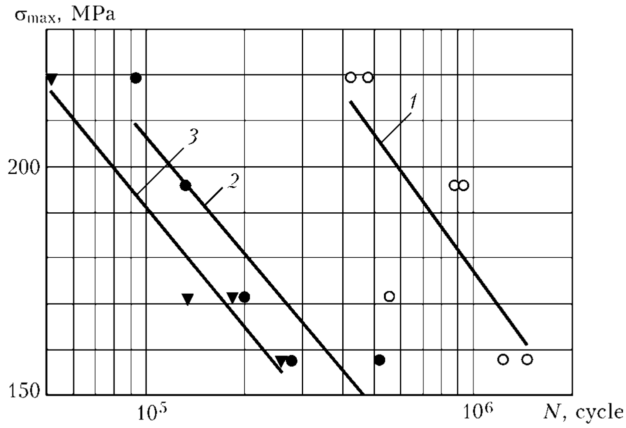

Figure 3. Fatigue curves of 09G2S steel welded joints with longitudinal stiffeners hardened by HFMP in as-welded condition: *1* — welding and peening; *2, 3* — correspondingly the first and second repairs by welding with subsequent HFMP treatment

Since fatigue curves of the studied welded joints strengthened and unstrengthened in as-welded condition, as well as after their repair by welding using HFMP technology and without its application, are located practically in parallel (see Figure 2 and 3), K_{FLI} for each concrete joint is equal at all levels of stresses. Comparison of the set K_{FLI} values shows (Figure 4) that after the first and second repairs by welding the cyclic service life of unstrengthened specimens is practically restored to the initial level. Cyclic service life reaches approximately 74 % of the initial value after the third repair welding. Additional HFMP of welded joints increases the specimen cyclic life by 4.6 times after the first repair welding, and after the second and the third — by 3.9 and 3.6 times, respectively. HFMP of welded joints in as-welded state increased the cyclic life of the specimens almost 5 times in as-welded state.

Cyclic life was about 95 and 63 % of that of specimens in the initial state after the first and the second repairs by welding with subsequent HFMP treatment of repair welds of joints strengthened by forging in as-welded state. Therefore, the efficiency of HFMP technology application after repair by welding of damaged by fatigue cracks, initially not hardened by HFMP joints of the given type, is higher than that of the joints strengthened by forging in initial state. Such regularity can be connected with a considerably greater number of cycles of fatigue damage accumu-

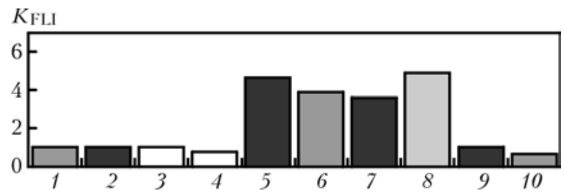

Figure 4. Extension of K_{FLI} service life coefficients of 09G2S steel welded joints: *1* — as-welded condition; *2–4* — correspondingly the first, second and third repairs by welding; *5–7* — correspondingly the first, second and third repairs by welding and peening of unhardened joints; *8* — welding and peening in initial condition; *9, 10* — correspondingly the first and second repairs by welding and peening of hardened joints

lation in the metal volume near the end of the longitudinal stiffener at higher stresses concentration under the conditions of biaxial tension in the strengthened joints in comparison with unstrengthened. The marked difference in cycles number is connected with the fact that in welded joints of the studied type unstrengthened after manufacturing, the fatigue cracks initiate at approximately 5 times smaller fatigue lives than in the joints strengthened by HFMP in as-welded state. Conditions of biaxial tension at some distance from the end fillet weld in the initially strengthened joints are determined by appearance of reactive tensile stresses balancing the compressive residual stresses in plastically deformed metal of the HAZ after its work hardening that are oriented perpendicularly to the direction of applied alternating loading. The features of repair by welding of the given type of joints are such that after removal of the material with the crack and welding up of the formed cavity the zone of transition to the base metal in repair welds (the place of fatigue crack formation) moves farther from the place of the longitudinal stiffener end at each repair by the width of repair weld to the zone of smaller stresses concentration. As for optimum number of repairs of the studied type of welded joint, it should be noted that already after the second repair with subsequent peening of repair welds, for joints both strengthened and unstrengthened in as-welded conditions, their base material uses all its load-carrying capacity and fatigue failures appear far or directly in the earlier-deposited welds of joints. In this connection it is not rational to perform repair welding with strengthening treatment more than two times on one joint.

CONCLUSIONS

1. The first and the second repairs by welding of unstrengthened joints, damaged by fatigue cracks, practically restore their cyclic life up to the level of their initial condition and by the time of their third repair their life does not exceed 75 % of initial value.

2. Additional HFMP of the transition zone from the repair welds to base metal increases the cyclic life of the joints after the first repair welding not less than by 4 times and after the second and third repair welding by not less than 3 times in comparison with the fatigue life of joints in as-welded condition.

3. HFMP of welded joints in as-welded condition improves the cyclic life of strengthened joints 5 times in comparison with as-welded condition.

4. It is rational to perform repair welding with strengthening treatment by HFMP technology not more than two times on one welded joint because the load-carrying capacity of base material and early made welds is used, as a result of their reaching the limited endurance limits.

1. Paton, B.E., Trufyakov, V.I. (1982) About increasing the load-carrying capacity and service life of welded structures. *Avtomatich. Svarka*, **2**, 1–6.
2. Trufyakov, V.I. (1998) Increasing the fatigue resistance of welded joints and structures. *Ibid*., **11**, 11–19.
3. Paton, B.E. (2000) Modern trends of increasing the strength and life of welded structures. *The Paton Welding J*., **9/10**, 2–8.
4. (1990) *Recommendations for inspection and reinforcement of welded span structures in operation*. Ministry of the Railways. Central Department of the Railways. Scientific Research Institute of Bridges of LIIZhT. Moscow.
5. Knysh, V.V. (2000) Determination of cyclic life of structure elements in arresting fatigue cracks. *The Paton Welding J*., **9/10**, 69–71.
6. Brodovoj, V.A., Mikheev, P.P., Knysh, V.V. et al. (2003) Effectiveness of fatigue crack retardation by the field of compressive residual stresses. *Ibid*., **8**, 49–50.
7. Vinokurov, V.A. (1973) *Tempering of welded structures for stress lowering*. Moscow: Mashinostroenie.
8. Ohta, A., Suzuki, N., Maeda, Y. (1996) Effective means for improving the fatigue strength of welded structures. *Welding in the World*, **37**, 84–89.
9. Kovalchuk, V.S., Knysh, V.V., Poznyakov, V.D. et al. (2007) Method for increasing the cyclic and service life of welded steel structures. *The Paton Welding J*., **3**, 37–39.
10. Trufyakov, V.I. (1973) *Fatigue of welded joints*. Kiev: Naukova Dumka.
11. Trufyakov, V.I., Mikheev, P.P., Kudinov, V.M. (1984) Increase of fatigue resistance by explosion loading. *Avtomatich. Svarka*, **12**, 50–52.
12. Mikheev, P.P. (1990) Increasing fatigue resistance of structure welded joints by ultrasonic impact treatment. In: *Transact. on Problems of Welding and Special Electrometallurgy*. Kiev: Naukova Dumka, 41–47.
13. Knysh, V.V., Kuzmenko, A.Z. (2005) Increasing fatigue resistance of welded joints by high-frequency mechanical peening. *Svarshchik*, **2**, 19–21.
14. Knysh, V.V., Kuzmenko, A.Z., Vojtenko, O.V. (2006) Increasing fatigue resistance of welded joints by high-frequency mechanical peening. *The Paton Welding J*., **1**, 30–33.
15. Lobanov, L.M., Kirian, V.I., Knysh, V.V. (2006) Increasing of life of welded metal structures by high-frequency mechanical peening. *Fiz.-Khim. Mekhanika Materialiv*, **1**, 56–61.

KSU KS 02 SYSTEM FOR AUTOMATIC CONTROL AND MONITORING OF RESISTANCE SPOT WELDING PROCESS

P.M. RUDENKO and **V.S. GAVRISH**
E.O. Paton Electric Welding Institute, NASU, Kiev, Ukraine

Methods for real-time quality control of resistance spot welding are considered. Universal system for control and monitoring, peculiar features of which are wide possibilities for real-time quality control, is suggested. Technical characteristics of the system are presented, and fields of its application in industry are shown.

Keywords: resistance spot welding, control system, quality control, fuzzy logic, neuron networks

State-of-the-art systems for controlling process of resistance spot welding are implemented on the basis of powerful single-crystal microcontrollers, functional capacity and productivity of which allow implementing (in addition to the functions of direct digital control of a welding machine) complex algorithms of a welded joint quality and process control. At present, taking into account impossibility of visual estimation of dimensions of a weld spot in the process of its fulfillment, as well as state-of-the-art production requirements in regard to certification and assurance of high quality of the produced products, real-time quality control of the resistance spot welding is one of main requirements to the spot welding machine control system.

As a rule, algorithms of quality control of the weld spots are based on measurement and use of the process parameters: welding current, voltage between the electrodes, resistance in the electrode--electrode area, and force of compression of the electrodes.

One can single out several methods of control on the basis of the process parameters. The simplest one is based on allowable deviations of, for example, welding current and voltage between the electrodes. Later this method was further developed due to application of the fuzzy logic algorithms, which made it possible to increase reliability of control [1].

For quantitative assessment of the welded joint quality, for example, diameter of the weld spot nugget, the assessment method based on assessment of the regression models, was used. The latter ones (usually in the form of polynomials of first or second order) are constructed on the basis of experimental welding data, using mathematical statistics method, whereby one tries to take into account in the experiments all disturbances, which influence the process under industrial conditions. In order to increase accuracy of the models, different algorithms for adjustment of the model factors, based on the data of experimental check of the conditions directly at the production site, are used.

Method of control on the basis of mathematical models was further developed after appearance of the neuron networks [2]. Mathematically application of the models on the basis of neuron networks is more complex than application of regressions models; however, in the first case one manages to increase accuracy and reliability of the resistance welding quality forecasting due to the fact that in the neuron network it is possible to forecast dynamic parameters of the process — change of the welding current and voltage between the electrodes during welding, which characterizes change of resistance in the welding area and more accurately reflects the spot welding process.

Each of mentioned processes — from the simplest to a complex one — has its advantages and shortcomings, and depending upon designation of the control system may be used in practice. Possibility of inclusion on requirement of a customer into software of the system and application of the listed quality control methods in resistance spot welding is main peculiarity of the KSU KS 02 system for the resistance welding machine control, developed by specialists of PWI and PWI Engineering Center «Pressure Welding», in comparison with known regulators of the RKS series, produced at present in Ukraine (plant «Selma», Simferopol) and of the RKM series, produced in Russia (plant «Elektrik», St.-Petersburg). The system is designed for controlling welding cycle and monitoring of the process applicable to pedestal and suspended single- and two-operator alternative current machines.

The KSU KS 02 system for the resistance spot welding machine control fulfills the following functions:

- direct digital control of a welding machine (control by the thyristor contactor and four (two pairs) electropneumatic valves for setting and fulfillment of the welding mode cyclogram: preliminary compression, compression, welding with modulation of current, cooling, annealing with modulation of current, forging with possibility of switching on during passage of current, and pause);
- stabilization of the welding process parameters (compensation of change of the power supply network voltage, stabilization of acting value of welding cur-

rent, automatic adjustment at cos φ of the welding machine, and automatic correction of welding current in case of the working surface wear of electrodes);

• welding quality control (on the basis of allowable deviations of welding current and voltage between electrodes or forecasting of the weld spot nugget diameter using mathematical model);

• auxiliary functions (storage in the system memory of eight preset welding modes in case of the voltage cut-off, and automatic selection of any of them by external control signal; self-diagnostics of the system; connection with a personal computer via sequential channels RS232 or RS485; programmable protection against unauthorized access to setting of the welding mode parameters, protection of output control circuits by pneumatic valve, thyristor contactor and auxiliary equipment against overloads).

The system has a convenient control panel with a membrane keypad and liquid-crystal display that ensures simplicity and visualization of a complex cyclogram of the welding process (Figure).

In the simplest case quality control is performed on the basis of allowable deviations of the process parameters. Optimal values of welding current and voltage between the electrodes, as well as range of allowable deviations of these parameters in percent are entered into the controller. The system forms messages about exceeding of allowances, relating to any parameter.

As a version of the allowance-based control, a control based on the fuzzy logic parameters is possible that was implemented in welding of inter-cell elements of storage batteries [1]. Because of complexity of estimation of a welded joint quality in this case, quantitative assessment of a parameter of the joint is insufficient, and a conventional allowance control does not allow using data obtained for control of the process, which would take into account technological peculiarities of welding of components from lead. In the used algorithm value of imprint from the electrode is controlled by voltage between the electrodes, and then for regulation of the current density the required value of welding current is determined, which has to be achieved during its stabilization.

In a case, when quality of a welded joint may be determined on the basis of a certain calculated parameter, for example, diameter of the nugget or depth of penetration, a mathematical model in the form of regression equation or neuron network equation is used. Although these methods of quality control of welded joints are almost equivalent, for certain welded materials, in particular, steels covered by protection layer, neuron networks allow achieving higher accuracy of forecasting, because it is possible to trace with their assistance change of parameters in time. It is known that behavior of the resistance curve in the process of welding of low-carbon steels well correlates with strength parameter of a welded joint.

In order to exclude storage in memory of big arrays of data on weight coefficients for different types of thicknesses and materials, an adaptive algorithm of quality control is used in the system. It consists in the fact that input parameters of the network are values of the latter, expressed in relative units in relation to optimal values. At such arrangement of the network transition from one optimal welding mode to another, for example, in welding of components of different thickness or materials for rearrangement of the network, it is necessary to set parameters of the new optimum modes. Adjustment of coefficients on the basis of experimental data is necessary in rare cases. However, number of required additional experiments is significantly lower than in case of construction of the neuron network in traditional form [2], whereby required accuracy of the nugget diameter assessment is achieved. Data on diameter of the weld spot nugget may be transmitted via sequential channel to the personal computer for formation of a protocol on quality of welding of a structure. Functions of quality control on the basis of a regression model or neuron network are on requirement of a customer fulfilled for a specific material and thickness.

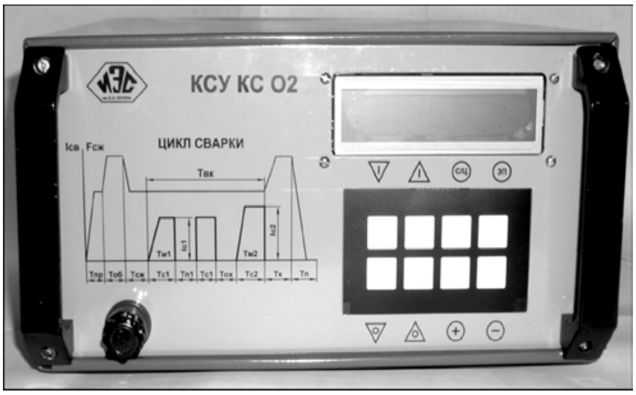

Appearance of KSU KS 02

As far as functions of the process control are concerned, in comparison with mentioned RKS and RKM the described system has the same possibilities, i.e. depending upon a preset control algorithm KSU KS 02 performs compensation of fluctuations of the network voltage or stabilization of welding current or voltage between the electrodes, as well as compensation of wear of the latter. However, like in the case of quality control, on requirement of a customer for compensation of wear of the electrodes in KSU KS 02 application of several algorithms is possible: from the simplest, when welding current is increased through preset number of weld spots, up to more complex and accurate ones. It is known that wear of electrodes depends upon welding conditions, intensity of cooling, material of the electrodes, method of their manufacturing, properties of the materials being welded, coating of their surface, and other reasons. It is rather difficult to measure wear of the electrodes in process of welding, and its estimation on the basis of number of weld spots is rather rough. In KSU KS 02 it is possible to install software for implementation of the algorithm, based on real-time monitoring of the welding mode parameters and welding current change according to a certain law, when correcting action is calculated on the bases of measured current data and voltage fall between the electrodes, taking into account density of current in the welding contact [3].

In addition to flexible structure of the software, KSU KS 02 is sufficiently universal. It is known that different types of machines are used for resistance spot welding, which require for different number of control signals. So, for alternative current machines as minimum three discreet control outputs are required, for direct current machines — five ones. For seam welding machines it is necessary to have one more control output. In addition, at plants a welding operator may turn on two-three welding machines, and switching on of a signaling system, based on results of welding or control of auxiliary mechanisms, is required. KSU KS 02 has seven discreet inputs (24 V, 10 mA), eight discreet outputs (24 V, 5 A) and two analogue inputs, if we do not take into account an internal channel for measurement of the power supply network voltage. All listed inputs and outputs are galvanically separated, and in case of modification of the software KSU KS 02 may be used arbitrarily. So, application of KSU KS 02 is possible for resistance spot machines, which require for development of special control algorithms. Application of KSU KS 02 is the most efficient in production of special-purpose structures and certification of welding production.

CONCLUSIONS

1. Main peculiarity of KSU KS 02 in comparison with known analogues consists in wide possibilities of the real-time welding quality control: control on the basis of allowable deviations, statistical models or neuron networks, taking into account voltage at the electrodes. By using it, it is possible to solve complex technological tasks and thus expand field of the resistance spot welding application.

2. The control system is universal and may be used for different types of machines for resistance welding and in welding production, for example, in automotive, agricultural machine building, instrument making, aircraft industries, etc.

1. Podola, N.V., Rudenko, P.M., Gorun, N.P. et al. (1999) Quality control of resistance spot welding of cell connections on the base of fuzzy logic. *Avtomatich. Svarka*, **5**, 42–45.
2. Podola, N.V., Rudenko, P.M., Gavrish, V.S. (2004) Application of adaptive algorithm for welding quality monitoring in control systems of resistance spot welding machines. *The Paton Welding J.*, **6**, 14–17.
3. Podola, N.V., Rudenko, P.M., Gavrish, V.S. (2005) Algorithms for compensation of electrode wear in resistance spot welding. *Ibid.*, **4**, 23–27.

WELDING-TECHNOLOGICAL PROPERTIES OF NEW AN-47DP GRADE FLUX

A.V. ZALEVSKY[1], **V.I. GALINICH**[1], **N.Ya. OSIPOV**[2], **V.I. NETYAGA**[2] and **O.P. KIRICHENKO**[2]

[1]E.O. Paton Electric Welding Institute, NASU, Kiev, Ukraine

[2]OJSC «Zaporozhie Plant of Welding Fluxes and Glass Items», Zaporozhie, Ukraine*

Results of tests of a new fused flux, designed for welding of high-strength low-alloy steels, are presented. The flux, produced according to the double-refining method and designated as the AN-47DP grade flux, was developed within the framework of innovation project of the «E.O. Paton Electric Welding Institute Technological Park».

Keywords: arc welding, low-alloy steels, pumice-like fused flux, formation of weld metal, separability of slag crust, narrow groove, impact toughness, production, double refining

Obligatory condition of successful operation of an enterprise in market economy is constant updating of products. Within the framework of the Technological Park innovation project the E.O. Paton Electric Welding Institute of NASU developed jointly with «Zaporozhie Plant of Welding Fluxes and Glass Items» company new fused flux of AN-47DP grade and technology for its production. New flux, which is an improved version of the AN-47 grade flux that is widely used for welding of low-alloy steels of increased strength [1], is designed for quality formation of the weld metal under specific conditions of welding — narrow groove, high speeds, corner joints — and ensuring resistance of the weld metal against brittle fracture, estimated by energy of the 47 J impact at –20 °C and 27 J impact at –40 °C according to ISO 14171 requirements [2].

Below test results of the AN-47DP flux properties are given in application to welding of a thick-sheet rolled metal, where along with impact toughness of the weld metal of special importance is separability of the slag crust. For the tests technology of a multilayer single-arc welding and welding wires of IMT 9, IMT 6 and IMT 9Si grades of 4 mm diameter were used, offered by the Polish company «Multimet». These wires according to ISO 14171:2000 classification ([2], Table 5A) correspond to the S2, S2Mo and

*Engineer R.N. Barannik participated in the work.

S2Si grades. For comparison also national welding wire of the Sv-08G2S grade of 3 mm diameter, corresponding according to this standard to the SU31 grade, was used ([2], Table 5B). Chemical compositions of the wires, base metal (steel 09G2S of 40 mm thickness) and weld metal are presented in Table 1.

Peculiarity of the welding technology consisted in bevel of the edges at 20° and making of a backing weld using the Sv-08G2S wire in mixture of 82 % Ar + CO_2, whereby width of the temporary weld was about 4 mm. As showed results of preliminary experiments with application of high-silicon manganese fluxes of AN-348-A and AN-60 grades, such technology of welding negatively effected separability of the slag crust from a narrow groove. That's why we carried out special investigations of separability of slag crust of the AN-47DP flux from a narrow groove.

A commercially produced flux was tested, quality parameters of which corresponded to TU U 05416923.0499–99 and GOST R 52222. Prior to welding it was dried at the temperature 300 °C within 3 h at thickness of the flux layer in the pan 30–40 mm. Quality of the flux drying was checked by the number and size of pores in the slag crust, produced during deposition of a bead on fettled surface of a plate at arc voltage 43 V (according to the TU U 05416923.0499–99 recommendation). The check did not detect pores in the slag crust.

As it is known, separability of slag crust of the flux in welding is not a standardized parameter of its quality, that's why a unified methodology for its assessment does not exist either. However, poor separability of the crust increases labor and time expenditures and consumption of materials in manufacturing of a welded structure. That's why when selecting flux for the groove welding separability of the slag is estimated, as a rule, only qualitatively in each specific case of welding. So, one is used to consider that flux has good separability, if on a planed surface of a steel plate the crust is separated from the weld metal surface spontaneously without application of any tools (a hammer, a chisel, etc.). Almost all existing fluxes demonstrate such capacity in welding of non-alloy or low-alloy steels, because such fluxes ensure good stability of arc process and do not contain in their composition components, which are able to form on surface of slag contact with the metal chemical compounds with crystalline lattice of the latter. In addition, separability of the slag is favorably affected by absence of limitations for spreading of the slag over surface of the molten pool metal. However, in case of the butt welding with deep groove preparation, which is characteristic of structures from the thick-wall rolled metal, situation significantly worsens — starting from the first run the crust in majority of cases is not removed from the butt without application of a tool.

It follows from analysis of the scheme of the weld metal and the slag crust formation in the butt groove (Figure 1) that width B_{sl} of the area of the slag contact with walls of the groove depends upon volume W_{sl} and width of the weld metal in the narrowest place of the groove (parameter b_n). However, the current and the speed of welding being the same, volume of the slag W_{sl} is function of arc voltage U_a, therefore at b = const increase of U_a expands width B_{sl} and thus worsens separability of the slag crust. In addition, in a general case reasons for worsening of the slag separation may be as follows: poor formation of the weld metal (presence of undercuts, sharp angles over the transition line, protrusions and «combs» over the weld axis), which stipulates mechanical jamming of the slag; influence of linear expansion coefficient of the slag; sticking of the crust to surface of the weld metal, stipulated by chemical compositions of welding consumables.

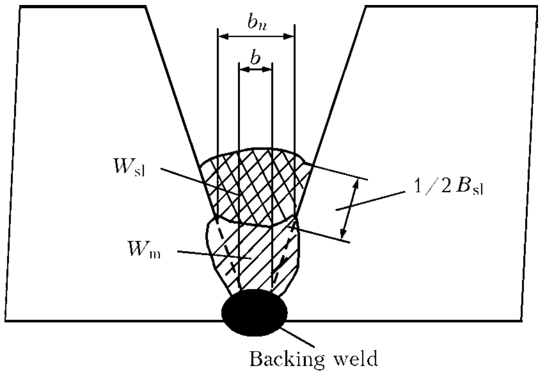

Figure 1. Scheme of butt groove filling by weld metal and slag crust (see designations in the text)

As shows practice, most difficulty the crust is removed from the deepest part of the groove with the smallest distance between walls of the latter. Having projected listed above factors on the described case of welding, one may assume that exactly sticking of the crust to surface of the butt walls is a decisive factor, which effects separability of the slag crust in case of narrow grove welding, because used welding materials did not have problems with separation of the slag in case of absence of the groove preparation. It follows from this that at constant welding conditions slag volume is also constant, and width B_{sl} depends just on the weld width of the previous run, i.e. distance between walls of the butt, measured over surface of the deposited metal (parameter b_n) and arc voltage.

In order to check this assumption, deposition of beads into grooves of a special specimen from the 09G2S steel was carried out, which simulated a real butt with deep edge preparation (Figure 2). The grooves had different initial parameter (b = 4 and

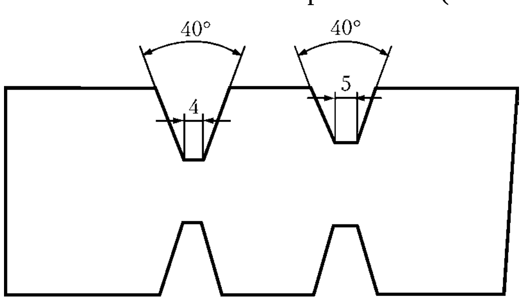

Figure 2. Sample section for determining separability of slag crust

Table 1. Chemical composition of base metal, welding wires and metal of welds, wt.%

Grade of materials	C	Si	Mn	S	P	Mo
09G2S steel (data of quality certificate)	0.12	0.56	1.30	0.021	0.018	–
Wire (data of quality certificate)						
IMT 9 (S2)	0.01	0.07	1.00	0.015	0.017	—
IMT 6 (S2Mo)	0.09	0.13	1.02	0.022	0.008	0.477
IMT 9Si (S2Si)	0.09	0.20	0.98	0.010	0.011	–
Sv-08G2S	0.06	0.87	1.88	0.017	0.023	–
Metal of welds (in case of welding with wire)						
IMT 9	0.059	0.316	1.30	0.025	0.017	–
IMT 6	0.051	0.378	1.37	0.031	0.012	0.350
IMT 9Si	0.053	0.430	1.38	0.022	0.013	–
Sv-08G2S	0.057	0.932	2.01	0.025	0.024	–
09G2S steel base metal	0.110	0.604	1.45	0.019	0.021	–

5 mm), which allowed studying separability of slag under the worst welding conditions, i.e. at the smallest values of parameter b and within wide range of arc voltages, and determining optimal welding conditions, at which the best conditions for the slag separation are achieved.

For the purpose of observation of identical surfacing conditions the groove was divided into four zones of 150 mm length, in each of which surfacing conditions differed from the previous only by a higher arc voltage (see Table 2). Greater part of the grooves was surfaced by the wire of 4 mm diameter (Sv-08GA), several grooves (for comparison) were welded up by wire of 3 mm diameter (Sv-08G2S); value of current (straight, reverse polarity) was unchangeable within one run in one groove and equaled 550–600 A in welding by wire of 4 mm diameter and 500–550 A for wire of 3 mm diameter. Speed of welding during performance of a run was constant all over length of the groove, but it changed in different runs depending upon previous results of deposition. It was maximum in first run (31.5 m / h for wire of 4 mm diameter) and minimal in the last run (24.6 m / h for wire of 3 mm diameter). In all runs electrode stick-out was 40 mm.

Separability of slag crust from the groove was estimated according to the three-mark system: excellent — slag separation without application of a tool; satisfactory — separation with application of a tool without significant force; unsatisfactory — separation with application of a tool and significant force. In each run quality of the weld metal formation was also estimated according to three-point system: excellent — surface of the weld is clean, without undercuts, overlaps and other defects of formation; satisfactory — insignificant unevenness on the weld surface; unsatisfactory — a weld is uneven with undercuts or overlaps.

As one can see from results of the slag crust separability tests of the AN-47DP flux, presented in Table 2 and in Figures 3 and 4, as arc voltage increases, the rest conditions of welding being the same, separability of the slag crust worsens. So, during fulfillment of first run in the groove with parameter b_0 = = 4 mm in the first zone (U_a = 30 V) the crust filled approximately 1 / 3 of the groove volume (Figure 3, *a*), in second run (U_a = 34 V, Figure 3, *b*) — 2 / 3, in third run (U_a = 38 V, Figure 3, *c*) — 4 / 5, and in fourth run (U_a = 42 V, Figure 3, *d*) the crust exceeded limits of the groove, whereby in the first zone the crust was removed practically spontaneously, while in the rest zones it was necessary to apply significant force. Formation of a weld in the first and second zones was practically equally good — without defects, with smooth transition to the butt wall, whereby surface of the weld was concave and smooth (Figure 3, *e*, *f*). Width of area of slag contact with the butt wall on crust of the first zone was less than 2 mm (Figure 4, *a*), of the second zone — about 4 mm, in the rest zones it was impossible to determine this parameter because of complete destruction of the crust during its removal. It should be noted that in case of good separability of slag crust from the groove the latter, as a rule, has convex (ellipsoid) shape (Figure 4, *a*, *b*). In case of formation of flat surface of the weld inside the groove, the crust has an angular shape (Figure 4, *c*, *d*) and it is, as a rule, difficult to separate it. Poor separability of the slag crust in fourth zone is stipulated, first of all, by unsatisfactory formation of the weld — over axis of the weld humps and rolls, undercuts and lacks of fusion appeared. It is evident that by means of the arc voltage increase stability of the process of the arc burning in a narrow groove reduces, and therefore formation of the weld and separability of the crust worsen. So, at certain dimensions of a groove good separability of the slag has to be expected at lower arc voltage or increase of b parameter. For specification of this assumption calculations of surface width of the deposited metal layer (parameters b_n) for each deposited layer were carried

Table 2. Welding conditions and results of AN-74DP flux tests for determining slag crust separability

No. of weld-run (parameter of joint b_n, mm)	Zone No.	U_a, V	I_w, A	v, m / h	Weld formation	Slag crust separability	Mean thickness of deposited layer, mm	Wire grade (diameter, mm)
1-1 (4)	1 2 3 4	30 34 38 42	550–.600	31.5	Excellent Same Satisfactory Unsatisfactory	Satisfactory Unsatisfactory Same »	4 4 – –	Sv-08GA (4)
1-2 (6.9)*	1 2 3 4	29 30 31 32	550–600	31.5	Excellent Same Satisfactory Same	Excellent Same Satisfactory »	4 4 3.5 3	
1-3 (9.5)*	1 2 3 4	29 30 31 32	550–600	27.8	Excellent Same » »	Unsatisfactory Excellent Satisfactory Unsatisfactory	2 2 2.5 2.5	
1-4 (11.3)*	1 2 3 4	31 32 33 34	550–600	27.8	Excellent Same » »	Excellent Same » »	2	
1-5 (12.8)*	1 2 3	32 33 34	550–600	27.8	Excellent Same »	Excellent Same »	1.5	
2-1 (5)	1 2 3 4	28 29 30 31	550–600	31.5	Excellent Same » »	Excellent Same Satisfactory Unsatisfactory	4	
3-1 (4)	1 2 3 4	30 31 32 33	550–600	31.5	Excellent Same Satisfactory Same	Unsatisfactory Same » »	4	
3-2 (6.9)*	1 2 3 4	29 30 31 32	550–600	31.5	Excellent Same » »	Excellent Same Satisfactory Unsatisfactory	3	
3-3 (9.1)*	1 2 3 4	30 31 32 33	550–600	31.5	Excellent Same » »	Excellent Same » Satisfactory	2.5	
3-4 (10.9)*	1 2 3 4	31 32 33 34	550–600	31.5	Excellent Same » »	Excellent Same » »	1.5	
4-1 (4)	1 2 3	28 29 30	400–450	24.6	Excellent Same »	Satisfactory Same »	N / D	Sv-08G2S (3)
4-2	1 2 3	28 29 30	500–550	24.6	Excellent Unsatisfactory Satisfactory	Excellent Satisfactory Unsatisfactory	Same	
4-3	1 2 3	28 29 30	500–550	24.6	Excellent Same »	Excellent Same »	»	
5-1 (5)	1 2 3	29 30 31	500–550	24.6	Excellent Same »	Satisfactory Same »	»	
5-2	1 2 3	29 30 31	550–600	27.8	Unsatisfactory Same »	Unsatisfactory Same »	»	

*Calculated value.

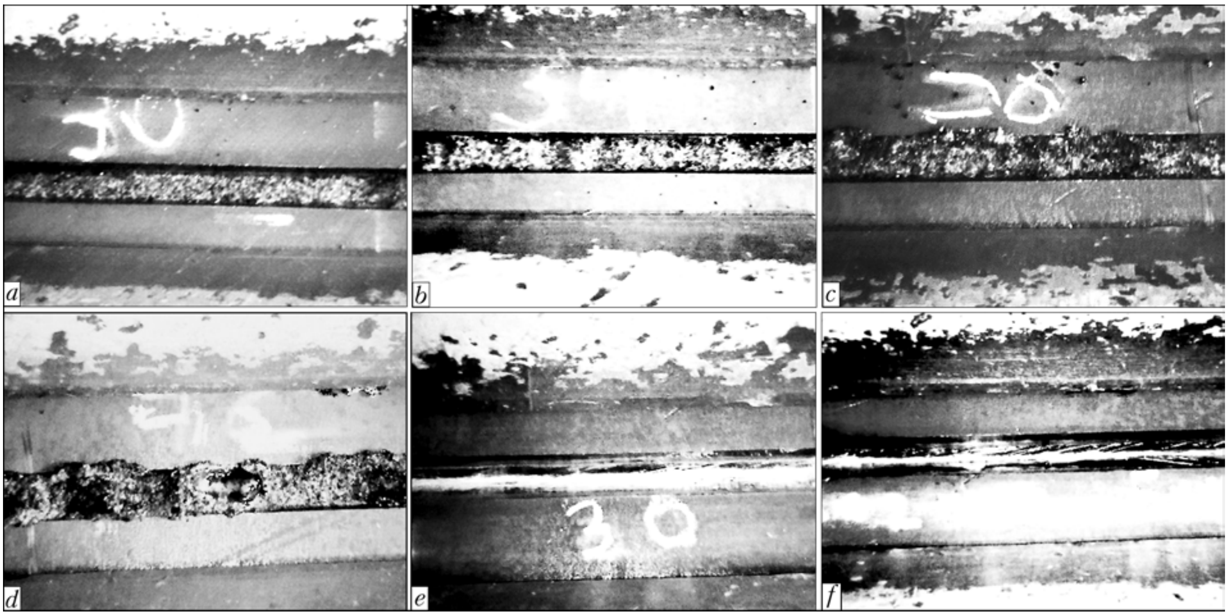

Figure 3. External view of internal surface of slag crust (*a*--*d*) and weld metal (*e*, *f*) (see description in the text)

out according to the formula: $b_n = (0.3640 \cdot 2h) + b_0$, where 0.3640 = tg 20°; h is the thickness of the deposited metal layer. One can see from data of Table 2 that by means of filling of the groove by the deposited metal (in case of superimposing of the next run or reduction of the welding speed) parameter b increases and, U_a being constant, separability of the crust improves (runs No. 3-2, 3-3, 3-4). The same regularity was observed in welding by wire of 3 mm diameter. However, this is fair only under stable conditions of welding, otherwise separability of the crust worsens (runs No. 4-1, 5-1, 5-2).

It is characteristic that for each value of parameter b limit value U_a exists, above which worsening of the crust separability is observed (Figure 5). So, it is established that for b_n = 4–5 mm voltage U_a constitutes 29–30 V, which is confirmed by surfacing results of the first run No. 1-1, 3-1 (b = 4 mm) and No. 2-1 (b = = 5 mm): in all surfacings separability of the crust is spontaneous or easy at $U_a \leq 30$ V, whereby form of the weld surface was concave with smooth transition to the base metal.

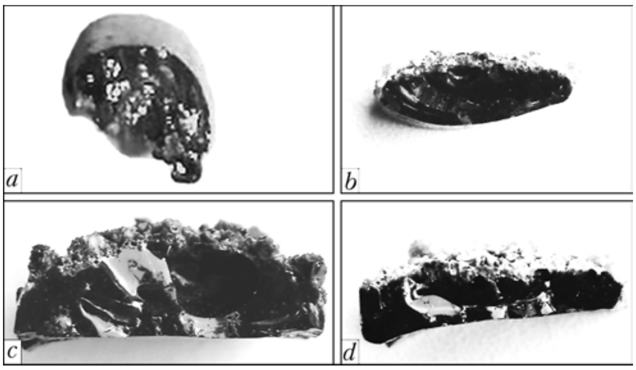

Figure 4. View of slag crust at different characters of its separability: *a* — excellent (U_a = 30 V, b_0 = 4 mm, No. 1-1); *b* — excellent (U_a = 34 V, b_3 = 4 mm, No. 1-4); *c* — unsatisfactory (U_a = 30 V, b_0 = 4 mm, No. 3-2); *d* — satisfactory (U_a = 31 V, b_0 = 4 mm, No. 3-2)

For comparing character of the slag crust separability of the AN-74DP flux with that of other fluxes, grooves with b_0 = 4 and 5 mm at arc voltage 29, 30, 31 and 32 V under AN-60 and AN-348-A fluxes were welded. In all cases of the first run welding the crust was separated by means of a tool after application of a significant force despite good formation of the weld metal in first zones of the groove, whereby volume of slag in the groove was in all cases bigger than in case of welding under the AN-47DP flux. Because of poor separability it was impossible to determine width of area of the slag contact B_{sl} with the butt walls. The result obtained evidently proves that under similar conditions of welding volume of molten within a time unit flux is different for different brands of flux and, therefore, better separability of the slag crust from the groove is ensured by flux with minimal value of mentioned volume, because in this case width B_{sl} is minimal.

Taking into account the results obtained in the investigations, welding of the test butts was performed according to the following technology: weld root was welded up by the Sv-08G2S wire in mixture 82 % Ar + CO_2 and then runs under flux were performed (five runs on each side). Current in all runs was invariable (550–600 A for wires of 4 mm and 500–550 A for wire of 3 mm diameter). Arc voltage and welding speed

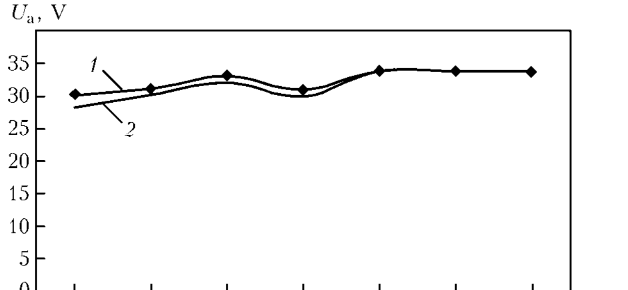

Figure 5. Dependence of limit value U_a upon parameter b_n: *1* — satisfactory separability; *2* — excellent

Table 3. Parameters of mechanical properties of welded joints made using AN-47DP flux on 09G2S steel of 40 mm thickness by the «Multimet» wires IMT 9 (S2), IMT 6 (S2Mo), IMT 9Si (S2Si) and Sv-08G2S wire (SU31)

Weld No.	Wire grade (diameter, mm)	σ_y, MPa	σ_t, MPa	δ_5, %	φ, %	Impact toughness KCV, J / cm^2 (impact energy according to ISO-V, J) at temperature, îÑ			
						+20	0	–20	–40
1	IMT 9 (4)	409.8 415.3	501.1 500.0	25.3 30.3	63.5 66.0	138.2--148.4 (114.6)	84.0–139.7 (86.8)	51.3--92.8 (53.3)	42.7--48.6 (35.8)
2	IMT 6 (4)	492.7 505.2	586.3 587.4	23.7 24.7	59.1 59.8	105.3--116.6 (88.0)	90.0–118.5 (84.5)	73.0--83.8 (61.5)	57.4--71.2 (50.8)
3	IMT 9Si (4)	421.7 434.9	523.7 545.4	30.0 31.7	60.0 62.1	134.0--152.6 (117.0)	108.1--120.2 (89.8)	83.4–108.1 (51.4)	42.5--61.2 (39.8)
4	Sv-08G2S (3)	546.6 585.1	642.0 659.4	25.0 27.3	55.4 59.8	158.2--189.7 (140.3)	115.4--142.8 (99.9)	54.5–103.7 (61.3)	56.1--60.0 (46.6)

for each run were selected from Table 2 and the following values were obtained: for wires of 4 mm diameter — first run 28–29 V and 27.8–31.5 m / h; second and third runs: 29 V and 31.5 m / h; fourth run: 29–31 V and 27.8 m / h; fifth run: 32 V and 24.6 m / h.

For wire of 3 mm diameter: first–forth runs — 29 V and 24.6 m / h; fifth run — 30–32 V and 21.7–27.8 m / h.

After performance of each run a weld was cooled in air down to a temperature below 200 °C, and for the purpose of reducing deformation of the butt the plates were turned over and two subsequent runs were made. The butt was completely welded up within five runs on each side, whereby spreading of the welds was not performed.

Welding of the reference butts showed that selected conditions ensured good formation of welds and easy separability of the slag crust even in first run. Due to physical-mechanical properties of the AN-47DP flux slag its crust cracked during cooling in all without exception subsequent runs and separated spontaneously.

Process of the groove filling in all reference butts was characterized by identity of welding conditions and absence of pores, cracks, and other defects in the weld metal (Figure 6).

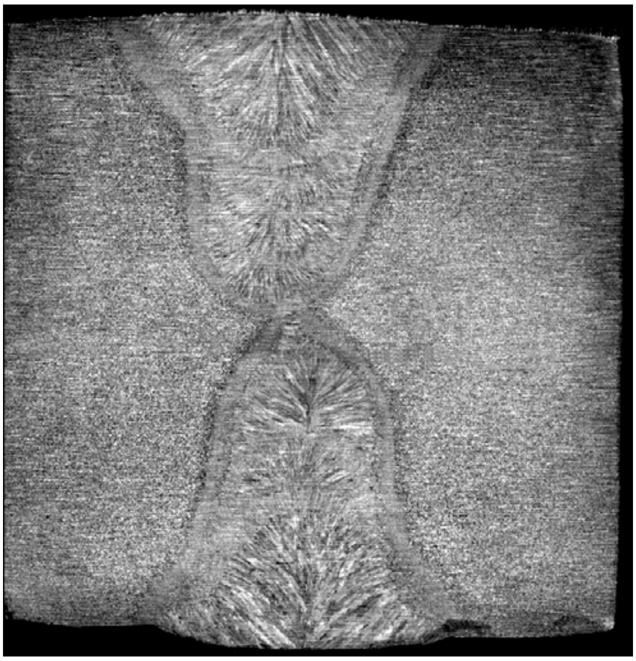

Figure 6. Metal welded using AN-74DP flux and IMT 9 wire (five runs on each side)

Parameters of mechanical properties of the produced joints exceeded the required ones (47 J at –20 °C). Neutral character of slag base of the fluxes containing ZrO_2, and its ability to oppose formation of silicate inclusions in metal of welds [3] allowed ensuring in welding with use of new flux necessary alloying of the weld metal in case of application of welding wires, containing manganese and molybdenum. So, while reached level of impact toughness exceeded the required one in all versions of welding by 10–30 %, for wires with molybdenum (MT 6) and manganese (Sv-08G2S) assigned level of cold resistance has preserved even at a lower test temperature (–40 °C). It follows from these data that application of the AN-47DP flux quite meets technology requirements of the multilayer single-arc welding of thick-sheet rolled metal both in regard to the welding-technological properties (free from defects formation of welds and easy separability of slag crust from a deep groove) and in regard to parameters of strength, plasticity, and resistance of the weld metal to brittle fracture.

So, new fused flux of the AN-47DP grade, produced by the method of double refining of the melt, may be recommended for production of special-purpose welded structures from low-alloy steels in combination with wires of the same class.

1. Zalevsky, A.V., Galinich, V.I., Podgaetsky, V.V. et al. (1977) Flux for welding of pipelines from low-alloy higher strength steel. *Avtomatich. Svarka*, **3**, 49.
2. *International standard ISO 14171:2002*: Welding consumables — Wire electrodes and wire-flux combinations for submerged arc welding of non alloy fine grain steels — Classification.
3. Zalevsky, A.V., Parfesso, G.I., Markashova, L.I. (1982) On metallurgical role of zirconium dioxide in welding fluxes. *Avtomatich. Svarka*, **4**, 54.

DEVELOPMENTS IN THE FIELD OF ALUMINIUM ALLOYS OFFERED BY THE E.O. PATON ELECTRIC WELDING INSTITUTE

TECHNOLOGY AND EQUIPMENT FOR FRICTION WELDING OF DISSIMILAR METALS AND ALLOYS

Friction welding can be successfully used for joining materials that differ in their mechanical and thermal-physical characteristics, as well as materials that enter into chemical interaction during their simultaneous heating process and form brittle intermetallic compounds.

The E.O. Paton Electric Welding Institute developed technologies and parameters for friction welding different metals and alloys in similar and dissimilar combinations, as well as commercial technologies for welding specific parts of different combinations of metals and alloys, including:

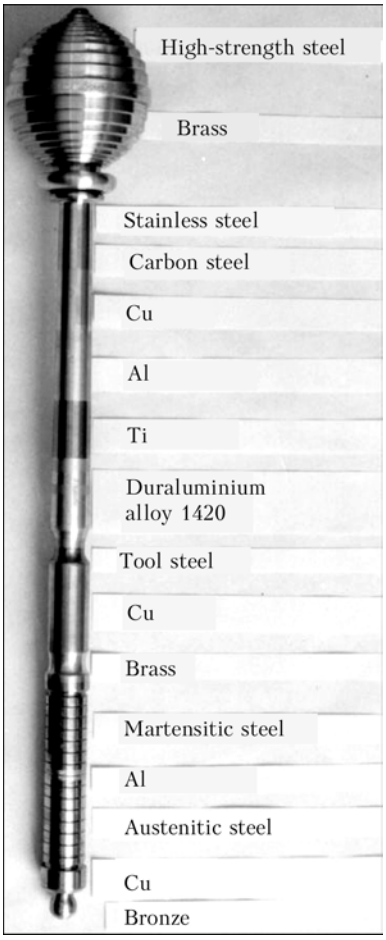

- tool steels to structural steels (sectional end metal cutting tool);
- corrosion-resistant steels to structural steels (shafts of chemical pumps, rollers of finishing machines for textile production);
- heat-resistant steels to structural steels (bimetal valves of car engines, rotors of diesel turbine compressors);
- alloyed high-strength steels to carbon steels of equal and different sections (casings of hydraulic cylinders, piston rods, shafts of axial-piston hydraulic machines);
- heat-hardened to cold-worked aluminium alloys (panels of alloy AMg6NPP to pins of alloy D16T);
- copper and aluminium to cermet (electrical equipment contacts);
- copper, bronze and brass to steel (cylinder blocks of axial-piston hydraulic machines);
- aluminium and its alloys to steel (bimetal transition pieces for aerospace engineering equipment);
- aluminium to copper (transition pieces for electrical engineering);
- titanium to steel.

A series of specialised machines for welding billets with a diameter of 10--100 mm is available to implement the technologies. The machines are characterised by simple design, reliability and durability, high degree of automation and productivity. Distinctive feature of the machines for inertia friction welding is utilisation of the electromagnetic force drive developed by the E.O. Paton Electric Welding Institute. The drive allows a simpler design of the machine, and provides high reliability, fast response, stable welding parameters, and possibility to vary the axial force according to any program.

Application. Welding of parts for machine building, electrical engineering, motor-car construction, aerospace engineering and other industries.

RESISTANCE BUTT WELDING OF PARTS FROM STEEL, ALUMINIUM, COPPER AND COMPOSITE MATERIALS

New advanced technologies have been developed for resistance butt welding of different structural materials and their combinations using a composite insert. The technologies are characterised by the use of a composite current-conducting insert, which provides uniform concentrated heating over the edge of a butt joint, and by creation of special conditions for deformation of the weld metal. These technologies feature a high thermal efficiency and small allowances for upsetting. They provide the high-quality butt joints in ferrous and non-ferrous metals, their combinations and composite materials.

Application. The technologies are intended to address the pressing production problems in welding of parts from carbon and low-alloy steels, aluminium and aluminium alloys of various profiles and sections,

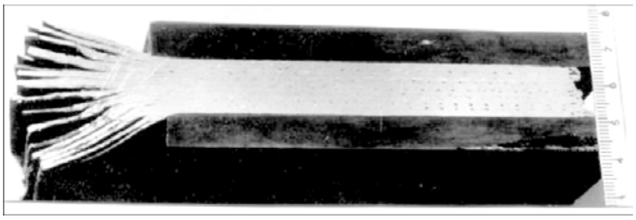

Overlap joining of stack of aluminium to steel busbars. Transition piece of electrolytic cell cathode with surface area of 20,000 mm^2

parts from copper, copper alloys and copper-based composites, steel-aluminium transition pieces for heavy-section (over 20,000 mm^2) current-conducting busbars, and can be applied in different industries, such as power generation, construction and machine building.

FLASH BUTT WELDING OF PARTS FROM ALUMINIUM-, MAGNESIUM- AND TITANIUM-BASE ALLOYS, STAINLESS AND HEAT-RESISTANT STEELS AND ALLOYS

Technology and equipment have been developed for flash butt welding of various parts from aluminium-, magnesium- and titanium-base alloys, stainless and heat-resistant steels and alloys with a cross section area of up to 40,000 mm^2, including rings of extruded sections, plates and forgings of high-strength aluminium-base alloys with a diameter of over 500 mm, sheets up to 2000 mm wide and up to 50 mm thick, and longitudinal welds on shells of the above sheets over 2000 mm in diameter.

In particular, available are the technologies for flash butt welding of similar and dissimilar combinations of high-strength aluminium alloys, and specialised equipment for implementation of these technologies.

Alloy grade (system)	$K = \sigma_{w.j} / \sigma_{b.m}$
AMg6 (Al–Mg)	0.95
1570 (Al--Mg–Sc)	0.92
1201 (Al–Cu)	0.90
D16 (Al--Cu–Mg)	0.90
V95 (Al--Zn–Cu–Mg)	0.90
AK6 (Al–Cu–Si)	0.92
1420 (Al–Mg--Li)	0.95
1460 (Al–Cu–Li)	0.90
1915 (Al–Zn–Mg)	0.90
AMg6 + 1201	0.90
D16 + ÀÊ6	0.90
V95 + ÀÊ6	0.90
1460 + AMg6	0.90

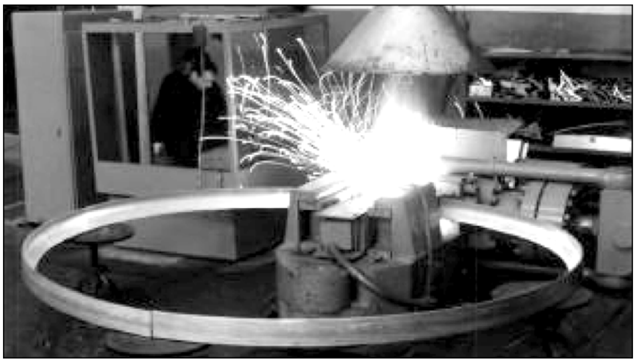

Flash butt welding of frames using machine K393

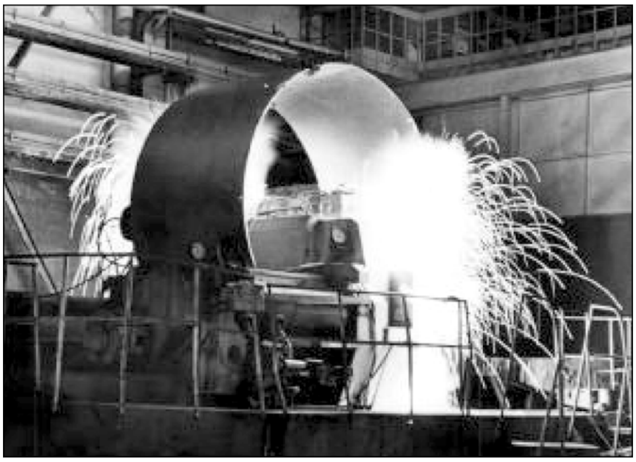

Flash butt welding of shells using machine K767

The technologies are applied for joining almost all high-strength aluminium alloys using no welding consumables. They provide:

- strength factor of a welded joint equal to not less than 0.9 (Table);
- high dimensional accuracy of parts of a large cross section (deviation on the perimeter being ± 1 mm), and absence of stresses;
- high productivity (welding time — 2–3 min).

Application. The technologies and equipment developed are intended for the manufacture of rings and shells for rocket and aircraft airframes and engine components. Also, they can be utilised for welding of parts of the type of bicycle and motorcycle wheel treads, various elements of building structures, for welding of large-size storage tanks for chemical, food processing and metallurgical industries, for ship building, etc.

UNIT FOR LOCAL VACUUM ELECTRON BEAM WELDING OF CUT-IN MEMBERS OF LARGE-DIAMETER SHELL STRUCTURES

Specialised unit has been developed for local vacuum electron beam welding of cut-in members of large-di-

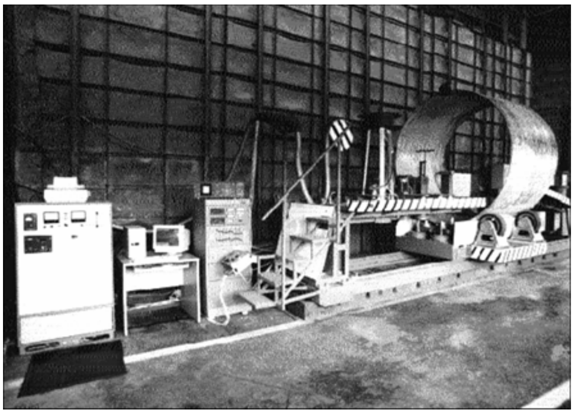

ameter shell structures made from high-strength aluminium alloys Al–Cu, Al–Mg–Mn, Al–Mg–Li and Al–Cu–Mg–Si. The unit comprises personal computer and programmed controllers. It provides for visualisation of the welding zone using a video monitoring device based on the principle of emission of secondary electrons (tenfold magnification). The unit is equipped with a power supply fitted with the breakdown protection system, which is characterised by a high operational stability.

Beam power is up to 15 kW at an accelerating voltage of 60 kV.

The use of electron beam welding instead of argon-arc welding allows a 5–6 times decrease in residual stresses within the zone of a cut-in member.

TECHNOLOGY FOR ELECTRON BEAM WELDING OF LIGHT ALLOY STORAGE TANKS AND OTHER SHELL STRUCTURES WITH WALL THICKNESS OF UP TO 150 mm

The integrated technology using electron beam welding has been developed for manufacture of 300 to 8000 mm diameter cylindrical or conical shells and tanks utilised as airframes of rocket-space vehicles, fuel systems, pressure vessels and cryogenic storage tanks made from aluminium and magnesium alloys. In addition to welding operations, the technology also solves the problems of design of weld edges in different types of welded joints, surface preparation of parts, and groove preparation prior to welding. It meets requirements to welding fit-up, provides selection of a spatial position and selection of rational methods for quality control and strength testing of welded joints, including at cryogenic temperatures.

The technology provides a 15–25 % increase in tensile strength of the welded joints on heat-hardened

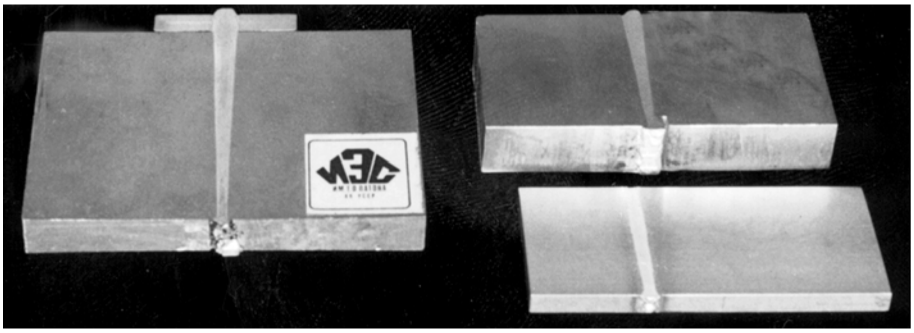

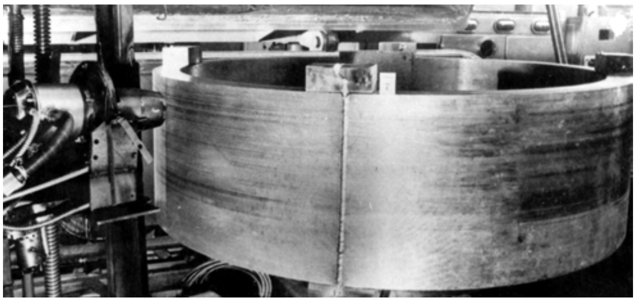

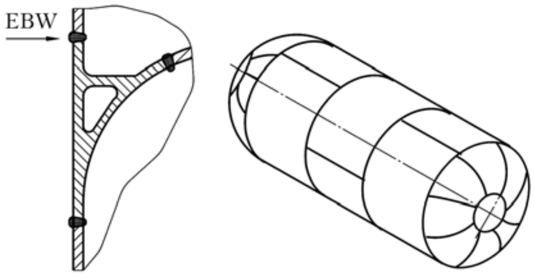

and intensively cold-worked aluminium alloys, 4–5 times decrease in residual welding distortions, and 5–7 times reduction in width of the heat-affected zone, compared with arc welding methods.

TECHNOLOGY FOR ELECTRON BEAM WELDING OF ALUMINIUM ALLOY PISTONS HAVING AN OIL COOLING CAVITY AROUND THE COMBUSTION CHAMBER

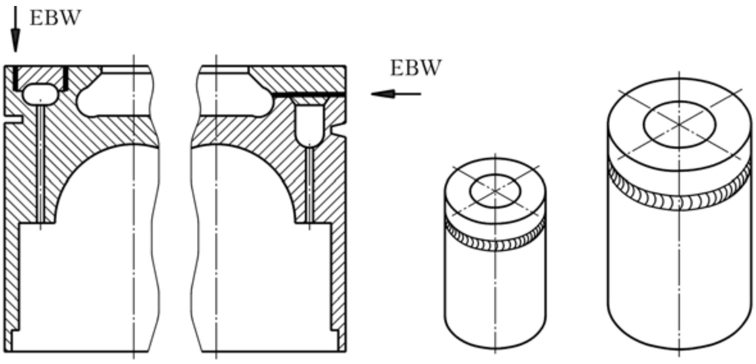

To improve operational reliability of diesels and extend service life of pistons, the most thermally stressed regions of a piston are treated by the methods of forced cooling, involving circulation of cooling oil via cavities made in the bottom part of the piston. In this respect, the cast-welded pistons of aluminium alloys meet most fully the corresponding requirements, and are not difficult to manufacture under mass production conditions.

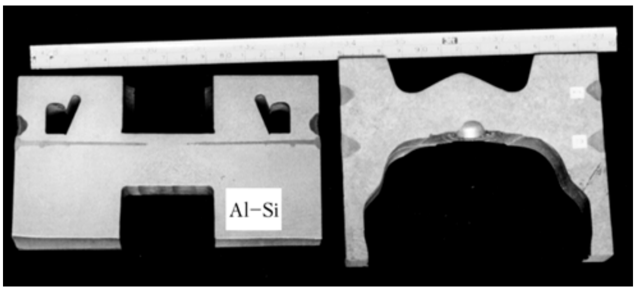

The developed design and technology of manufacture of the welded pistons allow selection of the most rational shape of a cooling cavity, its optimal location and almost 2 times decrease in labour consumption, compared with known manufacturing variants.

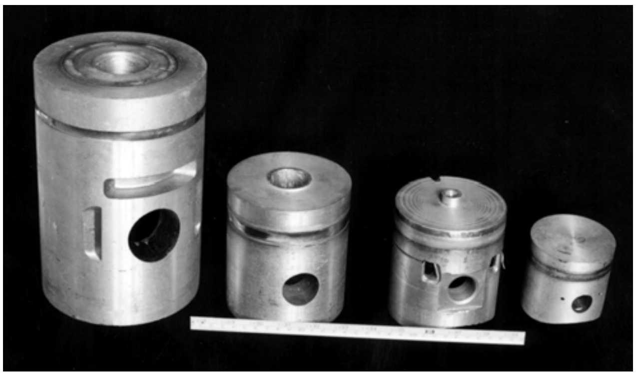

ELECTRON BEAM WELDING OF RIBBED HEAT EXCHANGERS (RADIATORS) OF ALUMINIUM ALLOYS

The environmentally clean and waste-free technology has been developed for manufacture of high-efficiency heat exchangers from aluminium and its alloys. It allows a 3--4 times decrease in weight characteristics of radiators, compared with conventional ones made from copper or brass, and 40--60 % improvement in their thermotechnical characteristics. The use of electron beam welding for joining ribbed tubular elements to tube sheets provides strength of the welded joints equal to that of the base metal, almost absolute absence of distortions, and retaining of initial rigidity of thin-walled ribs.

Main operations of the developed technology are environmentally clean and easy to automate and mechanise.

Application. Aluminium heat exchangers (radiators) can be applied in motor car and tractor construction, aircraft engineering, at refrigerating plants or compressor stations, in air conditioners, etc.

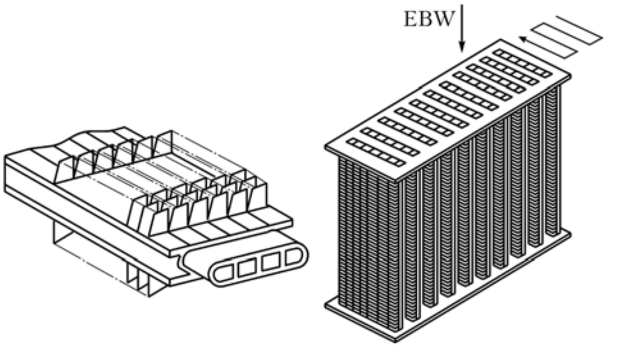

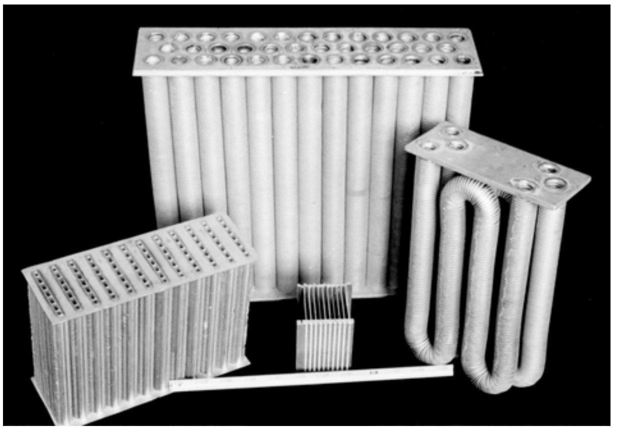

ELECTRON BEAM WELDING OF PRECISION PARTS AND ENCAPSULATION OF PACKAGES OF ELECTROVACUUM DEVICES

Precision electron beam welding was developed for joining packages of electric vacuum devices and gyroscopes, and for encapsulation of microcircuits in aluminium shells, the welding process being used as a final operation in the manufacture of high-precision devices.

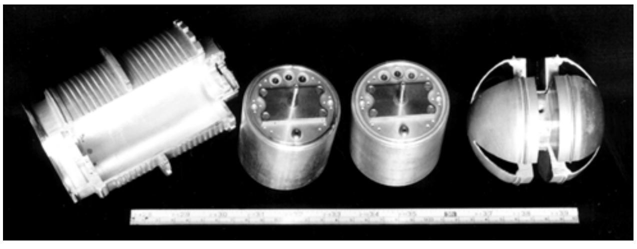

The technology provides minimal welding distortions (no more than 0.03 mm over a diameter of up to 100 mm) and insignificant (no more than to 60 °C) heating of mounting and microcircuit elements housed in a package or shell, and permits location of pressure seals on the package of a device at a distance of up to 2 mm from the weld. The pressure seals are joined to the package using different compositions of glues or sealants.

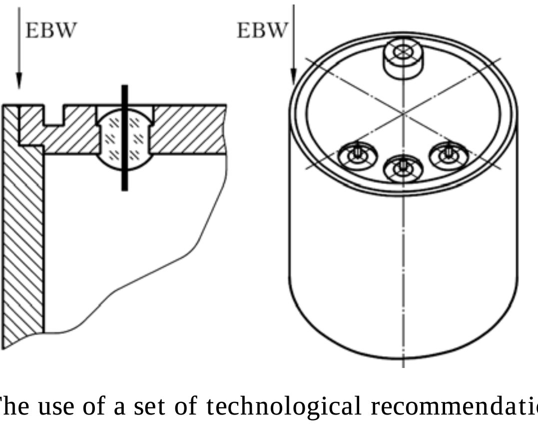

The use of a set of technological recommendations provides sound welds, as well as high reliability and performance of devices under complicated service conditions.

TECHNOLOGY FOR ELECTRON BEAM WELDING OF SHEET STRUCTURES WITH SIMULTANEOUS FEED OF FILLER WIRE TO THE WELD POOL

Semi-finished products in the form of sheet billets constitute a big portion in fabrication of different-application welded structures. Because of specific features of the process of electron beam welding of aluminium alloys, formation of welded joints is accompanied by some lowering of the surface of the weld metal relative to the upper plane of the sheets welded.

This defect in the welded joints on sheet billets can be prevented by the EBW technology that provides for the simultaneous feed of filler wire into the weld pool. Welding can be performed in different spatial positions and using no forming devices. The welds are deposited with formation of a reinforcement bead and through penetration to the reverse side of the joint.

During welding, the 0.8–2.6 mm diameter filler wire can be fed to the weld pool on any side relative to the melting front. This is particularly important in the case of a simultaneous use of devices for aligning and guiding of the beam over the joint, where the latter ahead of the beam should not be «closed».

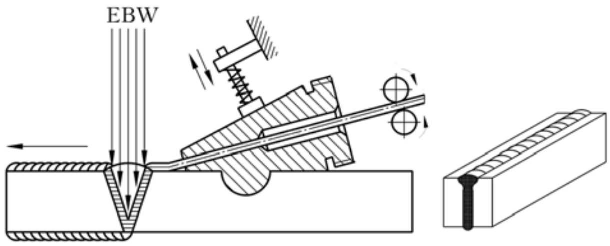

The developed technology and filler wire feed mechanism can also be used for performing surfacing operations, surface cladding, and filling up of wide gaps in multipass welded joints.

ELECTRON BEAM WELDING TECHNOLOGY FOR FABRICATION OF WELDED RIBBED THIN-SHEET STRUCTURES

Thin-sheet panels, i.e. sheets with a set of light alloy stiffeners, are widely applied in fabrication of large-size casing light-weight aerospace engineering structures, in ship building and transport. Such panels can be manufactured by hot pressing. However, this method can be employed only for high-ductility alloys and at certain proportions of cross section sizes of a sheet and stiffeners.

The advanced technology has been developed for the fabrication of welded panels, with which stiffeners of any cross section can be welded to a thin sheet. The developed technology based on the use of the preliminary elastic tensioning method provides suppression of residual distortions.

Welding of stiffeners to a sheet can be performed with a two- and one-sided fillet or slot weld. The stiffener to sheet thickness ratio in this case can range from 1:1 to 1:10 or more.

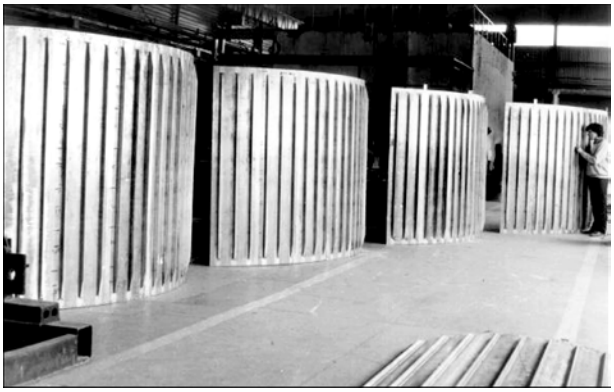

Panels made from high-strength aluminium alloys by electron beam welding are characterised by the highest values of structural strength. Residual longitudinal sag of such panels is no more than 1 mm per running metre of length of a panel.

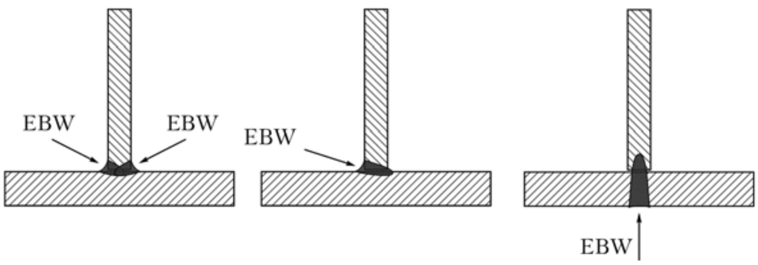

TECHNOLOGY FOR HARD-FACING OF COMPRESSION GROOVES IN ALUMINIUM PISTONS USING ADDITIVE MATERIALS

The trend in upgrading of internal combustion engines, and diesels in particular, is now to increase of their capacity, decrease of metal consumption and extension of service life. In this connection, the problems of extending service life of pistons take up special significance, as thermal and dynamic loads on a piston substantially grow with increase in capacity of the engines.

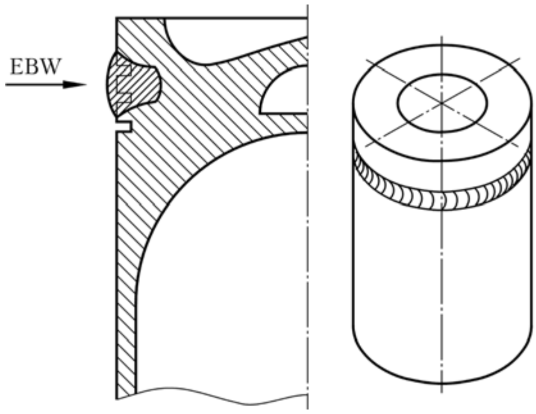

The technology for hard-facing of pistons within the zone of their upper compression groove by using alloying additives and highly concentrated electron beam heating has been developed to increase wear resistance and extend service life of the aluminium pistons.

The use of alloying materials provides the required values of hardness of the treatment zone equal to *HB* 150--180. Hot hardness of the treated layer in a temperature range of 100--360 °C is 2--3 times higher, compared with base metal of a piston.

The developed technology for hard-facing of pistons allows the life of a piston group of the engines to be increased 1.5--2 times.

TECHNOLOGY FOR FABRICATION OF WELDED LARGE-SIZE RIBBED PANELS AND SHELLS FROM LIGHT ALLOYS

The new technology is based on the use of both electron beam welding and metal-electrode argon-arc welding, which are performed at a high speed and combined with preliminary elastic deformation of the parts joined. Stiffeners are welded to a thin-sheet part using a two-sided fillet weld with small legs and full penetration through thickness of a stiffener. This provides a high accuracy of manufacture of the large-size structures, low level of residual welding stresses and strains, narrow zone of weakening of the base metal in HAZ, and high quality of the welded joints.

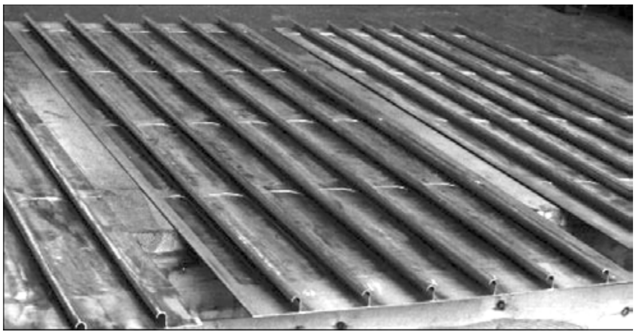

Compared with extensively applied milling of thick-plate billets and hot pressing of panels, the new technology is characterised by the reduced costs of manufacture of panel structures, much higher metal utilisation factor, and wider design capabilities in fabrication of high-efficiency structures.

PLASMA-ARC WELDING OF ALUMINIUM TO CARBON MATERIALS

In high-power thermal-electric resistance furnaces, such as Acheson furnaces, used for graphitisation of carbon materials (at currents of up to 200,000 A) and synthesis of silicon carbide (at currents of up to 30,000 A), metal busbars are connected to electrodes (current conductors) using pressure contacts, most often the bolted ones. Bus-lines of the furnaces are usually made from copper, which is expensive and difficult to obtain in Ukraine.

Contact assemblies of such furnaces are working in a cyclic mode — heating to 400--500 °C and cooling to a workshop temperature, which causes oxidation

Figure 1. Resistance furnace for synthesis of silicon carbide, designed for currents of up to 30 kA

of contact surfaces of the metal part of the contact, and associated rapid growth of contact resistance. For example, in graphitisation furnaces at the Dneprovsky Electrode Factory, contact resistance after a few campaigns of operation of a furnace ($I \sim 100 \cdot 10^3$ A) increases from 70–100 to 15,000 μOhm. Hence, the power losses at the end of a period amount to 19.6 % of the total power of the furnace.

The E.O. Paton Electric Welding Institute of the NAS of Ukraine has developed a new method for welding dissimilar metal to carbon materials, which allows the specific power consumption in thermal-electric furnaces to be substantially decreased.

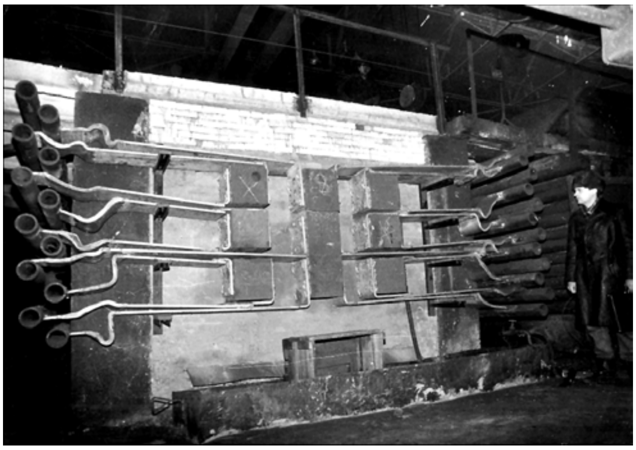

Figure 2. Resistance furnace for graphitisation of carbon materials, designed for currents of up to 100 kA

Electric-contact welded connections of metal busbars made by using electrodes based on carbon materials have the form of plugs, each being capable of working for a long time at currents of up to 600 A (aluminium-carbon material connection).

Contact resistance of welded connections measured at a contact temperature falls by 25–30 % in heating of a connection to an operating temperature, but, what is most important, it does not grow in long-time operation of the furnace. In addition to saving the electric power, the technology of making the welded contacts allows using light-weight and less expensive aluminium busbars instead of the copper ones. The technology has been successfully applied at the Production Association «Graphite» (Zaporozhie).

PACKAGE OF EQUIPMENT FOR WELDING THIN-SHEET ALUMINIUM STRUCTURES

Quality and high-productivity welding of structures of aluminium and its alloys with minimal power and resource costs is a pressing technical-economic problem for many industries. This problem has become even more pressing lately because of increase in requirements to the quality of welded joints on high-power busbars for power generating and electric metallurgical enterprises, including enterprises involved in electrolysis of non-ferrous metals. In this case, high saving of the electric power directly depends upon the quality of the welded joint. The entire package of problems encountered at a number of enterprises involved in electrolysis production of aluminium (TADaZ, Tajikistan, and AVISMA, Russia) was taken

Figure 1. Semi-automatic device PSh2107A

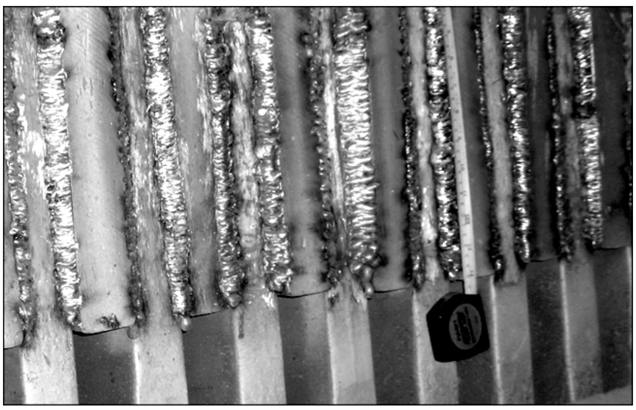

Figure 2. Welded aluminium joints for busbars

Figure 3. TRIPLET unit

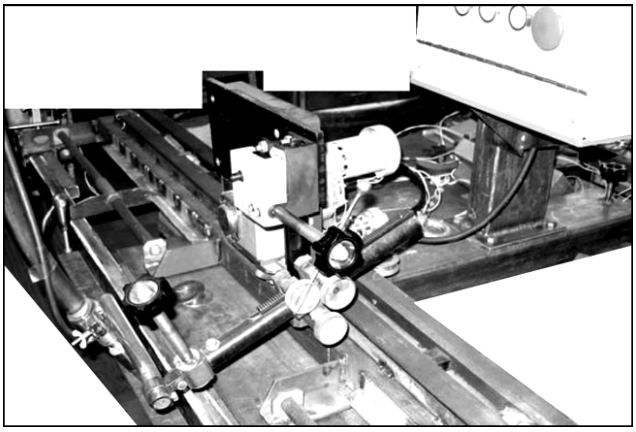

Figure 4. Automatic device for multilayer welding of aluminium structures

into account by the E.O. Paton Electric Welding Institute in development of ingenious technologies and equipment, including:

• semi-automatic device for arc welding of aluminium and its alloys of the PSh2107A type (Figure 1), which can be equipped with any type of the welding current source subjected to certain optimisation of static and dynamic characteristics. Distinctive and determining features of PSh2107A are the possibility of a reliable feed of 1.2--3.5 mm diameter aluminium electrode wires, as well as precise setting and maintenance of parameters of the welding process. It provides welding of structures of aluminium alloys up to 20 mm thick. Figure 2 shows the vertically welded joints on aluminium busbars of a magnesium electrolyser using the PSh2107A semi-automatic device;

• unit «Triplet» for arc welding of aluminium and its alloys with simultaneous or alternate feed of three electrode wires to one current-conducting tip using one welding current source. Advantages of this welding method consist in a substantial increase of process productivity, considerable saving of the electric power and resource consumption, and utilisation of the possibilities of modulation of the welding process through alternate feed of each of the three wires according to a certain algorithm. Manoeuvrability of the equipment is provided by availability of several modifications (mechanised, automatic). One design modification of the «Triplet» unit is shown in Figure 3. It is recommended for welding of structures with thicknesses of the members welded within a range of 10--60 mm;

• small-size (portable) automatic device for high-productivity multilayer welding of long thick-plate aluminium structures, e.g. busbars, longitudinal welds on storage tanks, etc., equipped with the mechanisms for feeding up to 4.0 mm diameter electrode wire, displacement devices, devices for adjustment and arrangement of welds, and welding cycle control devices with automatic arc ignition (Figure 4). It is recommended for welding of structures with thicknesses ranging from 20 to 100 mm.

Additional capabilities of the above equipment in power and resource saving provide the controlled pulse processes, which can be realised, among other things, by using ingenious adjustable pulsed feed mechanisms.

THESES FOR SCIENTIFIC DEGREE

E.O. Paton Electric Welding Institute, NAS of Ukraine

N.O. Chervyakov (PWI) on the 10th of October 2007 defended the thesis of Candidate of Sciences in engineering on the subject «Stress-Strain State and Technological Strength of Welded Joints of High-Strength Nickel Alloys».

The thesis is dedicated to study of peculiarities of thermal deformation processes for evaluation of crack resistance of welded joints and development of recommendations on this base for selection of effective technology methods of making sound high strength ($\sigma_t \sim 1000$ MPa) welded joints of nickel age-hardening alloys with γ'-strengthening.

Weldability of nickel alloys was studied by Varestraint Test. Brittle temperature intervals were built for nickel alloys with γ'-phase content from 40 to 60 %. The presence of two brittle temperature intervals, namely high (BTI-I) and low (BTI-II) temperature, were shown. Extent of brittle temperature intervals and critical deformation, exceeding which causes cracks initiation, were determined for each interval. It was established that when welding nickel alloys, the most critical is transverse crack formation in the low temperature interval of ductility dip (BTI-II) in the temperature range of 1150–700 °C.

Distribution of residual stresses and strains was experimentally studied and it was shown that with increase of γ'-phase content in the alloy from 40 to 60 %, the maximum tensile residual longitudinal stresses change from 750 to 950 MPa, and they were proportional to material yield point. It was determined that plastic deformation is located at the distance of up to 1000 μm from the fusion line towards the base metal, and the width of crack formation zone coincides with the size of plastic deformation zone. Temperature conditions of welded joint formation were studied by direct measurement of thermal cycles in the heat-affected zone (HAZ) at different distance from the weld axis. The influence of parameters of the process of tungsten electrode argon-arc welding on the parameters of weld pool and weld was examined. An experimental set-up was assembled, which allowed performing video filming of the moving weld pool surface and weld formation, by the results of which the liquid pool surface shape and geometrical sizes were determined. The obtained data were further used for mathematical model correction.

Mechanical and thermophysical properties of the studied alloy were determined experimentally at temperatures higher than 1000 °C, namely the yield point and linear expansion coefficient, that are important parameters for modeling the thermodeformation processes in the weld and HAZ. Maximum values of linear expansion coefficient are equal to $60 \cdot 10^{-6}$ 1 / °C for JS-26 alloy, practically two times increase of its values at the stage of heating occurring in the temperature interval of 1000–1200 °C. Yield point at room temperature is 950 MPa, and at heating up to the temperature of 900 °C it smoothly decreases to 850 MPa; quick drop of the yield point to 100 MPa occurs in the 950–1100 °C temperature interval.

The level and the kinetics of development of the stress-strain state during welded joint formation were studied by the experimental estimation method for evaluation of the probability of near-weld hot crack formation in fusion welding of nickel age-hardening alloys. Regularities of distribution and peculiarities of local plastic deformation development in nickel alloys HAZ were studied by calculation, and it was determined that longitudinal plastic deformations are localized at the stage of cooling in the narrow (up to 1000 μm) zone adjacent to the fusion line, and have positive increments, which values are more than 1.5 % on the macro level, thus considerably exceeding the critical value of deformation. The peculiarity of these deformations development is such that their reaching the maximum coincides in time with the HAZ metal (BTI-II) staying in the temperature interval of 1150–700 °C. Study of the kinetics of change of the longitudinal temporal stresses showed that the main role belongs to longitudinal σ_{xx} stresses relative to welding direction, the high values of which of up to $0.8\sigma_{0.2}$, are already achieved at the time when the HAZ metal stays the region of subsolidus temperatures that proves the fact of prior formation of transverse near-weld cracks. The correlation between stress-strain state and technological strength, i.e. susceptibility of welded joints to hot cracking in welding and heat treatment of high-strength nickel alloys, is shown on the base of analysis.

Methods of controlling the stress-strain state in welding of alloys prone to hot cracking in the HAZ are determined, and it is shown that the moment of the start of development of positive increments of plastic deformation in HAZ can be significantly delayed by heat input variation, and their values can be decreased to the level of less than 0.1 %, that does not exceed the critical values at which the crack forms in the corresponding brittle temperature interval.

A complex of recommendations was developed for creation of conditions at which the necessary technological strength of welded joints is provided.

On the 10th of October 2007 **I.A. Petrik** (OJSC «Motor Sich») defended the thesis of Candidate of Sciences in engineering on the subject «Processes of Reconditioning by Welding and Soldering GTE Blades from Difficult-to-Weld Alloys on Nickel and Titanium Base».

The thesis is devoted to development of industrial technological processes of reconditioning blades from high-strength titanium and high-temperature nickel alloys for the gas-air path of gas-turbine aircraft engines with the aim to prolong their service life. The main causes of GTE parts breakdown are examined and systematized in the study. It is shown that dynamic forces and temperature loadings and corrosion environment of gas flow affect the blades during operation. Thermal-force load distribution is nonuniform along the blade body and is of a gradient nature. Classification of originating operation damage of blades was carried out: by types of wear, by design features, by the zones of origination, by causes of failure, with the aim to establish their reapirability and repair conditions.

The main methodological aspects of work, methods and use of equipment are given. Chemical, spectrum and X-ray structural analysis, metallographic studies, standard mechanical tests, tests for short-term and long-term strength, including at working temperatures, and determination of fatigue point σ_{-1} (on 10^7 cycles base) were conducted. Procedure of technological «blade circular» sample together with dynamic deformation Trans-Varestraint Test method, were used for effective technological evaluation of blade metal weldability after their operation.

Influence of EBW, AAW modes, filler metal composition and heat treatment modes on the structure and mechanical properties of welded joints of VTZ-1 titanium alloy and heat resistant JS6U-VI nickel alloy were studied. It is shown that standard EBW and AAW processes and parameters considerably decrease the joint performance and require optimization. On the basis of analysis of the established dependences of the influence on the structure and properties, EBW and AAW heat input values were determined, at which optimal adaptability-to-fabrication of weld structure, and the highest level of mechanical properties are provided.

Calculation and analysis of working stresses distribution in blade volume were carried out. Calculation and graphic plotting of the stress fields were done for the case of GTE D-36 fan working blade. The procedure of determination of the possible zones for repair by welding was developed on the base of working stress comparison with strength properties of repair welded joints and gradient-strength model was suggested of selection of technological parameters, materials and methods of welded joints treatment. Weldability of structural materials was recognized to be the determinant factor in assignment of repair technologies. For working blades from two-phase titanium alloys of VTZ-1 type the generalized weldability criterion is fatigue strength value; and for repair welded and soldered joints from JS6U-VI it is the level of cracking sensitivity and strength properties of welded joint.

Application of gradient-strength principle of repair for fan blade from VTZ-1 alloy showed the possibility of repair volume expansion by 75–80 % in comparison with admissible zones determined in accordance with earlier adopted standard documentation.

The results and analysis of weldability of blades from high-temperature nickel alloys by AAW process are given. Investigations of the influence of filler material from VJ98, EP367 alloys and heat treatment for blades from JS6U-VI alloy on technological strength (cracking resistance) were carried out. Availability of the alloy brittle temperature interval in 950–1160 °C temperatures range at low (0.1 %) values of critical deformation was established. Welding and heat treatment modes, and technological methods of their realization that decrease the influence of thermodeformation processes on cracking in welding JS6U-VI alloy were substantiated and suggested. Express method of evaluation of complex-alloyed blade metal weldability after long-term operation under the influence of high-temperature gas medium and force loads was developed on the base of standard Trans-

Varestaint Test. «Blade circular test» that was done directly on the real blade body, was used. Complex Ω criterion of weldability evaluation, was proposed that takes into account the geometrical features of the parts and metal state, level of stressed state by location and total length of cracks being formed, was suggested.

The possibility of repair by brazing was studied in a number of cases when blades repair by welding was unacceptable. In-service defects that can be corrected by brazing were determined by the type and location. Possibility of standardized braze alloy application in aircraft industry was studied, conditions of ensuring of capillary gaps required for producing tight and strong brazed joints of high-temperature casting nickel alloys were determined.

The developed principle of gradient strength was grounded and realized in creation of repair technologies with application of welding and related technologies of both titanium and high-temperature alloys.

Recommendations and approaches were also realized for repair of casting defects, as well in manufacturing of new nozzle blades.

Normative documentation, instructions, group technologies and recommendations on repair were also developed that were agreed with engine development contractors.

Methodological and technological capability was provided for creation of repair processes of heavy-duty GAP blades under industrial conditions. The developments were introduced at OJSC «Motor Sich».

NEWS

NKMZ SIGNED A CONTRACT WITH MAGNITOGORSK METALLURGICAL WORKS

On June 13, the day of 75th anniversary of Magnitogorsk Works, the largest in the history of Novokramatorsk Machine-Building Works –– NKMZ Company –– (Kramatorsk, Donetsk reg.) contract has been signed for complete reconstruction of a continuous broad-strip hot rolling mill 2500 made at NKMZ and put into operation in 1960.

Preparation for a tender, in which such major manufacturers of metallurgical equipment as Danieli (Italy), Siemens-FAI (Austria), SMS-Demag (Germany) were involved alongside NKMZ, went on for a year. It turned into a struggle of ideas and technologies with the world trendsetters in the field of fabrication of rolling equipment.

Victory of the concept which envisages increase of the mill efficiency up to 5 mln t of rolled stock per year, lowering of the starting thickness to 1 mm, increase of slab weight up to 40 t, was followed by –– victory as to the equipment package.

Scope of delivery under the contract is equal to 37.5 thou t of equipment, its cost being 10 bln roubles RF. The equipment for reconstruction of 2500 mill should be made in 2.5 years.

We have never before gained a victory over the leading world manufacturers in such an uncompromising struggle for large-scale package deliveries of equipment. This is a great honour for NKMZ to earn the trust of the customer and receive congratulations from competitors, –– commented on the occasion G.M. Skudar, JSC President, in the press-conference on July 17.